



SOUTHERN PLAINS
TRANSPORTATION CENTER

Trends in Cold Extremes and Winter Weather for the SPTC Region

RENEE A. MCPHERSON, Ph.D.,
ESTHER D. MULLENS, Ph.D.

SPTC14.1-50-F

**Southern Plains Transportation Center
201 Stephenson Parkway, Suite 4200
The University of Oklahoma
Norman, Oklahoma 73019**

DISCLAIMER

The contents of this report reflect the views of the authors, who are responsible for the facts and accuracy of the information presented herein. This document is disseminated under the sponsorship of the Department of Transportation University Transportation Centers Program, in the interest of information exchange. The U.S. Government assumes no liability for the contents or use thereof

1. REPORT NO. SPTC14.1-50-F	2. GOVERNMENT ACCESSION NO.	3. RECIPIENTS CATALOG NO.	
4. TITLE AND SUBTITLE Trends in cold extremes and winter weather for the SPTC region		5. REPORT DATE May 31 2017	
		6. PERFORMING ORGANIZATION CODE	
7. AUTHOR(S) Renee A. McPherson, Ph.D., and Esther D. Mullens, Ph.D.		8. PERFORMING ORGANIZATION REPORT	
9. PERFORMING ORGANIZATION NAME AND ADDRESS South Central Climate Science Center 201 Stephenson Pkwy, Suite 2100 Norman, OK, 73019		10. WORK UNIT NO.	
		11. CONTRACT OR GRANT NO. DTRT13-G-UTC36	
12. SPONSORING AGENCY NAME AND ADDRESS Southern Plains Transportation Center 201 Stephenson Pkwy, Suite 4200 The University of Oklahoma Norman, OK 73019		13. TYPE OF REPORT AND PERIOD COVERED Final September 2014 – May 2017	
		14. SPONSORING AGENCY CODE	
15. SUPPLEMENTARY NOTES University Transportation Center, University Strategic Organization			
16. ABSTRACT <p>Extreme weather poses multifaceted hazards to transportation. There is now increased awareness of the threats of climate variability and change on transportation safety and state of good repair. In particular, a non-stationary climate will potentially change the frequency and severity of extreme events beyond those currently accounted for in design standards. Understanding regionally-specific climatic hazards is the first step necessary to adequately adapt to these changes and reduce the potential social, economic, and environmental impacts on the transportation system.</p> <p>This project performed an extensive climate analysis examining historical trends and future climate scenarios for the South Central United States, focusing on transportation-relevant conditions that reflect extreme and impactful events which stress transportation infrastructure and affect safety. These include cold weather, winter precipitation, and freeze thaw cycles, but also heatwaves and heavy precipitation. Key metrics, thresholds, and preferred formats for data analysis and dissemination were identified and guided by expert input via a transportation stakeholder survey. In Year 1, we developed and validating a model and observation derived spatial 36-year dataset for freezing precipitation which can be used for winter hazard and vulnerability assessment. Additionally, we use very high-resolution data (~1km) to construct freeze-thaw cycle spatial maps, climatologies, and trends between 1948 and 2015. Year 2 mined future climate projections from a large data ensemble to develop future scenarios for each transportation-relevant variable. Value-added data and graphics are generated for the entire SPTC region, and specific examples are provided for Central Oklahoma in this report. The research demonstrated that current infrastructure is likely to be benefitted over its lifetime by the reduction in winter weather and cold extremes, but will be adversely impacted by large projected increases in heat and extreme precipitation, particularly if climate change is not considered in planning and design. We provide links to expert recommendations and resources, including steps that various transportation agencies around the nation are taking to reduce their vulnerability, and incorporate climate projections into their long-term planning.</p>			
17. KEY WORDS Regional climate variability and change, climate projections, extreme temperature, extreme precipitation, winter weather, freezing precipitation, impacts and vulnerability		18. DISTRIBUTION STATEMENT No restrictions. This publication is available at www.sptc.org and from the NTIS.	
19. SECURITY CLASSIF. (OF THIS REPORT) Unclassified	20. SECURITY CLASSIF. (OF THIS PAGE) Unclassified	21. NO. OF PAGES 131 + cover	22. PRICE

SI* (MODERN METRIC) CONVERSION FACTORS

APPROXIMATE CONVERSIONS TO SI UNITS

SYMBOL	WHEN YOU KNOW	MULTIPLY BY	TO FIND	SYMBOL
LENGTH				
in	inches	25.4	millimeters	mm
ft	feet	0.305	Meters	m
yd	yards	0.914	Meters	m
mi	miles	1.61	kilometers	km
AREA				
in ²	square inches	645.2	square millimeters	mm ²
ft ²	square feet	0.093	square meters	m ²
yd ²	square yard	0.836	square meters	m ²
ac	acres	0.405	hectares	ha
mi ²	square miles	2.59	square kilometers	km ²
VOLUME				
fl oz	fluid ounces	29.57	milliliters	mL
gal	gallons	3.785	liters	L
ft ³	cubic feet	0.028	cubic meters	m ³
yd ³	cubic yards	0.765	cubic meters	m ³
NOTE: volumes greater than 1000 L shall be shown in m ³				
MASS				
oz	ounces	28.35	grams	G
lb	pounds	0.454	kilograms	Kg
T	short tons (2000 lb)	0.907	megagrams (or "metric ton")	Mg (or "t")
TEMPERATURE (exact degrees)				
°F	Fahrenheit	5 (F-32)/9 or (F-32)/1.8	Celsius	°C
FORCE and PRESSURE or STRESS				
lbf	poundforce	4.45	newtons	N
lbf/in ²	poundforce per square inch	6.89	kilopascals	kPa
APPROXIMATE CONVERSIONS FROM SI UNITS				
SYMBOL	WHEN YOU KNOW	MULTIPLY BY	TO FIND	SYMBOL
LENGTH				
mm	millimeters	0.039	inches	In
m	meters	3.28	feet	Ft
m	meters	1.09	yards	Yd
km	kilometers	0.621	miles	Mi
AREA				
mm ²	square millimeters	0.0016	square inches	in ²
m ²	square meters	10.764	square feet	ft ²
m ²	square meters	1.195	square yards	yd ²
ha	hectares	2.47	acres	Ac
km ²	square kilometers	0.386	square miles	mi ²
VOLUME				
mL	milliliters	0.034	fluid ounces	fl oz
L	liters	0.264	gallons	Gal
m ³	cubic meters	35.314	cubic feet	ft ³
m ³	cubic meters	1.307	cubic yards	yd ³
MASS				
g	grams	0.035	ounces	Oz
kg	kilograms	2.202	pounds	Lb
Mg (or "t")	megagrams (or "metric ton")	1.103	short tons (2000 lb)	T
TEMPERATURE (exact degrees)				
°C	Celsius	1.8C+32	Fahrenheit	°F
FORCE and PRESSURE or STRESS				
N	newtons	0.225	poundforce	Lbf
kPa	kilopascals	0.145	poundforce per square inch	lbf/in ²

*SI is the symbol for the International System of Units. Appropriate rounding should be made to comply with Section 4 of ASTM E380. (Revised March 2003)

Acknowledgements

The lead PI and Co-PI would like to thank Co-PIs Mark Shafer, Mike Richman, and Derek Rosendahl for their contributions to this work. Co-PI Rosendahl provided insight on climate model performance for the South Central U.S.; Co-PI Shafer along with his staff assisted in the development and testing of the stakeholder survey; Co-PI Richman aided in the extreme value analysis leading to the calculation of rainfall return periods from historical and future climate projections. Thanks also to Rachel Riley (Southern Climate Impacts Planning Program), and Toni Klemm (South Central Climate Science Center) who assisted with survey development. The assistance of Kelly Jones in formatting this report to ADA compliance was much appreciated. Colleagues at the Southern Plains Transportation Center have provided their support and important expertise to assist this research throughout its development and implementation. In particular we thank Professors Musharraf Zaman, and Gerald Miller, as well as Dominique Pittinger, Cerry Leffler, and Sonya Brindle at the SPTC offices in Norman. Thanks also to all those who participated in the survey, as their expertise, opinions and insights were critical in guiding this project. Finally, much of the computing work would not have been possible without the cyber-infrastructure provided by a grant from the National Science Foundation EPSCoR program, and its maintenance by the University of Oklahoma's Supercomputing Center for Education and Research (OSCER).

Trends in Cold Extremes and Winter Weather for the SPTC Region

Historical context and future projections in transportation-relevant weather and climate extremes

Final Report

SPTC14.1-50-F

Renee A. McPherson
Esther Mullens
The University of Oklahoma

Southern Plains Transportation Center
OU Gallogly College of Engineering
201 Stephenson Pkwy, Suite 4200
Norman, Oklahoma 73019

SPTC 14.1-50 Final Report

Table of Contents

TABLE OF CONTENTS	VI
LIST OF TABLES	VIII
LIST OF FIGURES	IX
EXECUTIVE SUMMARY	XVII
1. INTRODUCTION.....	1
2. METHODS	4
2.1 EXPERT INPUT – STAKEHOLDER SURVEY.....	4
<i>(i) Demographics.....</i>	<i>5</i>
<i>(ii) Weather and climate hazards and thresholds.....</i>	<i>6</i>
<i>(iii) Perspective of climate information.....</i>	<i>9</i>
<i>(iv) Usable output.....</i>	<i>12</i>
<i>(v) Summary.....</i>	<i>13</i>
2.2 CLIMATE DATA.....	14
<i>(i) Historical 20th and 21st century weather and climate</i>	<i>14</i>
<i>(ii) Future climate projections.....</i>	<i>15</i>
<i>(iii) Background on emissions scenarios.....</i>	<i>16</i>
2.3 APPROPRIATE SELECTION OF CLIMATE MODELS	19
<i>(i) Using a single climate model.....</i>	<i>19</i>
<i>(ii) Using existing datasets that best conform to a certain software or application.....</i>	<i>19</i>
<i>(iii) Using a range of climate models.....</i>	<i>20</i>
<i>(iv) Using a range of models across different downscaling methods.....</i>	<i>21</i>
2.4 DEFINITIONS OF INDICES AND VARIABLES	24
<i>(i) Freeze-Thaw Cycles.....</i>	<i>24</i>
<i>(ii) Winter Precipitation</i>	<i>24</i>
<i>(iii) Cold extremes.....</i>	<i>25</i>
<i>(iv) Hot extremes.....</i>	<i>26</i>
<i>(v) Heavy precipitation.....</i>	<i>26</i>
2.5 SUMMARY OF YEAR 1 ACTIVITIES	27
<i>(i) Data Mining.....</i>	<i>27</i>
<i>(ii) Output.....</i>	<i>29</i>
<i>(iii) Other synergistic activities.....</i>	<i>29</i>
<i>(iv) Changes from original proposal</i>	<i>31</i>
2.6 SUMMARY OF YEAR 2 ACTIVITIES	31
<i>(i) Data Mining.....</i>	<i>31</i>
<i>(ii) Output.....</i>	<i>33</i>
<i>(iii) Other synergistic activities.....</i>	<i>36</i>
<i>(iv) Changes from original proposal</i>	<i>37</i>
3. RESULTS: CLIMATE TRENDS	39
3.1 FREEZE THAW CYCLES AND WINTER WEATHER: PAST AND FUTURE.....	40
<i>(i) Context.....</i>	<i>40</i>
<i>(ii) Historical climatology (1948-2012) and future projections of freeze-thaw cycles.....</i>	<i>41</i>

3.2 COLD TEMPERATURES: SPATIAL PROJECTIONS FOR THE SOUTH-CENTRAL U.S.	52
3.3 WINTER WEATHER (SNOW AND ICE)	56
3.4 CASE STUDY: WINTER CONDITIONS IN CENTRAL OKLAHOMA	63
3.5 EXTREME HEAT: PAST AND FUTURE.....	68
3.6 CASE STUDY: EXTREME HEAT IN OKLAHOMA CITY	71
3.7 HEAVY PRECIPITATION: A CASE STUDY FOR CENTRAL OKLAHOMA.....	76
4. DISCUSSION	84
4.1 IMPLICATIONS	84
4.2 CAVEATS AND LIMITATIONS	92
4.3 FUTURE EFFORTS.....	93
5. RECOMMENDATIONS	94
6. REFERENCES.....	98
APPENDIX	1-A
A.1 RESOURCES ON PUBLICALLY AVAILABLE STATISTICALLY DOWNSCALED DATASETS.....	1-A
<i>A1.1 Delta Method.....</i>	<i>1-A</i>
<i>A1.2 Bias correction and Quantile Mapping.....</i>	<i>2-A</i>
<i>A1.3 Regression techniques</i>	<i>2-A</i>
<i>A1.4 Multivariate techniques.....</i>	<i>2-A</i>
<i>A1.5 Weather analogue techniques.....</i>	<i>3-A</i>
<i>A1.6 Other</i>	<i>3-A</i>
A.2 LIST OF DATA PRODUCTS GENERATED BY THIS PROJECT	4-A
<i>A.2.1 Freeze Thaw Cycles.....</i>	<i>4-A</i>
<i>A.2.2 Cold temperatures.....</i>	<i>5-A</i>
<i>A.2.3 Winter Precipitation.....</i>	<i>5-A</i>
<i>A.2.4 Hot Temperatures and temperature range.....</i>	<i>6-A</i>
<i>A.2.5 Precipitation, including average and extremes.....</i>	<i>7-A</i>
A.3 INTERPRETING DATA FORMATS.....	7-A
<i>A.3.1 Spreadsheet Readable formats.....</i>	<i>7-A</i>
<i>A.3.2 NetCDF.....</i>	<i>7-A</i>
A.4 LEVELS OF CONFIDENCE IN CLIMATE PROJECTIONS	9-A

List of Tables

Table 1: Survey participants were asked to rank (1=lowest concern, 5 = highest concern) their level of concern regarding various weather and climate extremes. The center column shows the percentage of responses that indicated high (3-5) concern. The response rate varied depending on the variable, with a minimum of 24 (tropical storm) to a maximum of 37 (heavy rainfall), with a mean of 34 (60% of surveys started). The right column shows the number of responses reflecting a desire for more climate data (trends, statistics, projections). Variables are ordered in the table in decreasing order of preference based on these two measures. 7

Table 2: Publicly available historical climate datasets used in this analysis. Their sources and use are briefly summarized in the table, along with the temporal length of the dataset (all have at least 30 years of data), and their spatial resolution (the distance separation between data points, in kilometers).....22

Table 3: Publicly available statistically downscaled climate model datasets used in this analysis. Their sources and use are briefly summarized in the table, along with the temporal length of the dataset (all have at least 30 years of data), and their spatial resolution (the distance separation between data points, in kilometers). The list of models used is included in the dataset/models column.23

Table 4: Threshold criteria used to designate locations by the frequency and magnitude of their cold temperatures. Integer values between -1 and 5 were assigned (higher value implies colder temperatures, and more frequent cold, and -1 indicates no freezing). For each location, the four variable fields were summed together (consisting of freeze-thaw cycle (FTC) days, FTC T_{min} , near lowest or 0.1th percentile annual temperature, and number of days with T_{min} less than or equal to 20°F), and then divided by 4, giving a mean value between -1 and 5. Climate class 2 and 3 in this table were condensed to category 2, as shown in the figures, and the no freeze category became category 0.....27

Table 5: List of winter weather (ice/snow) and related variables calculated from North American Regional Reanalysis data, and a brief description of the variable, including its unit, and temporal interval (e.g., 3-hourly, daily, monthly). The total data range is 1979-present. Data available at 3-hour intervals means that over this interval (1979-present), there is data available every 3-hours, and so on.30

Table 6: List of freeze-thaw cycle variables (including annual counts of FTC, EFTC, and FTC temperatures) calculated from high-resolution gridded observations. The temporal range of this data is 1948-2012 (Topographic Weather), and 1980-present (Daymet)....30

Table 7: Climate model historical and future projections of freeze-thaw cycle related variables, including annual FTCs and EFTCs, and FTC temperatures (annual or monthly mean, minimum and maximum). These are calculated from all available models used in this analysis, over the years 1950-2099 (1960-2099 for ARRM models). The same data is also calculated from the Livneh and Maurer observations.....33

Table 8: Cold temperature variables calculated from climate model datasets, including number of cold days at various thresholds (25, 20, 10°F), and the 0.1th percentile of annual temperatures. The length of the freezing season is also estimated for each

model. These parameters are calculated from the Livneh and Maurer observations, in addition to historical and future climate projections.....34

Table 9: Hot temperature variables calculated from climate model datasets, including days and consecutive days with maximum temperatures at or above 95, 100 and 110°F, and the annual 99.9th percentile temperature. The length of the 100°F season is also estimated for each model. These parameters are calculated for Livneh and Maurer observations, in addition to historical and future climate projections.....34

Table 10: Winter weather variables calculated from climate model datasets, including frequency (number of days per year), and accumulation (in the form of liquid water equivalent in inches). These variables are calculated for Livneh and Maurer observations, in addition to historical and future climate projections.....35

Table 11: Precipitation variables calculated from climate model datasets, including annual counts of days and consecutive days above thresholds ranging from 1-6 inches, and multiday (5 day) accumulations from 4-10 inches. Monthly and annual average precipitation accumulation is also calculated for each data point in the SPTC domain. Estimates of return period values and annual maxima are compiled by climate division. These variables are also assessed from Livneh and Maurer observations, in addition to historical and future climate data.....35

List of Figures

Figure 1: Map of the domain used in this analysis. All data was subset for this region, extending 110°W to 89°W, and 25°N to 40°N. Within the domain are the U.S. Department of Transportation Region 6 states of Oklahoma, Texas, Arkansas, New Mexico, and Louisiana. Image courtesy of ESRI-[ArcGIS](#)..... 4

Figure 2: The main employers of the survey respondents, which consisted of State DOT (39%), Federal DOT (17%), University researchers (20%), Private companies (22%), City or local government (5%), and other (10%). Respondents could pick multiple responses. 6

Figure 3: 'Word maps' depicting the type and frequency of responses to questions regarding hot and cold temperature thresholds, as described in the Section 2.1(ii) text. The larger the font, the more responses for that given threshold value. On the left is extreme heat, and the right, extreme cold..... 9

Figure 4: A gauge chart depicting the responses of participants to possible barriers in using climate information, the result of which are discussed in Section 2.1(iii). On the left panel a, are the seven respondents who indicated that they do not desire more climate information. On the right (panel b) are the responses of those who indicated that they would want more climate data. The response to each sub-query is shown in the chart as an average number between 1 and 5, where 1 (5) is strongly disagree (strongly agree) to a given statement. 11

Figure 5: A pie chart showing how respondents would prefer output climate data and information. The breakdown was as follows: 26% graphical summaries, 21% GIS, 19% report or information sheet, 19% spreadsheet compatible raw data, 15% original data from web portal. _____ 12

Figure 6: Pie chart describing the preferred formats for presenting or communicating climate data. The responses were: 27% for website that consolidates information, 20% graphics that use a spread of models (e.g., time series and range), 18% probabilistic likelihood of future climate state, 15% guidance document on reliable datasets, 14% mean future state compared to present state (and range), and 5% more direct communication with climate experts. _____ 13

Figure 7: Comparison of projected carbon dioxide concentrations associated with SRES emissions scenarios, used in CMIP3, and representative concentration pathways (RCP), used in CMIP5. The selected RCPs/SRES in the mid-range (RCP4.5/B1) and high categories (RCP8.5/A1Fi) both display similar carbon emission pathways to each other, meaning that they can be used in the same ensemble for each respective emission category. The grey line shows the 2016 concentration of CO₂. Base image from '[Climate Change Australia](#)'. Data from the Potsdam Institute. _____ 18

Figure 8: Top panel: Average annual number of freeze thaw cycles in Oklahoma, based on data from 1948-2012 taken from the Topographic Weather dataset (Oyler et al. 2012). Counties, highways and interstates are overlaid (think black, grey, and thick black lines respectively). FTC frequency ranges from 40-50 days in far southern Oklahoma, to 60-70 days along and south of I-44, 70-80 days parallel and north to I-44, increasing northwestward into the panhandle, to a maximum of 130-140 days in the far western Panhandle. Bottom panel: The percentage of freeze-thaw cycles that occurred within 3-days of precipitation >0.01 inch. Far southeastern Oklahoma has the highest percentage with 50-60%, decreasing north and west to 40-45% in a vertical line intersecting central Oklahoma, and a minimum in the Oklahoma Panhandle (25-35%). _____ 41

Figure 9: Multi-model average climate projections of annual average number of freeze thaw cycles for Oklahoma using mid-range emissions scenarios (RCP4.5/B1), based on 21 models. Top panel: 1970-2000, Middle panel: 2021-51, Bottom panel: 2060-90. The lower-resolution ARRM models are regridded to the MACA grid (6.6 km horizontal resolution). This regridding is performed for all spatial maps. Description of results provided in the main text. _____ 43

Figure 10: As Fig. 9, but for multi-model average climate projections of annual average number of freeze thaw cycles for Oklahoma using high emissions scenarios (RCP8.5/A1Fi), based on 19 models. _____ 44

Figure 11: Left panel: Average annual number of freeze thaw cycles in Texas, based on data from 1948-2012 taken from the Topographic Weather dataset (Oyler et al. 2012). Counties, highways and interstates are overlaid (think black, grey, and thick black lines respectively). FTC frequency ranges are discussed in the text, but freeze-thaw days are rare in south Texas, elevated over the Texas hill country (40-60 per year), and reach a maximum over the western Texas panhandle (120-140 per year). Right panel: The percentage of freeze-thaw cycles that occurred within 3-days of precipitation >0.01 inch. Eastern Texas east of I-35 has the highest percentage with 50-65%, decreasing north

and west to a minimum in the Chihuahuan desert (20-25%) and southern high plains (25-30%). _____ 45

Figure 12: Multi-model average climate projections of annual average number of freeze thaw cycles for Texas using mid-range emissions scenarios (RCP4.5/B1), based on 21 models. Left panel: 1970-2000, Center panel: 2021-51, Right panel: 2060-90. Description of results provided in the main text. _____ 46

Figure 13: As Fig. 12, but for multi-model average climate projections of annual average number of freeze thaw cycles for Texas using high emissions scenarios (RCP8.5/A1Fi), based on 19 models. _____ 46

Figure 14: Left panel: Average annual number of freeze thaw cycles in New Mexico, based on data from 1948-2012 taken from the Topographic Weather dataset (Oyler et al. 2012). Counties, highways and interstates are overlaid (think black, grey, and thick black lines respectively). FTC frequency is strongly dependent on altitude, with over 180-200 or more days per year in the mountains and high plains of northern and western New Mexico. The Tularosa valley and other low-lying regions of southern NM have the least number of FTcs annually (<50). Right panel: The percentage of freeze-thaw cycles that occurred within 3-days of precipitation >0.01 inch. The northern Sangre De Cristo Mountains have the highest frequency of proximal precipitation (some of which may be snowfall) at 45-50%, while the valleys and Chihuahuan desert have the lowest (20-25%). _____ 47

Figure 15: Multi-model average climate projections of annual average number of freeze thaw cycles for New Mexico using mid-range emissions scenarios (RCP4.5/B1), based on 21 models. Left panel: 1970-2000, Center panel: 2021-51, Right panel: 2060-90. Description of results provided in the main text. Note the different color bar magnitudes for this state (which range from 40-220 FTCs). _____ 48

Figure 16: As Fig. 15, but for multi-model average climate projections of annual average number of freeze thaw cycles for New Mexico using high emissions scenarios (RCP8.5/A1Fi), based on 19 models. _____ 48

Figure 17: Left panel: Average annual number of freeze thaw cycles in Arkansas, based on data from 1948-2012 taken from the Topographic Weather dataset (Oyler et al. 2012). Counties, highways and interstates are overlaid (think black, grey, and thick black lines respectively). FTC frequency is greatest over far northern Arkansas, and along the Ozark and Ouachita ranges (70-90 per year), and decreases southeast toward the Mississippi (40-60 per year). Right panel: The percentage of freeze-thaw cycles that occurred within 3-days of precipitation >0.01 inch. Arkansas has relatively abundant precipitation year-round, and 50-55% (North) to 60% (south) of FTC days are proximal to precipitation. _____ 49

Figure 18: Multi-model average climate projections of annual average number of freeze thaw cycles for Arkansas using mid-range emissions scenarios (RCP4.5/B1), based on 21 models. Left panel: 1970-2000, Center panel: 2021-51, Right panel: 2060-90. Description of results provided in the main text. _____ 50

Figure 19: As Fig. 18, but for multi-model average climate projections of annual average number of freeze thaw cycles for Arkansas using high emissions scenarios (RCP8.5/A1Fi), based on 19 models. _____ **50**

Figure 20: Left panel: Average annual number of freeze thaw cycles in Louisiana, based on data from 1948-2012 taken from the Topographic Weather dataset (Oyler et al. 2012). Counties, highways and interstates are overlaid (think black, grey, and thick black lines respectively). FTC frequency is greatest over far northern Louisiana (40-50 days), and decreases to the south. South of 1-10 freeze-thaw days are rare (0-10 per year). Right panel: The percentage of freeze-thaw cycles that occurred within 3-days of precipitation >0.01 inch. Louisiana has relatively abundant precipitation year-round, and 55 (north)-70 (south)% of FTC days are proximal to precipitation. _____ **51**

Figure 21: Cold climate class across the SPTC DOT region 6, expressed as the average for the period 1970-2000, calculated based on the frequency and magnitude of cold calculated from 4 temperature-related variables using applicable thresholds, described in section 2.4(iii), and Table 4. Top panel: The average of Livneh and Maurer observations (Maurer regridded to Livneh grid prior to calculation), Bottom panel: Climate model average, based on 21 models. _____ **53**

Figure 22: Cold climate class across the SPTC DOT region 6, expressed as the average for the period 2021-51. Top panel: mid-range emissions scenarios (RCP4.5/B1), 21 models. Bottom panel: high emissions scenarios (RCP8.5/A1Fi), 19 models. _____ **54**

Figure 23: Cold climate class across the SPTC DOT region 6, expressed as the average for the period 2060-90. Top panel: mid-range emissions scenarios (RCP4.5/B1), 21 models. Bottom panel: high emissions scenarios (RCP8.5/A1Fi), 19 models _____ **55**

Figure 24: Left panels: Seasonal climatology of freezing precipitation (freezing rain FZRA, freezing drizzle FZDR, and sleet IP) frequency, expressed as the average number of 3-hour periods with ice (1979-2013). 'NR-Alg' is the algorithm mean results, based on application of three precipitation type algorithms to the NARR data (see section 2, 'year 1 activities'), while 'NR_Cat' is the NARR native estimates of ice. Observations are from National Weather service observing station sites ('ASOS') at Amarillo (top), Oklahoma City (center) and Dallas Fort Worth (bottom). Right panels: Time series of winter (November-April) total ice frequency (also 3-hourly). Shown are both NARR-derived products, observations of all freezing precipitation types, and observations excluding freezing drizzle. It is evident from the Amarillo data that magnitudes of the reanalysis-derived ice frequencies are closer to estimates excluding freezing drizzle, as drizzle is not well resolved by the reanalysis. The maximum linear correlations between observations and reanalysis-derived data are shown, indicating high correlations in excess of 0.7 in all three locations. _____ **57**

Figure 25: General ice and snow climatological information, derived from a product developed by Co-PI Mullens and PI McPherson, available from 1979-2014 (2015 and 16 data coming soon). Panel a depicts the average annual number of 3-hour periods with freezing precipitation, revealing a northeastward increase in frequency through the region. Values over the far southeast domain, including Northern Texas, Louisiana, and south central Arkansas are known to be overestimated compared with observations, and regions to the northwest do not account for freezing drizzle. Panel b shows the average annual freezing precipitation accumulation in the form of liquid water equivalent (inches),

also showing a northeastward increase. Panel c shows the climatological ratio of freezing precipitation to snowfall, with values greater (less) than one implying more (less) freezing precipitation compared with snow. Panel d shows the annual average frequency of snowfall (also 3-hourly), which shows a maximum over the southern Rocky Mountains, and a latitudinal dependence over the region. _____ 58

Figure 26: Distributions of multi-algorithm mean freezing precipitation LWE for three decadal periods (inches, left) and locations of 1 in 50 year ice/damaging ice (right) obtained from the Army Core on Engineers [online GIS database](#). While not strictly comparable (more work is needed), qualitatively the regions of high ice liquid water often correspond with areas impacted by multiple events in the historical storm event database. _____ 59

Figure 27: Mid-range emissions climate projections in winter precipitation (ice/snow) daily frequency, expressed as a multi-model mean percentage change from the historical (1970-2000) average, and aggregated over climate divisions. Top left panel: difference in winter precipitation frequency for the mid-century, Top right panel: difference in winter precipitation frequency for the late-century. The bottom two panels show the average winter precipitation intensity change for the same periods, and expressed as a state average. Values within 5% of the historical period suggest very little change. Generally, the percentage changes in frequency for mid-century are between 15 and 45%, lowest in SW Texas, followed by the southern High Plains. Decreases over New Mexico, Oklahoma, and north Texas are between 30-40%, while Arkansas is generally 40-45%. A similar pattern is projected for late century, but with reductions between 30 and 60% (the greatest reductions are over northern New Mexico). Intensity changes are within plus or minus 5% (give or take 1%) during the two periods for all states except for New Mexico, which shows an 11% positive intensity change during the late 21st Century. _____ 61

Figure 28: As Fig. 27, but for high emissions. There are some sub-regional differences compared to the mid-range, mid-century projection, however for the region as a whole, the range of the decreases are similar (15-45%), with highest decreases over Arkansas, and far western New Mexico. The spatial pattern of the decreases is similar later in the century, but the magnitude of the decrease is larger, typically 60-70% (southern High Plains), 70-80% (eastern Oklahoma into Arkansas, and North Texas), and 80-80% (southern Arkansas, northern Louisiana, and far western New Mexico). The mid-century change in intensity is an increase across all states, greater than 5% for all states, but within 10% for all except Louisiana (15.9%). The late century change is within plus to minus 7%, and is generally slightly negative with the exception of New Mexico (+8.7%). _____ 62

Figure 29: Freeze-thaw statistics for Oklahoma City, based on 1948-2012 data (Topographic Weather, Oyler et al. 2012). A small grid was defined that encompassed the City, and the 1-km data was averaged over this grid. Top: probability distributions of T_{max} (left) and T_{min} (right) during FTC, with values at or greater than the criteria for EFTC shaded. Bottom: Time series of FTC activity from 1948-2012, FTC (left), and EFTC (right), including an estimated linear trend. A description of this information is provided in the text. _____ 63

Figure 30: Future projections of monthly freeze-thaw activity. Left panel: Mid-range emissions showing the observations (Maurer and Livneh); the model historical average

(MACA and ARRM are displayed separately and overlaid, as MACA=solid, and ARRM=stippled bars); the model mid-century; and the model late-century for months November through April. Individual model projections are shown by the black square markers (MACA), and grey square markers (ARRM). The vertical bars on the right hand side of the figure show the change in freeze-thaw cycle variance on the left, and proportion of freeze-thaw cycles that meet the 'enhanced' criteria (right). Right panel: As left panel, but for high emissions. The trends depicted in this figure are discussed in the text. _____ 64

Figure 31: Annual highest and lowest temperatures in the OKC area during the peak winter season (December-January-February) as simulated by climate models. The multi-model mean is depicted by the thin black line, and the model spread the shaded polygon. The thick dark grey and blue lines show the Maurer and Livneh observed temperatures respectively. Top panel: mid-range emissions, Bottom panel: high emissions. The model spread encapsulates the range of the historical observed conditions, indicating that the past variability is relatively well constrained. The trends depicted are discussed in the text. _____ 66

Figure 32: Output from the freezing precipitation dataset developed by Mullens and McPherson (2017), with statistics and time series shown here for Oklahoma County, OK. Top left panel: Time series of freezing precipitation (blue) and snowfall (purple) days 1979/80-2013/14, with a linear trend line. There is year-to-year variability in the counts, with a mean of approximately 4.5 days (snow), and 3.7 days (ice) and a general slight decreasing trend (not significant). Center left: Time series of freezing precipitation liquid water equivalent in inches, with a linear trend line. Prior to the year 2000 the peak LWE was lower and less variable than after 2000. Bottom left: Time series scatter plot of temperatures (daily average and daily minimum) during snow and freezing precipitation. In most cases temperatures range between 25 and 32°F with no apparent trend since 1979/80. Right hand side: Pie chart depicting the percentage probability that any given day in a given month experiences freezing precipitation. The peak month is January, followed by December, February, then March. Below this are some statistics regarding the frequency of moderate ice days and ice storm days in any given year (estimated). 67

Figure 33: Time series of the standardized winter precipitation (ice/snow) frequency (days) for Oklahoma climate division 5, encompassing Central Oklahoma. Standardized units are based on the departure of values from the standard deviation of the data, so a unit of 1 for example would indicate data is roughly 1 standard deviation above the mean (the mean used was the historical period). The black line is the multi-model mean, and the blue shading the mode 5th-95th percentile range. Observed data is the grey (Maurer) and yellow (Livneh) lines, and the 5th and 95th percentiles of the observed data are shown by the horizontal dashed black lines. The model suite captures the range of historical variability, and it can be seen that with both mid and high emissions, that winter precipitation in the form of ice and snow declines over the 21st Century, particularly after mid-century with high emissions. _____ 68

Figure 34: The average annual number of days $\geq 100^\circ\text{F}$ over the SPTC domain, based on historical period 1970-2000. Left panel: average of the two observations (Maurer and Livneh), Right panel: Multi-model historical mean (21 models). Interstate highways, State and county boundaries are shown. This figure is described in the main text. _____ 70

Figure 35: The average annual number of days $\geq 100^{\circ}\text{F}$ over the SPTC domain, based on future climate projections using the mid-range emissions scenarios. Left panel: Mid-century projections (2021-51). Right panel: Late century projections (2060-90). Interstate highways, State and county boundaries are shown. The results shown by this figure are described in the main text. _____ **70**

Figure 36: The average annual number of days $\geq 100^{\circ}\text{F}$ over the SPTC domain, based on future climate projections using the high emissions scenarios. Left panel: Mid-century projections (2021-51). Right panel: Late century projections (2060-90). Interstate highways, State and county boundaries are shown. The results shown by this figure are described in the main text. _____ **71**

Figure 37: Decadal climate projections for average annual number of days $\geq 100^{\circ}\text{F}$, shown here for Oklahoma climate division 5, which is central Oklahoma. The decadal periods include historical, ending 1980, 1990, 2000 for observations (grey), and climate model mean (yellow), Future ending 2030, 2040, 2050 (orange), 2070, 2080, 2090 (red). The solid bars are MACA, and the stippled bars ARRM. The range bars are the 5th-95th percentile range of all annual counts of 100°F days. The horizontal line is the number of 100°F days during 2011. The values at the top of the chart show (top) the average number years with 2011-like summers in each decade, and (bottom), the maximum number of 2011-like summers in each decade. Left panel: mid-range emissions, Right panel: high emissions. The results of this graphic are described in the main text. _____ **73**

Figure 38: Historical and future projections of the average onset and termination of 100°F days for a given year, based on all MACA and ARRM models used in this work. Bottom: 1970-2000, center: 2021-51, Top: 2060-90. The red box and dates depicted are the mean values, while the lighter pink shading denotes the 5th-95th percentile earliest/latest dates. Vertical dashed lines depict the equinox dates. Left panel: mid-range emissions, Right panel: high emissions. _____ **74**

Figure 39: Annual highest and lowest temperatures in the OKC area during the peak summer season (June-July-August) as simulated by climate models. The multi-model mean is depicted by the thin black line, and the model spread the shaded polygon. The thick dark grey and dark blue lines show the Maurer and Livneh observed temperatures respectively. Top panel: mid-range emissions, Bottom panel: high emissions. The model spread encapsulates the range of the historical observed conditions, indicating that the past variability is relatively well constrained. The trends depicted are discussed in the text. _____ **75**

Figure 40: 1 in 10-year 1 day return period precipitation events for Oklahoma climate division 5 (central Oklahoma) for Top: mid range emissions, and Bottom: high emissions. The return value in inches is shown by and in the bars, where grey is the observations (Livneh and Maurer), light blue is the historical period, and dark blue the mid and late century periods. The model spread is depicted by the range bars, and each individual model is displayed by a marker. The results shown by this figure are described in the main text. _____ **80**

Figure 41: 1 in 50-year 1 day return period precipitation events for Oklahoma climate division 5 (central Oklahoma). The layout of the chart is the same as that of Fig. 40, however the y-axis range has been expanded to account for the higher values. _____ **81**

Figure 42: 1 in 100-year 1 day return period precipitation events for Oklahoma climate division 5 (central Oklahoma). The layout of the chart is the same as that of Fig. 40. ___ **82**

Figure 43: Schematic representation of the change in return period frequency, based on 1-day multi-model mean return periods. The top shaded bar depicts the current estimated return periods and their precipitation values for 1 in 2 years to 1 in 100-year events. The middle panel shows how the return frequency of these events changes by later in the century for mid-range emissions, and the bottom panel is the same, but for high emissions. Return periods of 10 years or less approximately double in frequency (e.g., 1 in 5 year), while 1 in 50 to 100 year return intervals increase in frequency by a factor of 5-10, according to our estimates. _____ **83**

Figure 44: A ‘sensitivity matrix’ for central Oklahoma, including the Oklahoma City Metropolitan area, specifically examining temperature-related climate stressors and their potential impact on various transportation assets, including roads (paved, unpaved, asphalt and concrete), bridges (superstructure and substructure), rail (tracks, transit support infrastructure, power systems), and aviation (airports, runways, aircraft). The climate stressors examined include freeze thaw cycles, freeze thaw intensity (based on the temperature range of a cycle), extreme cold, extreme heat, mean summer temperatures, and temperature variation. The table (which is rendered as a figure here) identifies sensitive assets or activities, and approximates the degree of positive or negative impact based on the climate projections over the lifetime of the asset. The method used to construct this table, and its results are described in the main text. ___ **90**

Figure 45: As Fig. 44, but for precipitation-related climate stressors and their potential impact on various transportation assets. The climate stressors examined include winter weather frequency, winter weather intensity (the amount of winter precipitation associated with a given event), drought, and heavy precipitation. The table (which is rendered as a figure here) identifies sensitive assets or activities, and approximates the degree of positive or negative impact based on the climate projections over the lifetime of the asset. The method used to construct this table, and its results are described in the main text. _____ **91**

EXECUTIVE SUMMARY

Adverse weather poses multifaceted hazards to transportation safety and state of repair. In recent years there has been an increased awareness of the threats of climate variability and change on transportation. Climate change is leading to underlying trends in temperature and precipitation, which are likely to be outside of the range of historical conditions from which many design paradigms are currently based. Understanding regional climatic hazards is the first step necessary to adequately adapt to these changes and reduce the potential social, economic, and environmental impacts on the transportation system.

This project examines future climate scenarios for the South Central United States, focusing on transportation-relevant conditions that reflect extreme and impactful events that can stress transportation infrastructure, and affect safety. These include cold weather, winter precipitation, and freeze thaw cycles, but also heatwaves and heavy precipitation. Expert input identified from a transportation stakeholder survey motivated the focus on these variables. The survey also identified key metrics, thresholds, and preferred formats for data analysis and dissemination, and provided important perspective on current and anticipated challenges to using climate information in planning and decision-making. In general, additional climate data, including climate futures, was desired, but the use of this information can be impeded by its complexity, and incompatibility with existing standards.

A comprehensive climate data analysis was performed, using multiple statistically downscaled global climate models from two sources, a series of high-resolution historical observations and model products, and four emissions scenarios, the latter of which represent the projected magnitude of climate change. Using a large suite of data from multiple sources allows for an assessment of spread in climate projections, and therefore represents both the model central tendency for a projected trend, and a broader range of possible future conditions.

In Year 1, we focused on deriving key variables and trends using historical data. This included developing and validating a model and observation derived spatial dataset for freezing precipitation (freezing rain and sleet), available from 1979-2016. This climate-length dataset can be applied to evaluate existing winter weather hazards for a given region, and for retrospective case studies. Additionally, we use very high-resolution data (~1km) to construct freeze-thaw cycle spatial maps, climatologies, and trends between 1948 and 2015. This data, which in addition to graphics are also available in quantitative formats, provides an additional climate data source that can be used to assess current vulnerabilities of transportation infrastructure. Year 2 developed a future climate assessment encompassing all aforementioned weather and climate extremes. Trends, changes in frequency, and changes in intensity were examined for areas throughout the SPTC area of responsibility (DOT Region 6) for one historical period (1970-2000) and two future

periods (2021-51, or 'mid-century', and 2060-90 or 'late century'). In this report, we show examples of data output focusing on central Oklahoma. The work revealed:

- A decrease in winter hazards such as extreme cold, freeze thaw cycles, and winter precipitation. Each model magnitude differs, and the decrease is typically greatest later in the 21st Century, with high emissions of greenhouse gases. In such a scenario, winter temperatures in Oklahoma City, for example, become similar to present-day Dallas, and Dallas similar to present day San Antonio. Freeze-thaw cycles decline by 20% by mid-21st Century, and up to 50% by later in the century. Winter precipitation does not change discernably in intensity in most regions, but decreases in frequency, especially later in the century.
- An increase in hazards such as heat, drought, and heavy precipitation. The frequency of days above 100°F increase everywhere in the domain, by 200-400% by mid-century, and up to 800% by later in the century. Heatwave years analogous to that of 2011 in central Oklahoma become more common, and could be an average annual occurrence in Oklahoma later in the 21st Century. Extreme precipitation also shows a pronounced increase throughout most of the domain, based on return periods estimated from daily precipitation accumulations. The rate of change in extremes is greatest between the recent past, and mid-21st Century, and is less dependent on the emissions scenario and more dependant on the climate model. Events such as the 1 in 100-year rainfall could occur as often as 1 in 10-years within the next 20-50 years.

The report concludes by evaluating the confidence in these anticipated hazards, and including expert recommendations from within the transportation sector, such as current steps that other transportation agencies are taking to reduce their vulnerability. Links to some applicable tools and resources from credible transportation agencies and organizations are provided. Ultimately, the research has demonstrated that current infrastructure is likely to be benefitted over its lifetime by the reduction in winter weather and cold extremes, but also stands to be adversely impacted by the projected increases in extreme heat, and heavy precipitation. In either case, planners should be aware that the ongoing non-stationary nature of climate conditions in the SPTC region will require possible revision of design standards and paradigms so that critical long-duration infrastructure can meet its design life, maintain durability, and be cost-effective. This work provides the context, and some value-added data products, supplying detailed climatological information to aid regional vulnerability assessments.

1. INTRODUCTION

Weather conditions impact broad sectors of the transportation industry, including degradation to roadways and bridges, changes in traffic patterns, impacts on safety, and economic pressure due to potentially increased maintenance requirements (Meyer et al. 2013). Every year, extreme weather conditions lead to damage in one or other portion of the Southern United States, requiring additional maintenance, disbursement of emergency funds, and/or delays resulting in economic impact. While environmental conditions are but one of numerous factors influencing transportation, the majority of multi-year infrastructure requires engineering that confers protection against adverse risk associated with extreme and unusual weather. For example, developing durable construction materials that are economically viable and resilient to freeze-thaw cycles and high temperature, or by designing storm water infrastructure to operate to a certain extreme rainfall tolerance.

Assessment of climate-related risk to this point has been based on historical climate information from available datasets. While this provides a measure of recent conditions and potential vulnerabilities, the underlying climate system is not stationary. Human-contributed global climate change, associated predominantly with the burning of fossil fuels, has already become evident in the climate record. The United States nationally has observed an average annual temperature rise of nearly 2°F (~1°C) over the past 50 years, and an average 5% increase in precipitation. Changes in the frequency and characteristics of extreme events have been observed ([National Climate Assessment, 2014](#)). It is now known that climate change is contributing to the shift in the character of various extreme events regionally and globally, and this is expected to continue. This means that the historical records that many design paradigms are based on may no longer adequately capture the range of risks that new infrastructure, and those that use it, is likely to experience.

In order to help provide a 'road map' for how transportation-relevant weather and climate conditions are changing, it is useful to have reliable, regionally specific

information on historical climate, obtained from high-resolution datasets, and future trends, obtained from climate models. Valuable, but general, guidance on the plausible impacts of climate change on transportation are provided by the [Federal Highway Administration](#) (FHWA), the [Transportation Research Board](#) (TRB), and the [American Association of State highways and Transportation Officials](#) (AASHTO). These resources provide links to tools, information, and case studies that help transportation professionals understand why climate information is important and how it can be incorporated into the transportation planning process. Nonetheless, in order to provide more tailored and applicable information, climate trends should be evaluated on the regional to local scale, and for variables that are known to be impactful to the sector. Mills and Andrey (2002) in conjunction with the U.S. Department of Transport (DOT) in a collaborative interagency workshop suggested that a regional research approach was critical to have information specific enough for planning and adaptation. This contention was reaffirmed in 2013, as AASHTO hosted a symposium specifically addressing the impacts of extreme weather on transport (Meyer et al. 2013). Interregional differences in specific transport sensitivities were highlighted, as was the need to better understand regional risk factors.

Our work supports the vision of the [Southern Plains Transportation Center](#) (SPTC) in promoting 'climate-resilient' transportation by developing value-added climatological datasets and climate projections. This study develops an important component of the assessment of risk, which is to have regional, relevant, and accurate information on past and future trends in key variables. A particular focus of this work is to improve understanding of the climatological characteristics of winter weather in the region, and subsequently to identify whether, or the degree to which, winter weather-related transportation hazards will be ameliorated by climate change. Winter season hazards, including freeze-thaw cycles, extreme cold, and snow and ice storms, are associated with travel delays (Chin et al. 2002, OFCM 2002), accidents and fatalities, and costly maintenance. Ye et al. (2013) estimated that \$2.3 billion is spent per year nationwide on winter weather-related maintenance activities, such as salting, road clearing, and road surface improvement. Winter weather is anticipated to decrease during the 21st Century; however, the extent of this decrease, and other changes relating to winter weather precipitation types and intensity is not well understood. In addition, long-duration historical information for freezing rain in particular is difficult to find, particularly over a

broad spatial region. In addition to winter weather, temperature extremes and heavy precipitation have notable impacts to transportation, and these are also examined in this analysis. We use reliable, publically available historical and future climate datasets for this study, all of which are described in the report.

The subsequent sections provide a comprehensive description of the activities undertaken to develop value-added information, including datasets, and a description of climate trends for key parameters coupled with visualizations that depict these trends. We also examine climate projections specifically for central Oklahoma, including the Oklahoma City metropolitan area, generating a cursory climate-related sensitivity analysis for the area (e.g., based on the sensitivity matrix developed by Rowan et al. 2012). The information and output we have generated is designed to provide transportation planners with information for the SPTC domain that could assist in hazard planning, risk assessment, and other strategic planning activities that incorporate environmental hazard information. Furthermore, the information and data output from this work is intended to be a resource for transportation professionals who may wish to incorporate past and future climate information, where appropriate, into their planning process, which has been recommended by major federal highway authorities.

The area of study for which data were analyzed and developed is the SPTC domain of responsibility, including the states Oklahoma, Texas, New Mexico, Arkansas, and Louisiana, shown in Figure 1. For the sake of space, detailed climate assessments have not been provided for each state in this document. However, we will develop some state-by-state informational products, described toward the end of this report.

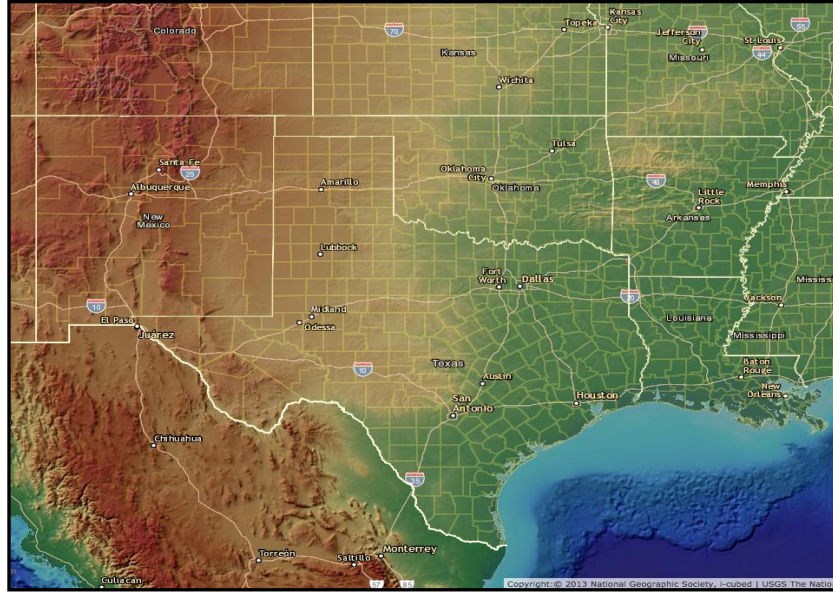


Figure 1: Map of the domain used in this analysis. All data was subset for this region, extending 110°W to 89°W, and 25°N to 40°N. Within the domain are the U.S. Department of Transportation Region 6 states of Oklahoma, Texas, Arkansas, New Mexico, and Louisiana. Image courtesy of ESRI-[ArcGIS](https://www.esri.com)

2. METHODS

2.1 EXPERT INPUT – STAKEHOLDER SURVEY

There is a tendency for disconnect between climate science, and the data generated by climate models or climate reanalysis, and other sectors where use of such information is important in adapting to or mitigating risk. Climate data are often not of a form or resolution that can be directly utilized by other tools and can require some advanced technical expertise. There is also the possibility of erroneously interpreting the data, or under-sampling the potential magnitude of future climate change. The temporal scales of climate change, being on the order of years to decades in the future, are generally perceived to be less valuable information relative to short-term concerns. The uncertainties posed by climate change, particularly for precipitation, also tend to be difficult to incorporate to the current paradigms of infrastructure planning. Since this project is attempting to at least understand, if not bridge, some of these gaps between climate science and transportation, it was important to receive input by the community on current hazards and whether or to what extent climate information is needed.

A survey entitled 'Weather and Climate data needs for Transportation,' was developed using 'Qualtrics' [software](#), which is an online tool for survey development, dissemination, and analysis. Co-PI Mullens attended trainings on utilizing this software, and in conducting human subject research, and obtained Institutional Review Board approval from the University of Oklahoma to conduct the survey. The survey asked a series of questions, including very basic demographic information, restricted to region (State, City), and type (job description) of work. Subsequently, participants were guided through a series of questions establishing and ranking the most hazardous weather conditions from their professional perspective, and assigning thresholds to hazardous temperature and precipitation conditions. The survey then asked respondents to evaluate whether or not climate data was useful to them, and what climate data resources they currently utilized. Those for whom climate data was not important were directed to exit the survey, and their opinions on climate data veracity and utility were gauged. For those who did indicate that they would use climate information, follow up questions asked for guidance on preferred data formats, data types, and data/information outputs. After a brief testing phase, where the survey was refined through the feedback of colleagues at the [South Central Climate Science Center](#), [Southern Climate Impacts Planning Program](#), and [Southern Plains Transportation Center](#), it was released to the broader community in September 2015 via the SPTC email list serve, and closed December 2015. In total 57 respondents accessed the survey, with 38% partial completions and 62% full completions. Efforts to increase participation were made by contacting each State Department of Transportation in the five-state area; all but one did not respond to our requests. We suspect that this is an inherent limitation in attempting to survey respondents with whom a prior relationship has not been established. Despite the comparatively low sample size, some highly useful information was gathered from participants, which is summarized below. The complete list of survey questions is provided in the appendix (Sec. 7.5).

(i) Demographics

The majority of those surveyed were transportation and engineering researchers (46%), followed by engineers in construction (30%), maintenance (26%), infrastructure (22%), and other (22% did not fit in any of the listed categories). Many respondents fit

into more than one category. Additional respondents were listed as in planning, operations, and urban design. Figure 2 below shows demographics by employer. Ten respondents declined to provide job information. The majority of respondents were in Oklahoma (80%), followed by Texas (6%). There were 1-2 responses for each remaining State (Arkansas, Louisiana, New Mexico). Thirteen respondents did not provide their location.

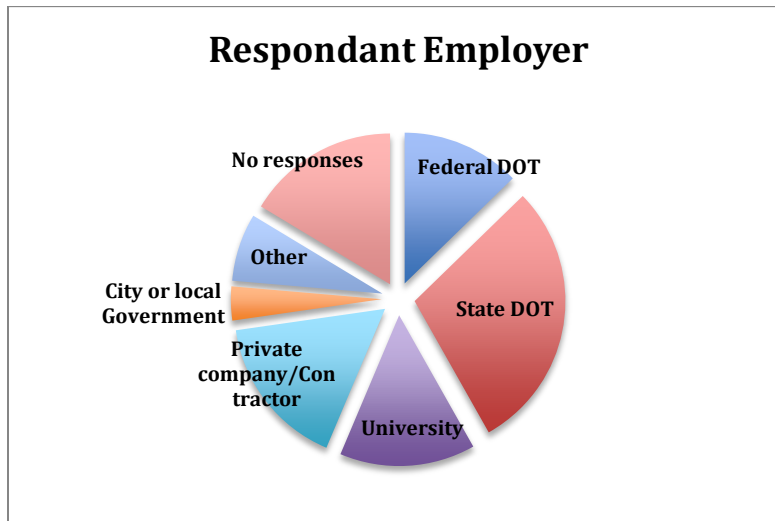


Figure 2: The main employers of the survey respondents, which consisted of State DOT (39%), Federal DOT (17%), University researchers (20%), Private companies (22%), City or local government (5%), and other (10%). Respondents could pick multiple responses.

(ii) Weather and climate hazards and thresholds

Two questions asked respondents to rank various weather and climate variables, such as extreme heat, cold, precipitation, snow, freeze-thaw, etc. The first asked: *“Based on your experience, please rank weather conditions that most frequently and/or significantly impact surface transportation in your region...”* A follow-up query then reframed this in the context of ranking the variables and indices most desired from climate data. Table 1 summarizes this information, expressed by ranking the variables based on the desire for climate data. Not all participants completed this question, and the number of responses varied depending on the variable, with a mean of 34 (60% of surveys started). This suggests that some respondents chose to skip a variable for which they could not estimate its impact, or it was not applicable.

Ultimately, as depicted in the table, the top 10 ranked variables of concern were (1) heavy rainfall and flooding; (2) snowstorms; (3) extreme heat or maximum surface temperature; (4) freeze-thaw cycles; (5) freezing rain; (6) wind speed or high wind; (7) cold extremes or minimum surface temperature; (8) thunderstorms; (9) tornado; and (10) heating degree days. Since the majority of respondents were situated in Oklahoma, the ranking of these hazards reflect predominantly inland hazards common to the State. Other states and locations would likely alter these ranks to some degree. This particular year (2015) was also marked by excessive precipitation in Oklahoma, cumulating in

Table 1: Survey participants were asked to rank (1=lowest concern, 5 = highest concern) their level of concern regarding various weather and climate extremes. The center column shows the percentage of responses that indicated high (3-5) concern. The response rate varied depending on the variable, with a minimum of 24 (tropical storm) to a maximum of 37 (heavy rainfall), with a mean of 34 (60% of surveys started). The right column shows the number of responses reflecting a desire for more climate data (trends, statistics, projections). Variables are ordered in the table in decreasing order of preference based on these two measures.

Variable	% indicating high concern presently	Number of responses indicating desire for climate information
Rainfall/flooding	90	24
Snowfall/snowstorm/blizzard	64	19
Maximum air temperature at surface/extreme heat	49	17
Freeze-thaw cycles	62	17
Freezing rain/drizzle/ice storm	72	15
Wind speed/high winds	44	15
Minimum air temperature at surface/cold extremes	30	14
Thunderstorm	50	11
Tornado	67	11
Heating degree days		10
Humidity at Surface	13	10
Cooling degree days		8
Solar radiation		8
Drought	30	7
Fog		6
Tropical Storm/Storm surge	38	8
Other		3

multiple flooding events, and two flood-related Federal disaster declarations (Oklahoma Climate Survey 2015, FEMA). As a result, heavy precipitation was particularly salient, potentially contributing to its prominence in both queries. The survey also confirmed that winter-season variables are consistently among the top concern, further justifying the initial focus for our research.

Once key variables were established, participants were asked to disclose a typical threshold used by their profession to distinguish hazardous conditions from normal operation for hot and cold temperatures (in °F), and rainfall, snow, and ice (inches or return periods). Many left this question blank, as they were directed to do if they did not know or have an applicable threshold. Figure 3 below shows the results for hot and cold temperatures, based on 20 responses, showing that 100°F (38°C) was the most commonly cited threshold for hot temperatures (followed by 110°F), and 32°F (0°C) for cold temperatures (with a second common response of 20°F or less). Thresholds may be dependent on location, for example, respondents in the more arid southwest, (such as Lubbock and El Paso, TX, n=3) supplied lower minimum temperatures (0-10°F), and higher heat values of 110°F. A respondent from Baton Rouge, LA suggested a heat threshold of 105°F, and prioritized concern and data needs toward coastal hazards, such as tropical storms, sea-level rise, and flooding. Precipitation thresholds were generally more mixed, and respondents offered a wide range of values. For those in areas that experience freezing rain and ice storms, the majority of respondents (n=23) suggested that only a small amount (<0.1 inch) is detrimental, with the second most prevalent response being at or greater than 0.25 inch – the current National Weather Service criteria for an Ice Storm. Snowfall values of 5 inches or less were noted by nearly 75% of respondents (n=24), with a few supplying much higher amounts, such as 10 inches or greater. The respondents (n=5) who provided higher snow depth thresholds typically worked in infrastructure and construction (80%). Rainfall thresholds (n=24) were particularly varied. 42% used a rainfall rate of typically 1 inch per hour or more. 30% used a static threshold above zero. Most common was 0.5-3 inches (n=5), followed by 5-8 inches in a single event or 24-hours (n=4). Two respondents gave return period thresholds of 1-in-50 year, and 1-in-100-year events. Our results suggest that precipitation thresholds are highly contextualized to the sub-discipline and location, or the application of this information, e.g., for example highway safety, versus culvert

design. Subsequently, it is difficult to generalize precipitation information derived from climate data.

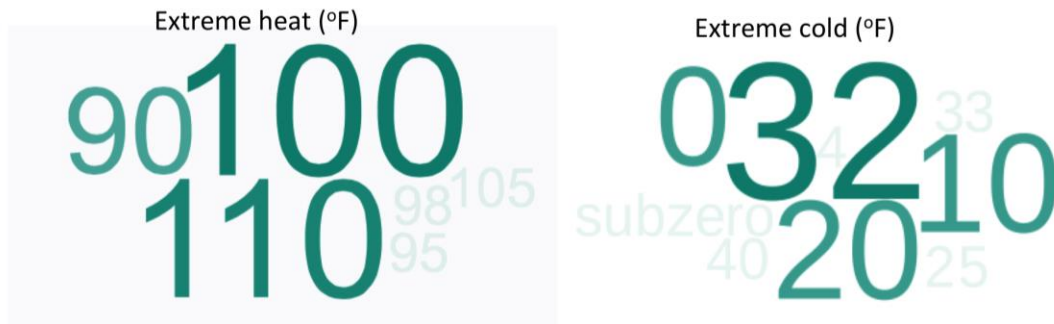


Figure 3: ‘Word maps’ depicting the type and frequency of responses to questions regarding hot and cold temperature thresholds, as described in the Section 2.1(ii) text. The larger the font, the more responses for that given threshold value. On the left is extreme heat, and the right, extreme cold.

(iii) Perspective of climate information

Survey participants were asked about their current use of climate data. Responses (n=27) indicated that National Weather Service (NWS) observations were most commonly used (70%), followed by the Oklahoma Mesonet (56%), and observations archived at the National Centers for Environmental Information (formerly known as the National Climatic Data Center, 44%). Participants’ noted additional sources tailored more specifically to transportation professionals, such as Iteris, return period atlases, and USGS flood databases. Most respondents who completed the survey (80%) suggested that they would be interested in using climate data and information further. However, one respondent did express a caveat:

“Generalizations are made based on personal and professional experience that is not easily translate able [sic] to weather data. I have personally used information from NOAA to determine general patterns on rainfall to project for future trends but this is rare. Generally researching actual data is not considered practical in Oklahoma. Unless it’s a standard it is not used.”

This suggests that transportation professionals, particularly those working within state and local government, typically employ data that have been used in the past or are part of an approved standard for climate measurement, thereby having limited ability to incorporate new data or information.

Respondents' perception of the reliability of climate data was ascertained by asking participants to agree or disagree with a series of statements. Figure 4 below shows these responses for (a) respondents who were open to using climate data, and (b) those who did not want to use climate data. Values of 5 (1) indicate strong agreement (disagreement) with each statement, with a value of 3 being neutral (neither agree nor disagree). There was a clear contrast between users (and potential users) versus non-users (>1 point change) for three particular statements:

(1) *'Use of climate data is not a current priority'*. Non-users agreed with this statement, whereas users did not, on average.

(2) *'Spacing between data points is insufficient to generate decision-relevant guidance'*. In other words, the data was too coarse to resolve important features needed in transportation activities. Non-users agreed to strongly agreed, while users were generally neutral.

(3) *'I don't know where to locate useful resources'*. Non-users agreed with this statement, while users were neutral on average.

There were less significant differences between users and non-users for the other statements. Notably, both parties agreed that climate data is typically not compatible with their software and tools, and had some reservations on the reliability of climate data and projected trends. They also were neutral-to-agree that the current information is lacking in terms of the quantity or types of variables provided. The respondents were offered the opportunity to provide further feedback. Below are three particularly noteworthy responses:

"Climate data is frequently important in traffic safety analysis, but we do not have enough staff to take advantage of it."

"There hasn't been serious effort to incorporate this data into the transportation planning process [in our State]."

“I am relatively new to the world of DOT's and civil engineering. However, in my two years, it seems as though civil engineers and professors of civil engineering do not like to look outside their field for expertise, even to fields like meteorology and climate. Nationally, of course, USDOT and AASHTO are aware of the challenges posed by climate change, as is the SPTC, but collaboration between climate experts and civil engineers still seems relatively small compared to the potential benefit. Civil engineering has a number of mathematical formulae for estimating the effect of weather on infrastructure (bridge and drainage design) and on crashes (highway safety manual), but these tools are not particularly helpful to understanding the big picture implications of increased numbers of extreme weather events or to understanding the big picture in how to prevent infrastructure damage from weather.”

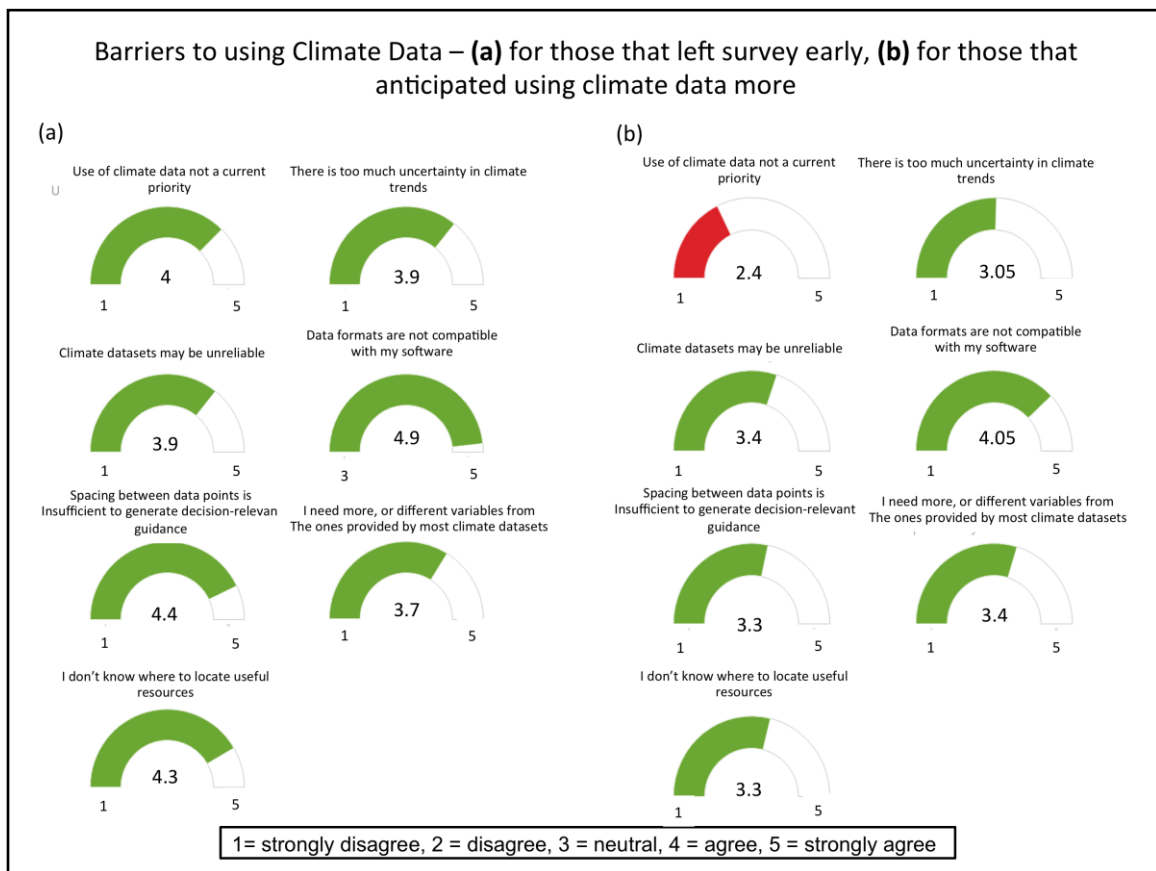


Figure 4: A gauge chart depicting the responses of participants to possible barriers in using climate information, the result of which are discussed in Section 2.1(iii). On the left panel a, are the seven respondents who indicated that they do not desire more climate information. On the right (panel b) are the responses of those who indicated that they would want more climate data. The response to each sub-query is shown in the chart as an average number between 1 and 5, where 1 (5) is strongly disagree (strongly agree) to a given statement.

(iv) Usable output

A final series of questions asked respondents to provide opinions on how data and information is best disseminated. In other words, what are the best ways to ‘package’ data and information that are more utilizable and relevant? Firstly, respondents were asked to choose the most useful options for *data and information packaging, i.e., data formats*. The results are shown in Figure 5 (n=24 responses). There was an even split between participants that would accept data in the form of graphics, tables, and other summarized resources, such as information sheets, that could be accessed (45%). A further 40% indicated that raw data that are spreadsheet readable or available in GIS would be most helpful. Raw data simply deposited to a web portal were generally slightly less useful to this respondent group.

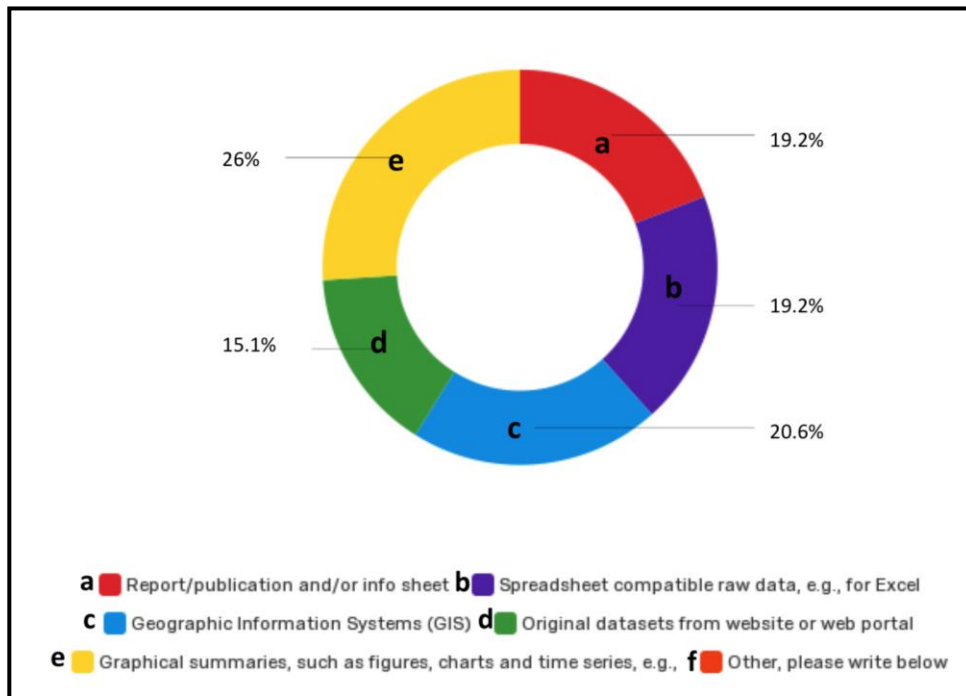


Figure 5: A pie chart showing how respondents would prefer output climate data and information. The breakdown was as follows: 26% graphical summaries, 21% GIS, 19% report or information sheet, 19% spreadsheet compatible raw data, 15% original data from web portal.

In addition to how data are packed, the way data are to be *displayed* was also ascertained, shown in Figure 6. This information assists our analysis, and allows us to better tailor graphical or tabulated output to end-users. In general, results identified that websites consolidating climate information and resources are most useful (27%),

followed by graphics that depict a mean and spread of climate trends from multiple datasets or models (19%), and probabilistic likelihood of a future climate state (18%). Direct communication with scientists was not considered useful by most (only 5%). One respondent commented that trend information was “*captivating*”, and that cases of existing conditions (perhaps relating to climate variability), and information on technologies that currently assist in mitigating vulnerabilities to extremes would be helpful.

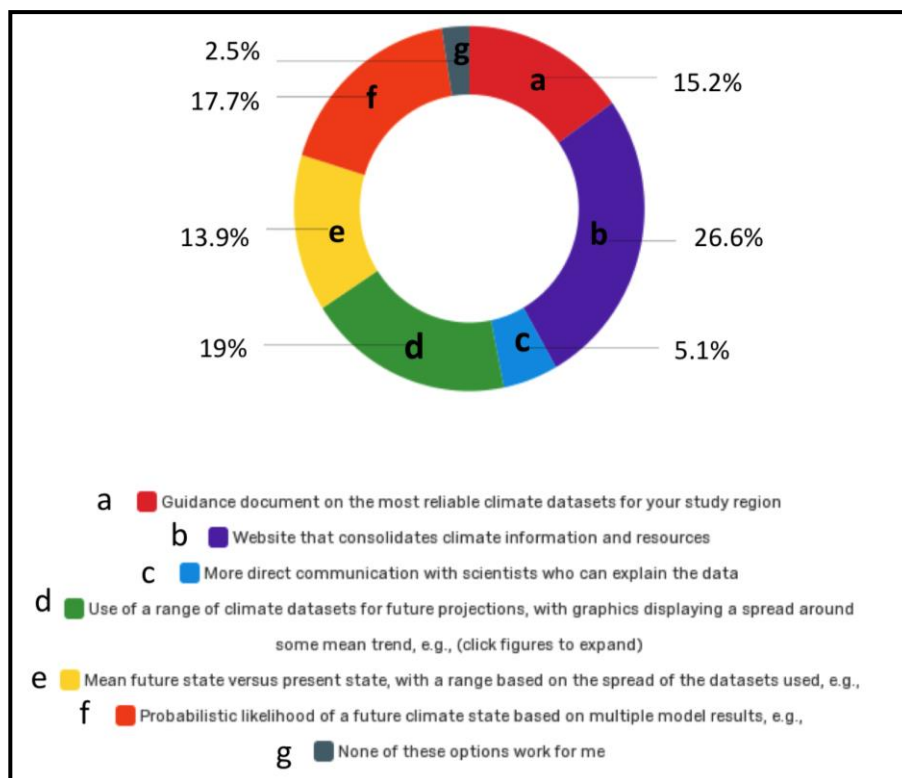


Figure 6: Pie chart describing the preferred formats for presenting or communicating climate data. The responses were: 27% for website that consolidates information, 20% graphics that use a spread of models (e.g., time series and range), 18% probabilistic likelihood of future climate state, 15% guidance document on reliable datasets, 14% mean future state compared to present state (and range), and 5% more direct communication with climate experts.

(v) Summary

The responses to our survey have provided highly useful guidance for this project and can be used by others seeking to better tailor climate data guidance and other tools or resources to the transportation community. This survey was limited in its reach, and so the number of responses was low. As a result, testing for the statistical significance of

responses, and other higher-level analyses with this information was not considered.

The survey information is used in the following way throughout our project:

- To develop thresholds and metrics for weather and climate variables that reflect those provided (e.g., for freeze-thaw days, hot and cold extremes).
- To design interpretable and useful graphics which display our results.
- To output raw data in spreadsheet-readable formats, and to work toward GIS-readable datasets.
- To recognize the caveats of this project in fully addressing data concerns and institutional limitations in data usability. Hopefully, over time, and with more relationship building between these communities, these critical challenges can be more effectively addressed through co-production of knowledge/information/data.
- To design a series of state-by-state information brochures that detail historical climate trends, and future climate impacts for the region, as well as highlighting useful resources, and summarizing case studies of current adaptation measures. This is similar to current informational sheets provided by the Federal DOT and FHWA, but injects substantially more regional detail, and more tailored information. These documents have a planned release date of late summer 2017.

2.2 CLIMATE DATA

(i) Historical 20th and 21st century weather and climate

For this project, historical data were restricted to use of 'gridded' datasets of at least 30-year duration. Gridded refers to regular spacing between data points, typically in degrees or kilometers. Data are often gridded through interpolation and statistical techniques that adapt unevenly spaced station-based data to a regularly spaced grid, or from model-derived data that is output onto a grid. The use of data spanning 30 years or greater allows for analysis of climate trends, since we are sampling a greater diversity of weather and climate variability over years and decades, while also increasing the sample size of extreme events.

Table 2 shows the historical datasets used for this work and the context in which they were used. The data source is also provided; all data used in this project was publically available, meaning that it was free and downloadable from the web (although

some data may require registration to access). Documentation on these datasets, their development, and any caveats is also provided at the source sites.

(ii) Future climate projections

Climate models represent complex Earth system processes through mathematical equations that describe the behavior of heat, solar radiation, momentum, and other physical mechanisms that influence Earth's climate system. In contrast to numerical weather prediction models, global climate models (abbreviated GCMs) must represent processes that impact the environment over decadal to centennial time scales. This includes ocean circulation, land-surface feedbacks and changes, biosphere, and the cryosphere (ice). Climate models are able to represent how climate can be influenced from both natural circulations and other internal forcings such as volcanic eruptions. They can also project the changes in climate-system properties, such as temperatures and precipitation, resulting from radiative imbalances associated with greenhouse gas emissions. A climate model cannot provide a 'forecast', i.e., a weather type on a particular day; however, it can represent the evolving trends and changing statistics of weather conditions with time.

There are a number of major modeling centers around the world that have the capacity to develop and run GCMs. In the United States, for example, this includes the [National Centers for Atmospheric Research](#) (NCAR), and NOAA's [Geophysical Fluid Dynamics Lab](#) (GFDL). These centers participate in a regular set of coordinated climate model experiments, with data made available every several years. The most recent of these comprehensive experiments was the '[Coupled Climate Model Inter-comparison Project Phase 5](#)' (CMIP5). This project involved the use of over 30 climate models from 20 modeling centers. The data have been comprehensively evaluated regionally and globally (e.g., The Intergovernmental Panel on Climate Change, IPCC 2013).

For regional climate change projections and for decision-relevant information, GCMs tend to be limited in their utility. GCM data are spatially coarse, with a single data point ranging from every 100-300 km. Furthermore, GCM temperatures and precipitation can be biased, so they do not represent the historical climatology you would expect when looking at observations for a given region, though their projections on the continental to global scale remain useful in this form. In order for GCM data to be valuable for local decision-makers, such as transportation planners and engineers, two main things must

happen; Firstly, the data must be *bias corrected*. This is done through statistical techniques that adjust the distributions of the GCM data to be reflective of the historical observations for a given location or region. Secondly, the data must be *downscaled*, meaning that its horizontal resolution (number of data points in a given area) must be increased. There are a number of well-established statistical and model-based techniques that can adjust GCM data in these ways. These techniques do not artificially impose or remove trends associated with climate change; trends stay fundamentally true to the GCM projection. Some web links to information on these techniques are provided in the appendix to this report.

For this project, we used two statistically downscaled, publically available datasets. Table 3 shows the datasets used and their sources. The first is ‘MACA’ or ‘multivariate adaptive constructed analogues’ (Abagatzou and Brown, 2012), which refers to the statistical downscaling method used. This project used MACAv2Livneh, which downscaled 20 CMIP5 GCMs to a 6.6 km spatial resolution and includes daily projections for temperature, and precipitation. A few other variables, such as humidity, winds, and solar radiation, were also available but not used for this project. From this dataset, 15 of the 20 models were used. Five models were excluded based on their poor simulation of past climate in the south central United States (D. Rosendahl, personal communication, not shown). The second dataset was ‘ARRM’, or ‘asynchronous regional regression model’ (also a reference to the technique used), developed by Stoner et al. (2013). This dataset had a smaller sample available, and the base data were an older form of the coupled model experiments (CMIP3). This dataset was used to provide another set of models that were downscaled using a substantially different statistical technique (regression methods, as oppose to weather pattern typing used in MACA). This additional selection increases the breadth of the model sample, and it accounts for some uncertainties contributed from newer versus older model inter-comparisons, statistical methods, and emissions pathways (see next sub-section). In all, up to 21 models were utilized for this analysis with a maximum temporal range of 1950-2100.

(iii) Background on emissions scenarios

One of the most pivotal aspects of representing future climate is to make effective projections of greenhouse gas emissions, as they are the fundamental driver of human-contributed climate change. To do so, assumptions regarding how human

societies will grow technologically, socially, and economically are required. For CMIP3, these representations were in the form of 'SRES' scenarios (Special Report on Emissions Scenarios, Nakicenovic et al. 2000). These scenarios developed fixed assumptions, or 'storylines' regarding emissions growth, associated with the above considerations. Projected trends in the various assumptions were quantified and run through integrated assessment models to generate the final set of quantitative emissions projections employed in the models. Scenarios were grouped into 'families'. For example, the 'A1' scenarios describe a world with varying degrees of rapid economic growth, a population that peaks in the mid 21st century, and a subsequent introduction of more efficient and advanced technologies in the late 21st century. The highest emission scenario 'A1FI' suggests current and future fossil fuel-intensive energy production and use. The 'B1' scenarios experience the same economic and population trajectories as A1, however the global economy transitions more toward service and information, and away from material-intensive activity. There is increased use of clean energy and resource-efficient technology in this scenario.

For the most recent climate assessment (CMIP5), the scenarios were adjusted significantly, now denoted 'Representative Concentration Pathways' (RCPs, Van Vuuren et al. 2011). They no longer employed fixed assumptions between populations, economies, etc. and emissions. Instead, they focus on developing scenarios for the degree of *radiative forcing* contributed by a variety of greenhouse gases. The same radiative forcing can be associated with multiple different emission scenarios involving socio-economic, technological, and environmental factors. For CMIP5, users can identify how various policy options would be consistent with each RCP. For example, by examining the different energy/technology/economic solutions that would result in a temperature change of less than 3°C by 2100 (approximately equivalent to RCP4.5). There are four RCPs: RCP2.6, RCP4.5, RCP6.0, and RCP8.5, with the numbers representing the anthropogenic portion of the total radiative forcing (in Watts per square meter) at the top of the atmosphere. The higher values denote greater radiative forcing, and thus more substantial climate change, with RCP8.5 describing a fundamentally carbon-intensive future.

Figure 7 shows the projected growth in carbon dioxide (CO₂) emissions associated with the various SRES and RCP scenarios. Here, we used two equivalent

SRES and RCPs, RCP4.5 and SRES B1, which we call 'mid-range', and RCP8.5 and SRES A1FI, which are 'business as usual' or 'high' emissions. As shown by the figure, the difference between RCP and SRES for these options is minor in terms of future emissions, and we can therefore combine the models with these scenarios.

Using more than one scenario provides a wider range of anticipated climate change projections. At this stage, it is unknown how emissions will evolve decades into the future. The Paris Agreement (2015), and continuing United Nations negotiations aim to keep the global temperature rise to 1.5°C or less (UNFCC, COP21, 2015), following closely to RCP2.6. However, a willingness to pursue this target does not necessarily translate to its successful implementation, so decision-makers should be aware of the potential impacts of climate change should current trends in greenhouse gas emissions continue with limited or no abatement.

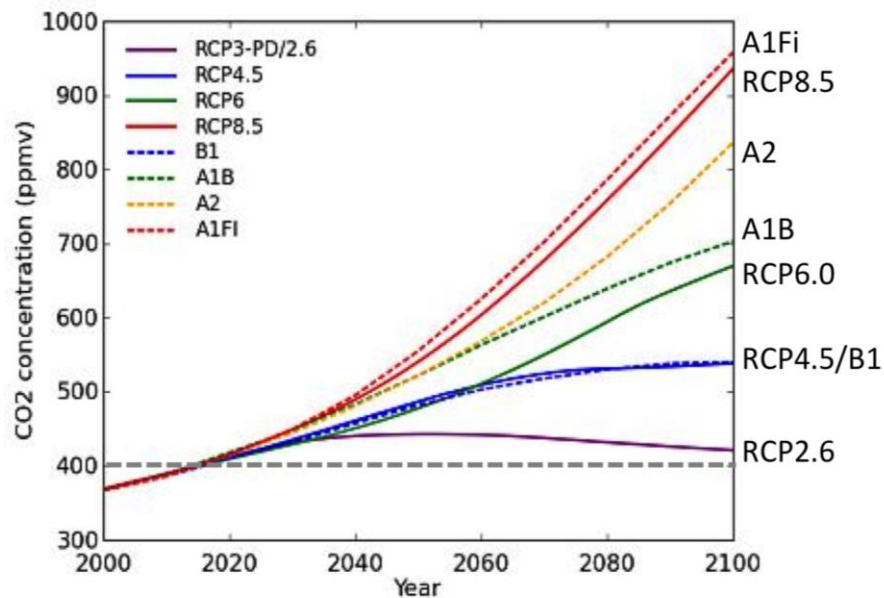


Figure 7: Comparison of projected carbon dioxide concentrations associated with SRES emissions scenarios, used in CMIP3, and representative concentration pathways (RCP), used in CMIP5. The selected RCPs/SRES in the mid-range (RCP4.5/B1) and high categories (RCP8.5/A1FI) both display similar carbon emission pathways to each other, meaning that they can be used in the same ensemble for each respective emission category. The grey line shows the 2016 concentration of CO₂. Base image from 'Climate Change Australia'. Data from the Potsdam Institute.

2.3 APPROPRIATE SELECTION OF CLIMATE MODELS

This project adhered to the wisdom put forth by climate scientists regarding careful data selection to account for uncertainty in future projections. A number of options are available to end-users when evaluating if or how climate data can be incorporated into their research:

(i) Using a single climate model

Researchers or decision-makers sometimes utilize output from a single climate model, which is more efficient if a project is resource- or time-limited. However, as will be demonstrated later in this report, different climate models can produce very different future climate states from the same scenario. This result is because each model represents the response of the climate system to external and internal forcing differently. Some are more sensitive to greenhouse gas radiative forcing than others, which will result in a greater degree of warming. While most climate model architectures are similar, various parameters and processes are constructed differently. It is therefore not recommended that only a single model be used. This advice is particularly true for examining trends in regional precipitation, which are more uncertain than temperature trends.

(ii) Using existing datasets that best conform to a certain software or application

Particularly when applying information across disciplines, use of a well-known software or tailored application is beneficial in making data more accessible to end users. The U.S. Federal Highway Administration (FHWA) has developed tools that aim to allow transportation professionals better access to future climate projections, such as the [‘CMIP5 climate data processing tool’](#), and [‘vulnerability assessment scoring tool’](#), both macro-enabled excel-based programs. In addition, extensive resources on climate impacts, and reports from pilot projects, have provided some detailed resources on using climate information in planning. Further initiatives have attempted to apply climate data in urban flood modeling (e.g., Rosenberg et al. 2010) or in predictions for pavement quality (e.g., the ‘enhanced integrated climate model’, Ongel and Harvey, 2004). Where models have been developed from historical station-based data, it can be difficult to

adjust these to incorporate climate change data, as the latter often have fewer variables and only daily temporal resolution, whereas traditional pavement or flood models may require sub-daily information and non-standard variables (e.g., solar radiation, humidity, evapotranspiration, soil type).

For this project, we recognized the benefit of the tools developed by the FHWA; however, we did not apply these here as our goal was to create a series of spatial datasets, as opposed to analyzing output primarily designed for point locations. Furthermore, the toolkit had a more restrictive pre-defined series of variables, whereas this work required the freedom to define our own metrics and indices from the information provided by our survey, and other expert input. Finally, we were able to examine a greater range of data options, and provide some additional regional datasets and resources to expand upon those currently available.

(iii) Using a range of climate models

Many climate change analyses now utilize multiple climate models, which provide a greater range of plausible climate futures, as simulated by GCMs. The optimal number and range of models to use often is highly dependent on the region, research activity considered, and the resources available. For projects where resources require constraining the number of GCMs to a minimum, it may be useful to consult with experts regarding the choice of models that best reflect the climatology of the region, e.g., Rupp et al. 2013. For larger model ensembles, there has been discussion amongst scholars as to whether or not to weight models by their historical veracity, or to ascertain how many models are required to capture the spread of uncertainty (e.g., Tebaldi and Knutti 2007, Weigel et al. 2010, Knutti et al. 2010). In general, research has shown that the use of several models outperforms using only a single model, with respect to the ensemble mean projection. The effect of weighting models by their historical performance may not provide discernable benefit over a suite of equally weighted projections. For this work, we weight all model data equally. We utilize the ensemble mean, particularly for the spatial graphics shown in later sections. However, gauging the spread of the model solutions should be considered, particularly for decisions that involve understanding how extremes may change in the future.

(iv) Using a range of models across different downscaling methods

It is common for regional applications to utilize data that have been downscaled from a single downscaling method. Using multiple models samples the variability amongst GCMs. Nonetheless, the downscaling method is likely to also create some degree of uncertainty in the projection, with different methods yielding slightly different results, particularly at the extremes (e.g., heat waves, cold waves, and heavy precipitation). Uncertainties due to downscaling methods have generally been less studied than those resulting from GCMs, and so the degree to which the downscaling method contributes to uncertainty is it is not fully understood. However, some studies have suggested that the uncertainty contributed by these different approaches could be significant when using the data for impacts assessments, specifically those that are sensitive to extremes, such as hydrologic changes (e.g., Sunyer et al. 2012). Users of these data may also need to consider that downscaling techniques can generally be grouped into ‘families’ of similar methods, with some methods being updates and revisions to prior approaches. This is true of the constructed analogues methods ‘MACA’ and ‘BCCA’. MACA represents an improvement over certain approaches in BCCA (particularly for extreme precipitation), while the newest approach ‘LOCA’ suggests improvements over MACA in certain aspects (Pierce et al. 2014). Other common methods include quantile mapping and regression (e.g., ARRM) approaches, with the most basic (not recommended) using simple adjustment for regional climate (i.e., the ‘Delta method’). Our choice to employ ARRM with its lower sample size and older form, as oppose to BCCA (used in the FHWA toolkit as of 2016) was based on the fact that BCCA and MACA possess substantial similarities, whereas ARRM and MACA are different techniques entirely. ARRM is currently in the process of being updated and re-run with CMIP5 datasets; however, we were not able to access these newer data, due to be released during 2017. The appendix provides brief information on publically available statistical downscaling methods.

Table 2: Publicly available historical climate datasets used in this analysis. Their sources and use are briefly summarized in the table, along with the temporal length of the dataset (all have at least 30 years of data), and their spatial resolution (the distance separation between data points, in kilometers)

Dataset	Temporal and Spatial Range	Uses in this project	Source/Access date (approx.)
North American Regional Reanalysis (NARR)	3-hourly, daily, monthly, 1979-present, 32 km grid	Deriving freezing precipitation and snow frequency, and liquid water equivalent.	NOAA Earth System Research Lab. Accessed March 2015, updated October 2015.
Topographic Weather (TopoWx)	Daily, 1948-2012, 800m grid	Freeze-thaw cycles	Jared Oyler University of Montana Accessed April 2015
Daymet	Daily, 1980-present, 1km	Freeze-thaw cycles. Information on extremes during 2015 (precipitation), and 2011 (heat)	NASA & Oak Ridge National Lab distributed active archive center Version 3
Livneh	Daily, 1950-2005 (can extend from 1915-2011), 6.6 km	Hot and cold temperatures, freeze thaw cycles, heavy precipitation, winter precipitation. Used for climate model historical verification.	NOAA Earth System Research Lab. Livneh et al. (2013) Accessed August 2016
Maurer	Daily, 1950-1999, 12.2 km	As Livneh	Ed Maurer personal webpage Maurer et al. (2002) Accessed April 2016
Climate Prediction Center Unified Gauge	Daily, 1948-present, 0.25° (~28 km)	Precipitation proximate/during freeze-thaw cycles	NOAA Earth System Research Lab Accessed October 2014.

Table 3: Publicly available statistically downscaled climate model datasets used in this analysis. Their sources and use are briefly summarized in the table, along with the temporal length of the dataset (all have at least 30 years of data), and their spatial resolution (the distance separation between data points, in kilometers). The list of models used is included in the dataset/models column.

Dataset/Models	Temporal and Spatial Range	Uses in this project	Source
MACAv2LIVNEH- Consisting of the following CMIP5 models: <i>BNU-ESM, CanESM2, CCSM4, CNRM-CM5, CSIRO-Mk3-6-0, GFDL-ESM2G, HadGEM2-CC, HadGEM2-ES, Inmcm4, IPSL-CM5A-LR, IPSL-CM5A-MR, MIROC5, MIROC-ESM, MIROC-ESM-CHEM, NorESM1-M</i>	Daily data, 1950-2100, 6.6 km	Hot and cold temperatures, freeze thaw cycles, heavy precipitation, winter precipitation (the latter a proxy measure based on daily surface temperature)	John Abagatzou, Katherine Hegewisch University of Idaho Link
ARRM – consisting of the following CMIP3 models: <i>HadCM3, GFDL-CM2.1, CCSM3, PCM (A1fi only), CNRM (B1 only), ECHAM5 (B1 only), CGCM3-t63 (B1 only)</i>	Daily data, 1960-2100, 12.2 km	As MACA	Katherine Hayhoe, Anne Stoner, Texas Tech University Link

2.4 DEFINITIONS OF INDICES AND VARIABLES

The weather and climate variables that were assessed in this project were initially defined in our summary of survey results (Table 1). Here, we provide a definition of each metric, and a brief rationale for the thresholds used.

(i) Freeze-Thaw Cycles

The basic definition of a freeze-thaw cycle (FTC) is a day with a maximum temperature (T_{\max}) greater than 32°F (0°C) and a minimum temperature (T_{\min}) less than 32°F. The data available are for surface air temperature, typically referring to a measurement height roughly 2m above ground level. Therefore, the freezing level at this height may differ from road surface freezing. Nonetheless, data limitations preclude deriving a true ground surface temperature. Freeze-thaw damage may be exacerbated by larger temperature swings, and so a second definition is employed to account for a more substantial freeze-thaw event. This ‘enhanced freeze thaw cycle’ or EFTC was defined by Haley (2011), and refers to a freeze thaw day where T_{\max} greater than or equal to 41°F (5°C) and T_{\min} less than or equal to 23°F (-5°C).

(ii) Winter Precipitation

Winter precipitation, in the form of ice and snow, can be difficult to measure. Long-term records of precipitation type are typically restricted to ‘first-order’ National Weather Service stations situated in major cities (Mullens and McPherson, 2017). Our goal was to provide a spatial dataset that ‘filled in’ some of the data gaps that exist between these *in-situ* stations, particularly for freezing precipitation (freezing rain and sleet), where records are more limited than snow (see Year 1 activities, below). Because the datasets used to derive freezing precipitation are both model-derived and observation-derived, the precipitation amounts (expressed as a liquid water equivalent) could not be directly translated to estimates of ice accretion, or snow depth. Thus, we infer the *presence and frequency* of winter precipitation from the number of times ice or snow was identified from the dataset over a given day, month, or year (the minimum time resolution was 3 hours for historical data and daily for future projections). The *amount* of winter

precipitation is calculated from the total liquid water equivalent (LWE). However, while more LWE implies a higher magnitude event, there is not a simple or direct conversion of LWE to snow amounts or ice accretion. Historical datasets split winter precipitation into ice and snow; however, future datasets include surface-based precipitation only, precluding the delineation of phase types (further explanation provided in Year 2 activities). In this case, winter precipitation is simply defined as each day and daily LWE where T_{\max} is less than or equal to 32°F.

(iii) Cold extremes

The frequency, duration, and magnitude of cold temperatures are often evaluated by the atmospheric science community through the use of percentile anomalies. These anomalies express the frequency (duration or magnitude) relative to a base climatology, such as the 30-year mean temperature for a given day, week, or month. While these definitions are useful, from the perspective of revealing the statistically rare events, we opt to use definitions that will be more easily interpreted and relevant. Other than the freezing-point threshold, there was no consistent definition for an adverse cold temperature extreme, based on our survey. Thus, we calculated frequencies of days with T_{\min} below 25, 20, and 10°F, and examined the trends in the lowest 0.1% of values.

Unfortunately, none of these values individually served to give a complete picture of the changing facets of cold temperatures in the region. Thus, we defined a series of thresholds for cold temperatures and freeze-thaw cycle frequency, and assigned a numerical value to each threshold, from 0 to 5. The numerical value corresponded to various ranges of the frequency and magnitude of cold conditions in a given region. Subsequently, the average numerical index value of each parameter provided a measure of the 'cold climate class' of a given location within the SPTC domain, with a higher value reflecting a cooler winter climate. This class is the 'typical' climatological condition experienced by a given location over a 30-year period. Table 4 defines these parameters and thresholds. The rationale behind this classification is to provide users with a visual representation of their climate region, with respect to cold temperatures. This then allows for better interpretation of how climate change impacts the cold temperature magnitude and frequency at a given location, shown in the results section.

(iv) Hot extremes

While the focus of this work was primarily on cold-season conditions, there was merit in considering trends and projections in hot temperatures, based on its known adverse impact to transportation. Our survey also ranked hot temperature extremes above cold temperature extremes in terms of concern and data needs. In this case, the survey revealed clear thresholds for adverse heat, which we define as a daily maximum temperature greater than or equal to 100°F (37.8°C). Further definitions were employed but not shown in this report, including days and consecutive days with T_{\max} greater than or equal to 95°F (35°C) and 110°F (43.3°C).

(v) Heavy precipitation

We provided a cursory examination of future trends in extreme precipitation, based on its high ranking by the survey and motivated by recent damaging heavy precipitation events in the Southern Plains. The survey revealed a general lack of consistency in thresholds of extreme precipitation. We opted to calculate values for return periods of 2, 5, 10, 20, 50, and 100 years for 24-hour precipitation (in inches). Since the datasets from which extreme precipitation was derived were of daily temporal resolution, sub-daily information is unavailable; therefore intensity-frequency-duration curves cannot be calculated for any time periods less than a day. (Due to time constraints, we were unable to scale the investigation up to multi-day precipitation amounts.) Trends in return-period frequencies on the daily time-scale are likely reflected by other time durations, and thus the information provided would be of interest to decision-makers. The results section on heavy precipitation describes the methods used to calculate return-period values.

Table 4: Threshold criteria used to designate locations by the frequency and magnitude of their cold temperatures. Integer values between -1 and 5 were assigned (higher value implies colder temperatures, and more frequent cold, and -1 indicates no freezing). For each location, the four variable fields were summed together (consisting of freeze-thaw cycle (FTC) days, FTC T_{min} , near lowest or 0.1th percentile annual temperature, and number of days with T_{min} less than or equal to 20°F), and then divided by 4, giving a mean value between -1 and 5. Climate class 2 and 3 in this table were condensed to category 2, as shown in the figures, and the no freeze category became category 0.

Value assigned	FTC days	FTC average T_{min} (°C)	0.1th % T_{min} (°C)	Days with $T_{min} \leq 20^\circ\text{F}$
5 Frequent severe frost	≥ 100	≤ -6	≤ -20	≥ 25
4 Frequent cold frost	80-99	-5 to -5.99	-16 to -19.99	20 to 24
3 Frequent moderate frost	60-79	-4 to -4.99	-12 to -15.99	15 to 19
2 Frequent mild frost	40-59	-3 to -3.99	-8 to -11.99	10 to 14
1 Infrequent frost	20-39	-2 to -2.99	-4 to -7.99	5 to 9
0 Rare frost	≤ 20	≥ -2	≥ -4	1 to 4
-1 No Frost	0	0	≤ 0	0

2.5 SUMMARY OF YEAR 1 ACTIVITIES

(i) Data Mining

A large portion of year 1 activities was to develop a method to effectively obtain freezing and frozen precipitation from gridded meteorological reanalysis. The dataset chosen for this investigation was the North American Regional Reanalysis (NARR), combining actual meteorological observations with model reforecasts using a complex and robust data assimilation system (Meisinger et al. 2006). This dataset is of sufficient temporal and spatial resolution to capture processes that result in ice and snow. Furthermore, it contains a large suite of meteorological variables at the surface, and various layers of the atmosphere that can be used to determine where ice and snow are occurring. The NARR product also derives its own estimates of freezing rain, sleet, and snow, which can be compared to the methods we have employed to identify precipitation type. The data extends from 1979 through the present day.

The methods used to derive ice and snow were described in detail in the publication Mullens and McPherson (2017), and so will not be covered extensively here (Readers

are encouraged to email the principle investigator for the publication if they cannot obtain it online). The basic approach was to use a series of common precipitation type algorithms. These algorithms identify ways in which a hydrometeor (precipitation droplet) can melt and freeze as it travels from its generation region in the cloud to the surface. We employed three methods of varying complexity to account for differences in their representation of these processes, with the final product being the mean of these methods. We also combined freezing rain and sleet into a single definition of 'freezing precipitation', necessitated by the difficulty in separating those precipitation types reliably through our approach. Once the algorithm-based data were collected, it was extensively validated against observations of precipitation type that were collected from several first-order stations throughout the Southern Plains. Ultimately, the data was found to reproduce the temporal trends and variability seen in the observations, with the exception of freezing drizzle, which was not well resolved in NARR. Snowfall was not evaluated to the same degree of detail, however, in cursory examination of the snowfall climatology from NARR versus satellite (not shown), the spatial distribution was well reproduced. Additionally, the algorithm-derived estimates were compared with the freezing precipitation information directly from the NARR variable suite, and in general, no significant differences were found. Using the native NARR variables improved magnitude estimates for individual storm events in all regions bar the northwest (Southern High Plains), while the algorithm approach better constrained the climatological frequencies and magnitudes over the Southern High Plains. Additional variables were output in associated with ice and snow events, shown in Table 5.

Additional research activity during year 1 was developing high-resolution spatial climatological maps and datasets for freeze-thaw cycles. We investigated the utility of employing lower-resolution reanalysis for this activity (NARR, for example, has a data point every 32 km). However, for the best representation of more local features, such as orography, urban climates, and river valleys, and for better access to precise spatial location data, we use an 800-m daily surface temperature dataset, developed by Oyler et al. (2014). The dataset, which extends from 1948-2012, incorporates historical station observations, digital elevation model information, atmospheric reanalysis, and satellite-based land skin temperature (MODIS satellite). Statistical methods involving station homogenization (for temporal consistency), interpolation, kriging, and geographically weighted regression are used to create the very high-resolution end product. Freeze-

thaw cycles (FTCs and EFTCs), and associated temperature condition products and output are shown in Table 6. Since this product does not extend to the present day, freeze-thaw cycles were also calculated using the dataset 'Daymet', which is available at roughly the same resolution, from 1980-present.

(ii) Output

The tables below highlight the output generated from our data analysis from year 1. This output will be available online by summer 2017 via contact requests to Co-PI Mullens, and subsequently through the South Central Climate Science Center cybercommons web-portal (email PI or Co-PI). Data formats are discussed in the appendix to this report.

(iii) Other synergistic activities

Other activities related to this project involved informal meetings with SPTC Faculty (e.g., G. Miller, M. Zaman) on the subject of climate data, including Co-PI Mullens and Rosendahl developing a brief report detailing climate data options. Formal year 1 activities included:

Conference and Workshop Presentations

- *McPherson, R.* Opening/Closing comments. Southern Plains Transportation Center, Region 6 Transportation-Climate Summit. September 30 2014, University of Oklahoma, Norman, OK.
- *Mullens, E. and McPherson, R.* Weather and Climate Impacts on Transportation for SPTC Region 6. Southern Plains Transportation Center Research Day, October 21, Oklahoma City, OK.
- *Mullens, E. McPherson, R. and Rosendahl, D.* Developing high-resolution climatologies and future climate projections for the transportation community. Informal seminar, January 20 2015, Geophysical Fluid Dynamics Lab, Princeton, NJ. Presentation slides available upon request.
- *Mullens, E. D., McPherson, R. A, and Rosendahl, D* 2015: Developing a high-resolution freezing precipitation dataset for climatological research (Poster). SPTC Openhouse, June 30, Norman, OK

Table 5: List of winter weather (ice/snow) and related variables calculated from North American Regional Reanalysis data, and a brief description of the variable, including its unit, and temporal interval (e.g., 3-hourly, daily, monthly). The total data range is 1979-present. Data available at 3-hour intervals means that over this interval (1979-present), there is data available every 3-hours, and so on.

Variable	Description
Freezing precipitation accumulation	Accumulation of freezing rain and sleet over a given time interval (3-hourly, daily, monthly, annual). <i>Liquid water equivalent in inches</i>
Snow accumulation	Accumulation of snow over a given time interval (3-hourly, daily, monthly, annual) <i>Liquid water equivalent in inches</i>
Freezing precipitation counts	Occurrence of freezing rain and sleet (3-hourly, daily, monthly and annual total)
Snowfall counts	Occurrence of snowfall (3-hourly, daily, monthly and annual total). Estimates of snow-cover days not considered.
Surface air temperature during freezing precipitation	Air temperature at the surface during freezing rain and sleet (3-hourly only, °C)
Surface air temperature during snowfall	Air temperature at the surface during snowfall (3-hourly only, °C). Incidences of snowfall in above-freezing conditions likely not resolved by the algorithms.
Precipitable water (moisture) during freezing precipitation	Total atmospheric column water vapor, observed during freezing rain and sleet (3-hourly mean, and daily maximum, in mm)
Precipitable water during snowfall	Total atmospheric column water vapor, observed during snowfall (3-hourly mean, and daily maximum, in mm)
Wind speed and direction during freezing precipitation	Wind speed in knots, and direction in degrees, during freezing rain and sleet (3-hourly, and daily maximum for wind speed)
Wind speed and direction during snowfall	Wind speed in knots, and direction in degrees, during snowfall (3-hourly, and daily maximum for wind speed)

Table 6: List of freeze-thaw cycle variables (including annual counts of FTC, EFTC, and FTC temperatures) calculated from high-resolution gridded observations. The temporal range of this data is 1948-2012 (Topographic Weather), and 1980-present (Daymet).

Variable	Description
FTC days	Total number of freeze-thaw days per year (1 value per year)
EFTC days	Total number of enhanced freeze-thaw days per year (1 value per year)
FTC temperatures	Surface minimum and maximum temperatures during each freeze-thaw cycle (daily)
FTC temperatures (annual mean)	Annual mean maximum and minimum surface temperatures during each freeze-thaw cycle (1 value per year)
FTC precipitation (average)	Average precipitation in inches within 3 days of a FTC (total average over year)
FTC wet/dry ratio	The ratio of wet to dry FTC cycles (total ratio per year). Precipitation from Climate Prediction Center 'Unified Gauge'.

Conference and Workshop Presentations (cont'd)

- *McPherson, R. A.*, 2015: Oklahoma's Rainfall Extremes: Past, Present, and Future. Invited Presentation, HUD All Grantee Meeting: H2O Past, Present, and Future, U.S. Dept. of Housing and Urban Development, Oklahoma City, OK, August 19, 2015.

Guest Lectures

- *Mullens, E. D.*, 2015: Invited guest lecture on weather, climate, and transportation. GEOG4513/5513, 15 students.

Reports/Articles

- *Mullens, E. D., R. A. McPherson and D. Rosendahl*, 2015: Trends in weather extremes, new datasets for transportation safety and infrastructure research. *SPTC Newsletter, Fall 2015*, [<http://www.sptc.org/publications/>]

(iv) Changes from original proposal

Notable changes from plans outlined in the proposal included:

- No longer considering additional low-resolution global reanalyses products. After a brief investigation, it was identified that these products tended to depict less precipitation (particularly heavy precipitation) and freeze-thaw activity compared with local observations. They were also too coarse spatially to maximize utility to end-users. Low-resolution data products listed in the proposal, such as NCAP-NCAR reanalysis, were replaced with high-resolution observations such as the topographic weather dataset.
- As mentioned previously in the subsection on cold extremes, our definition of cold-air outbreak was augmented to better reflect the thresholds and concerns of the transportation community, as opposed to a merely scientific analysis.

2.6 SUMMARY OF YEAR 2 ACTIVITIES

(i) Data Mining

Year 2 activities initially focused on development, dissemination, and analysis of survey information described in Section 2.1. Concurrently, climate model datasets (discussed in Section 2.2, Table 3) were downloaded and archived to the South Central Climate Science Center data servers. The variables and metrics outlined in Table 1 and

Section 2.4 were calculated from the base data and themselves written to new data files. Data were subset for the south-central U.S. domain shown in Fig. 1. For spatial plots, shapefiles of counties, interstates, highways, and secondary roads were obtained from the [U.S census](#) (2014 versions), and incorporated into visualizations of climate data. While the temporal length of most datasets extended from 1950-2100, we defined three time periods to examine future climate trends in climatological conditions, forming most of the spatial plots shown in this work. The historical period was 1970-2000, the mid-21st century period was 2021-51, and late 21st century was 2060-90. Most transportation planning would likely prioritize shorter-term changes, within 5-20 years, as many shorter-term issues associated with safety, maintenance, and construction occur at this time-scale. However, infrastructure that is ideally built for a long-design lifetime, in excess of 50-years, will likely encounter more pronounced impacts from climate variability and change, and so the late-21st century information is included to provide planners and engineers with a sense of where the climate system may be heading.

In addition to generating spatial maps of climate trends for the transportation-relevant variables, analyses and visualizations of temporal trends and model-ensemble spread were calculated by aggregating data over smaller sub-domains throughout the region. These sub-domains can essentially be any geographical region that a user desires, such as a point or county. However, for the majority of this work, we opted to utilize geographical climate regions known as '[Climate Divisions](#)' (CDs), defined by NOAA's National Climatic Data Center. Climate divisions have been used for decades to generate historical spatial climate information. They reflect regions of similar climate and other geographical and human factors, including forecast areas of responsibility, rivers, agriculture, and county boundaries (Guttman and Quayle, 1995). These domains are generally recognizable to decision-makers, and are well used by climatologists. Nonetheless, it should be noted that climate divisions vary substantially in their areal extent, particularly in Texas, and so output in large CDs is based on a larger number of data points, which are not weighted for area. Larger CDs also increase the risk that the area average is less representative of all locations within the division, since we may average over a more inhomogenous set of conditions or sharp gradients in certain variables.

(ii) Output

Historical and future climate projections were obtained from each model and emissions scenario for the selected variables shown in Table 1, and described in Section 2.4. Tables 7-11 (separated by variable) show the data products calculated from the base data, and their temporal and spatial availability. As with year 1 output, information on data formats is provided in the appendix.

Table 7: Climate model historical and future projections of freeze-thaw cycle related variables, including annual FTCs and EFTCs, and FTC temperatures (annual or monthly mean, minimum and maximum). These are calculated from all available models used in this analysis, over the years 1950-2099 (1960-2099 for ARRM models). The same data is also calculated from the Livneh and Maurer observations.

Variable	Description
Total FTC days	Annual and monthly total number of freeze-thaw days 1950 (1960 ARRM) – 2099.
Total EFTC days	Annual and monthly total number of enhanced freeze-thaw days 1950 (1960 ARRM) – 2099.
Average FTC T_{max}	Annual average daily maximum temperatures on freeze-thaw days 1950 (1960 ARRM) – 2099 ($^{\circ}C$)
Average FTC T_{min}	Annual average daily minimum temperatures on freeze-thaw days 1950 (1960 ARRM) – 2099 ($^{\circ}C$)
Maximum FTC T_{max}	Annual maximum daily maximum temperature on freeze-thaw days 1950 (1960 ARRM) – 2099 ($^{\circ}C$)
Minimum FTC T_{max}	Annual minimum daily maximum temperature on freeze-thaw days 1950 (1960 ARRM) – 2099 ($^{\circ}C$)
Maximum FTC T_{min}	Annual maximum daily minimum temperature on freeze-thaw days 1950 (1960 ARRM) – 2099 ($^{\circ}C$)
Minimum FTC T_{min}	Annual minimum daily minimum temperature on freeze-thaw days 1950 (1960 ARRM) – 2099 ($^{\circ}C$)

Table 8: Cold temperature variables calculated from climate model datasets, including number of cold days at various thresholds (25, 20, 10°F), and the 0.1th percentile of annual temperatures. The length of the freezing season is also estimated for each model. These parameters are calculated from the Livneh and Maurer observations, in addition to historical and future climate projections.

Variable	Description
Number of days and consecutive days with $T_{min} < 25^{\circ}F$	Annual total counts (1950, 1960 ARRM – 2099).
Number of days and consecutive days with $T_{min} < 20^{\circ}F$	Annual total counts (1950, 1960 ARRM – 2099).
Number of days and consecutive days with $T_{min} < 10^{\circ}F$	Annual total counts (1950, 1960 ARRM – 2099).
Cold climate classification	Averaged for each of the climatological time periods, 1970-2000, 2021-51, 2060-90
Annual 0.1th percentile of T_{min}	Near lowest annual temperature ($^{\circ}C$, 1950, 1960 ARRM – 2099).
First and last 32°F days during the cold season	Annual first and last 32°F day of year (1=September 1, 365 = August 31), 1950 (1960 ARRM) – 2099.

Table 9: Hot temperature variables calculated from climate model datasets, including days and consecutive days with maximum temperatures at or above 95, 100 and 110°F, and the annual 99.9th percentile temperature. The length of the 100°F season is also estimated for each model. These parameters are calculated for Livneh and Maurer observations, in addition to historical and future climate projections.

Variable	Description
Number of days and consecutive days with $T_{max} \geq 95^{\circ}F$	Annual total counts (1950, 1960 ARRM – 2099).
Number of days and consecutive days with $T_{max} \geq 100^{\circ}F$	Annual total counts (1950, 1960 ARRM – 2099).
Number of days and consecutive days with $T_{max} \geq 110^{\circ}F$	Annual total counts (1950, 1960 ARRM – 2099).
Annual 99.9th percentile of T_{max} ($^{\circ}C$)	Near highest annual temperature ($^{\circ}C$, 1950, 1960 ARRM – 2099)
First and last 100°F days annually	Annual first and last 100°F day of year (1=January 1, 365 = December 31), 1950 (1960 ARRM) – 2099

Table 10: Winter weather variables calculated from climate model datasets, including frequency (number of days per year), and accumulation (in the form of liquid water equivalent in inches). These variables are calculated for Livneh and Maurer observations, in addition to historical and future climate projections.

Variable	Description
Winter precipitation days	Monthly and annual total number of days with winter precipitation (ice, snow) (1950, 1960 ARRM – 2099)
Winter precipitation accumulation (liquid water equivalent)	Monthly and annual total accumulated winter precipitation, expressed as a liquid water equivalent in inches (1950, 1960 ARRM – 2099)

Table 11: Precipitation variables calculated from climate model datasets, including annual counts of days and consecutive days above thresholds ranging from 1-6 inches, and multiday (5 day) accumulations from 4-10 inches. Monthly and annual average precipitation accumulation is also calculated for each data point in the SPTC domain. Estimates of return period values and annual maxima are compiled by climate division. These variables are also assessed from Livneh and Maurer observations, in addition to historical and future climate data

Variable	Description
Number of days and consecutive days with precipitation \geq 1 inch	Annual total 1 inch precipitation days (1950, 1960 ARRM – 2099)
Number of days with precipitation \geq 2 inch	Annual total 2 inch precipitation days (1950, 1960 ARRM – 2099)
Number of days with precipitation \geq 3 inch	Annual total 3 inch precipitation days (1950, 1960 ARRM – 2099)
Number of days with precipitation \geq 4 inch	Annual total 4 inch precipitation days (1950, 1960 ARRM – 2099)
Number of days with precipitation \geq 5 inch	Annual total 5 inch precipitation days (1950, 1960 ARRM – 2099)
Number of days with precipitation \geq 6 inch	Annual total 6 inch precipitation days (1950, 1960 ARRM – 2099)
Number of times 5-day accumulation exceeds 4 inches	Annual total event counts (1950, 1960 ARRM – 2099)
Number of times 5-day accumulation exceeds 6 inches	Annual total event counts (1950, 1960 ARRM – 2099)
Number of times 5-day accumulation exceeds 8 inches	Annual total event counts (1950, 1960 ARRM – 2099)
Number of times 5-day accumulation exceeds 10 inches	Annual total event counts (1950, 1960 ARRM – 2099)
Return periods of maximum annual precipitation from 2-100 years (inch)	Return periods of extreme annual precipitation, calculated using Gumbel/GEV extreme value distributions, using data sampled from each climate division over the three climatological time periods. Not gridded. Climate divisions only.
Annual maximum precipitation (inch)	Annual maxima, (1950, 1960 ARRM – 2099)
Average precipitation (inch)	Monthly and annual total precipitation amount (1950, 1960 ARRM – 2099)

(iii) Other synergistic activities

Conference and workshop presentations:

- Mullens, E. D., R. A. McPherson, D. Rosendahl, and Gaitán Ospina, C, 2015: Developing transportation-relevant climatologies and projections for the south central U.S (Oral). *TRB First International Conference on surface transportation resilience to climate change and extreme weather impacts. Washington D.C, September 16-18, 2015.*
- Mullens, E. D., and R. A. McPherson, 2015: Climate trends and data resources for freezing precipitation and surface freeze-thaw cycles in DOT Region 6 (Poster), *SPTC Transportation Research day, Oklahoma City, OK, October 20, 2015*
- Mullens, E. D., and R. A. McPherson, 2016: A high-resolution freezing precipitation dataset for the South-Central U.S (Oral). *AMS 32nd Conference on Environmental Information Processing Technologies, New Orleans LA, January 14, 2016.*
- Mullens, E. D., and R. A. McPherson, 2016: A multi-algorithm Reanalysis-based freezing precipitation dataset for climate studies in the South Central U.S. (Oral), *AMS 22nd Conference on Applied Climatology, New Orleans, LA, January 14, 2016.*
- Mullens, E. D., and R. A. McPherson, 2016: Supporting end-user needs in the South Central U.S: Sector-specific climate change projections (Oral). *SCENARIO NERC DTP Conference, University of Reading, United Kingdom. June 11, 2016*
- Mullens, E. D., and R. A. McPherson, 2016: Current trends and future projections of transportation- relevant temperature and precipitation extremes in the South Central U.S. Invited Keynote presentation. *South Central Climate Science Center, and Southern Plains Transportation Center Climate Transportation Summit, Norman, OK, November 14, 2016.*
- Mullens, E. D., and R. A. McPherson, 2016: Come rain or shine: Multi-model projections of climate hazards affecting transportation in the South Central United States (Poster). *American Geophysical Union, Poster PA31A-2198, Climate Change Impacts on the Transportation Sector, San Francisco, CA, December 14, 2016*

Reports and Publications:

- *Mullens, E.D., and McPherson R.A*, 2017: A multi-algorithm reanalysis-based freezing precipitation dataset for climate studies in the South-Central U.S. *J. Appl. Meteor. Clim.* **56**, [DOI: 10.1175/JAMC-D-16-0180.1](https://doi.org/10.1175/JAMC-D-16-0180.1)

Other activities:

- Conversed with several engineering researchers in the region regarding climate-related project ideas.
- Assisted in developing and hosting a climate and transportation seminar series, with a first seminar on November 30 at the University of Oklahoma, National Weather Center, and a second on April 18, 2017. Additional seminars are anticipated later in 2017.

(iv) Changes from original proposal

- The proposal called for developing collaboration between the PI, Co-PIs, and researchers at the SPTC, leading to quarterly communication, and assistance with establishing appropriate metrics and threshold for climate and weather information. To a certain extent, this aspect was fulfilled, although perhaps in a less structured manner than had been planned. In particular, while beneficial communication was established between a few SPTC researchers, outreach to the wider transportation community, particularly to the State Departments of Transportation, did not yield fruitful results. Part of this was the lack of time allotted to cultivate these relationships, difficulty establishing whom to contact, and some lack of interest at the State DOT level. Instead, we opted for the survey approach, which did produce some very useful information. Collaborative relationships take time to develop, and we have found that the latter part of our timeline has been the most productive in this area. This is motivation for continuing to reach out to interested individuals in the transportation community, and to pursue formal engagements, such as the climate and transportation seminar series.
- The proposal anticipated the development of a web-based portal system where users could access the datasets developed for this project. During the latter part of year 1 through year 2, an IT professional affiliated with University of Oklahoma libraries has been assisting the South Central Climate Science Center with data

management, and has developed some preliminary infrastructure for a portal. However, personnel and resource constraints limited the time allotted to this work. Currently, our system permits datasets to be available on the web, but only in very basic form (as a simple file list). The plan is to develop a portal able to subset data for a given variable or location or domain, and provide that data in a spreadsheet-readable format, or a GIS shapefile. SC-CSC researchers are looking for funding options to complete this work. Data from our work will be available through this basic portal as it currently stands.

- Low-resolution GCM data was replaced by high-resolution statistically downscaled data, providing much improved spatial precision.
- Some variables planned in year 1 and 2 quarterly reports were eliminated, based on lack of time and perceived benefit. Final variables were constrained (and in a few cases, expanded) as the survey results were incorporated into our work.
- Information on high temperature and precipitation extremes were added to the suite of data analysis, as both were shown to be important to our survey respondents.

3. RESULTS: CLIMATE TRENDS

This section describes the main findings of data mining and analysis for both past and future datasets, using graphics where possible to highlight key findings. The section is arranged to showcase these findings for each meteorological and climatic variable in turn. The next section (discussion) brings these results together and links them to transportation concerns. In addition to providing visualizations of climate trends over spatial domains ranging from individual states to the full SPTC domain, we also examine some location-based output, here shown for the Central Oklahoma/Oklahoma City area as an example.

The rationale for selecting the Oklahoma City region was in part motivated by its proximity to the location of the PI and Co-PI research team, and the SPTC main office. However, the region is currently undergoing some significant reinvestment in infrastructure (Oklahoma DOT 8-year construction plan, 2017). These changes include recently completed I-40 relocation and widening, I-240/I-35 interchange replacement, bridge replacement and repairs (e.g., I-44 Belle Isle), and numerous resurfacing projects ([Oklahoma DOT](#)). In recent years, the State has recognized problems posed by its aging infrastructure. The state as a whole scored low in a recent Infrastructure scorecard assessment (ASCE, 2013), particularly for the condition of roads and bridges. The Oklahoma City metropolitan area also has ranked first in the number of deficient bridges in a city of 1-2 million people, a statistic the Governor's '[bridge improvement and modernization plan](#)' (HB2248/49) hopes to improve. Oklahoma City roads average a 60 for pavement condition index ('fair' PCI), and many areas have roadway infrastructure that is past its planned lifetime. Unfortunately budget constraints have made improvements challenging and have stretched resources. Given the planned works over the next several years, the expectation of additional investment in infrastructure, and the likelihood that many current infrastructure decisions do not incorporate future climate risk, we highlight some of the environmental hazards that new (and current) infrastructure many encounter over its lifetime, as well as provide some resources decision makers could use to evaluate whether incorporating future climate information may reduce long-term vulnerability.

3.1 FREEZE THAW CYCLES AND WINTER WEATHER: PAST AND FUTURE

(i) Context

Climatologically, much of the northern half of DOT Region 6 experiences ‘wet freeze’, which refers to numerous freeze-thaw cycles of generally low temporal persistence in an environment with semi-regular precipitation. Portions of the Texas High Plains and New Mexico experience ‘dry freeze’, especially in elevated New Mexico, where sub-freezing temperatures can persist for longer periods with minimal precipitation. Past studies of freeze-thaw cycles have identified that the southern states north of ~32 °N experience roughly 60 FTCs per year, with a maximum of close to 200 at higher-elevations in central and northern New Mexico (Hershfield 1974).

Repeated freezing and thawing have been linked to premature pavement failure, in conjunction with other non-climatic stressors such as traffic volume, construction practice, and subgrade composition. Application of deicing chemicals can exacerbate some surface scaling. Concrete durability to freeze-thaw is an ongoing active area of materials research. Concrete is typically exposed to an idealized series of high-amplitude freeze thaw cycles in a lab environment before deployment (e.g., ATSM C666/C666M). Simulations of pavement performance based on climatic and other factors have suggested that ridged pavement on active subgrade soils in wet freeze climates can experience more non-wheel-path (i.e. not load-related) longitudinal cracking. Moderate wet and dry freeze regions also experience more rutting, and transverse cracking (flexible pavement) over a 20-year period than no-freeze regions (Jackson and Puccinelli, 2006). In general, field studies of freeze-thaw damage are more rare than modeling analyses, potentially due to time and resource constraints. However, identifying how pavement degrades over time *in situ*, and/or identifying the potential lifetime exposure of pavement to freeze-thaw may be useful. It is therefore necessary to have a high-resolution, long-term climatic dataset that can resolve the mean and variability of freeze-thaw cycles over the SPTC region. Duration of at least 30-50 years of observations captures a greater degree of the range of FTCs, and provides historical information spanning the lifetime of much of the region’s highway infrastructure.

(ii) Historical climatology (1948-2012) and future projections of freeze-thaw cycles

We supplement historical FTC information to develop a very-high resolution spatial FTC product that depicts FTC frequency (cycles per year), and associated temperature statistics. The historical characteristics of freeze-thaw in the region are graphically summarized by state below. Subsequently, visual depictions of future projections in the frequency of freeze thaw cycles are shown, illustrating the degree of anticipated change in these events.

(a) Oklahoma

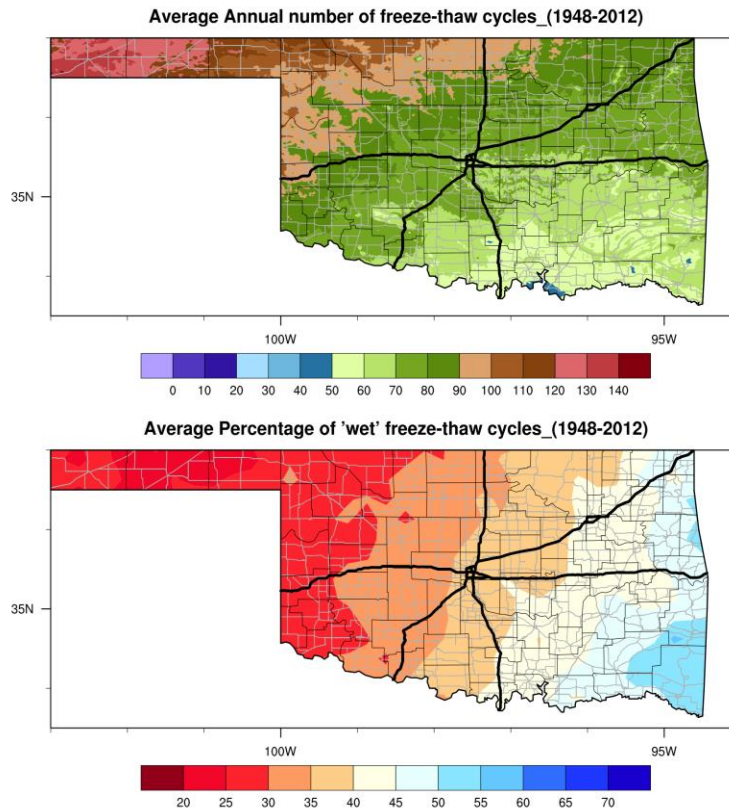


Figure 8: Top panel: Average annual number of freeze thaw cycles in Oklahoma, based on data from 1948-2012 taken from the Topographic Weather dataset (Oyler et al. 2012). Counties, highways and interstates are overlaid (think black, grey, and thick black lines respectively). FTC frequency ranges from 40-50 days in far southern Oklahoma, to 60-70 days along and south of I-44, 70-80 days parallel and north to I-44, increasing northwestward into the panhandle, to a maximum of 130-140 days in the far western Panhandle. **Bottom panel:** The percentage of freeze-thaw cycles that occurred within 3-days of precipitation >0.01 inch. Far southeastern Oklahoma has the highest percentage with 50-60%, decreasing north and west to 40-45% in a vertical line intersecting central Oklahoma, and a minimum in the Oklahoma Panhandle (25-35%).

Freeze-thaw cycles in Oklahoma (Figure 8) show a pronounced gradient from northwest to southeast, and urban and topographic variation. FTCs are most pronounced, but also driest and more intense (in terms of daily temperature change, not shown) in the Panhandle and Northwest Oklahoma, with a 65-year mean in Boise City of 130-140 days per year, and 35-30% within 3 days of precipitation. The number gradually declines toward Oklahoma City, with a 65-yr mean closer to 70 days per year, and 40-45% within 3 days of precipitation. Values in the south and southeast average 50-60 days per year, with higher values along the ridgelines of the Ouachita Mountains. Northeast Oklahoma averages 70-80 days per year, with apparently lower values in the vicinity of large lakes. In the east, the proportion of FTC days within 3 days of precipitation increases to 45-60%.

Future projections of FTCs were evaluated from climate model projections averaged for years 1970-2000 (past), 2021-51 (mid-century) and 2060-90 (late-century) using the mid-range emissions scenarios, shown in Fig. 9. This data is lower-resolution than the historical data, and so specific gradients revealed with the highest-resolution product will not be captured. The magnitudes in the historical period also vary due to different temporal length and model representation of the climatology. What is apparent is a reduction of FTCs everywhere in the region by at least 10-20% of the historical mean by mid-century, and 30-40% late century. Boise City and the Panhandle now suggest 110-120 FTCs per year over a 30-year period, decreasing to 90-110 by late-century. Oklahoma City area decreases to 50-60 by mid-century, and 40-50 late-century. Tulsa decreases to 60-70 by mid-century, and 50-60 late century. Most areas in the south and east also show similarly proportionate decreases.

Projections for the high emissions scenario are shown in Figure 10. The mid-century reduction in FTCs is very similar to that of the mid-range emissions. However, by late century, the reduction in days per year compared with the historical period is 50-70%. For example, Boise City now has 70-90 FTC days per year on average, Oklahoma City 30-40 days per year, and Tulsa 40-50 days per year. Precipitation changes that occurred in conjunction with freeze-thaw days were not assessed; however, more than 60% of models in this sample suggest a slight increase in average winter (December-February) and spring (March-May) precipitation (not shown).

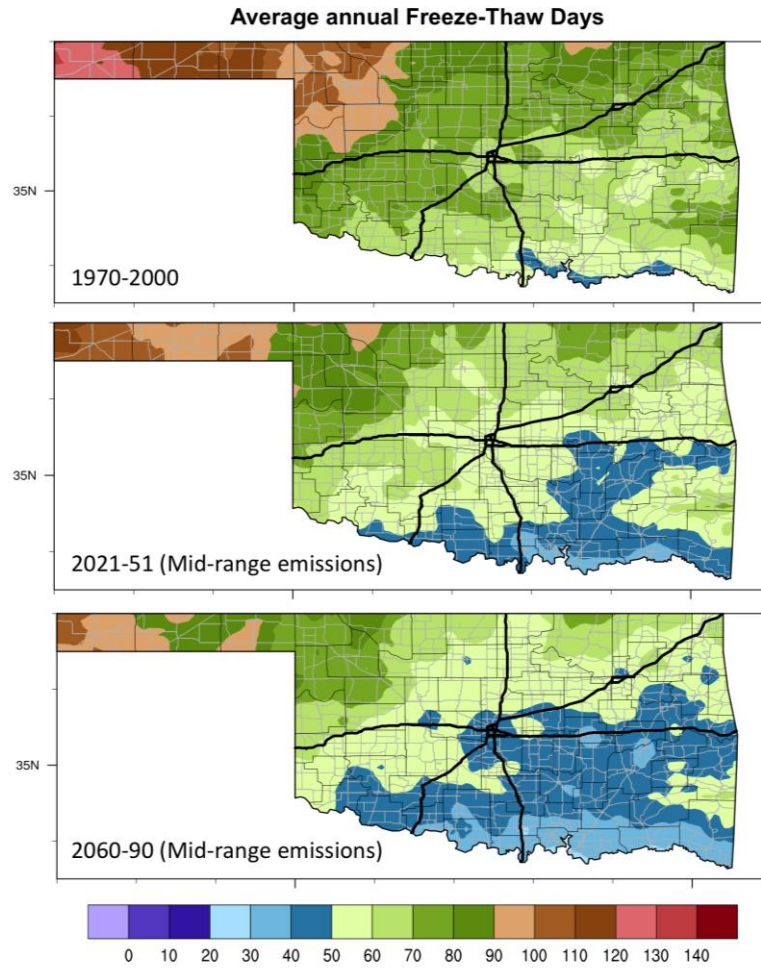


Figure 9: Multi-model average climate projections of annual average number of freeze thaw cycles for Oklahoma using mid-range emissions scenarios (RCP4.5/B1), based on 21 models. **Top panel:** 1970-2000, **Middle panel:** 2021-51, **Bottom panel:** 2060-90. The lower-resolution ARRM models are regridded to the MACA grid (6.6 km horizontal resolution). This regridding is performed for all spatial maps. Description of results provided in the main text.

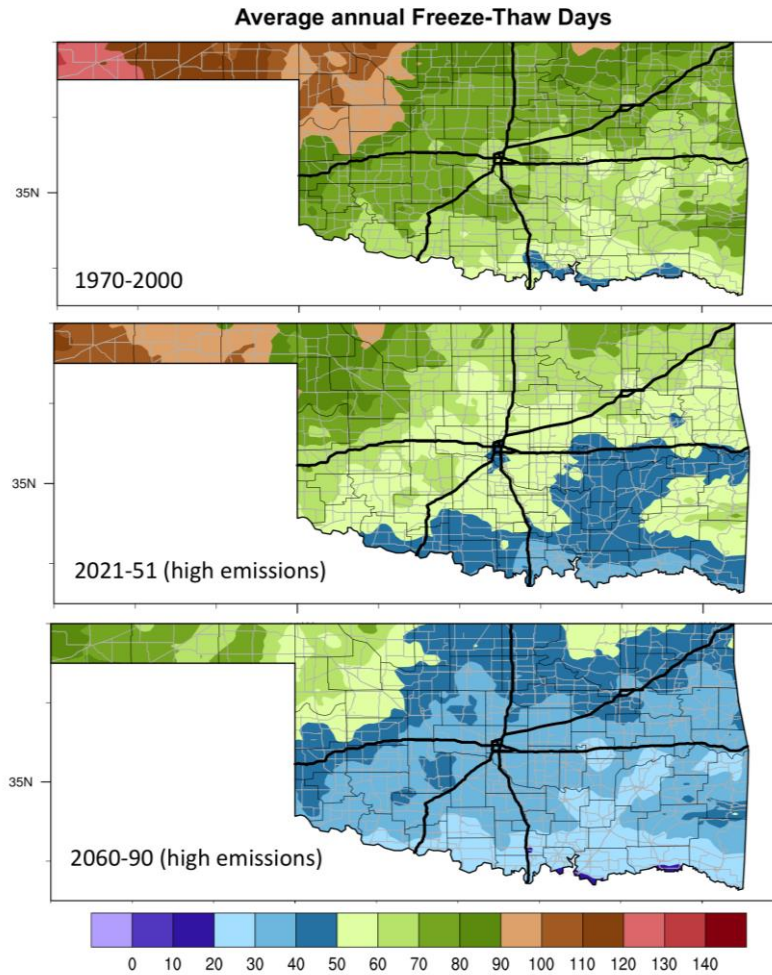


Figure 10: As Fig. 9, but for multi-model average climate projections of annual average number of freeze thaw cycles for Oklahoma using high emissions scenarios (RCP8.5/A1Fi), based on 19 models.

(b) Texas

Texas, like Oklahoma, shows pronounced topographic variation in freeze-thaw cycles (Figure 11). The most numerous are in the western Southern High Plains, occupying the western and northern Texas panhandle, the higher terrain of the Permian Basin, and the mountains of the Chihuahuan Desert. These areas have in excess of 100 FTCs up to 150 FTCs per year on average. Most of those regions would be considered ‘dry’ FTC. Further east, the Texas hill county northeast of San Antonio experiences more FTC days than areas at this latitude to the east (50-60 days, versus less than 20 in San Antonio). Freeze-thaw cycles in eastern Texas have the highest probability of being temporally

proximal to precipitation (55-65%), decreasing westwards. The metroplex of Dallas Fort Worth averages 40-50 FTCs per year.

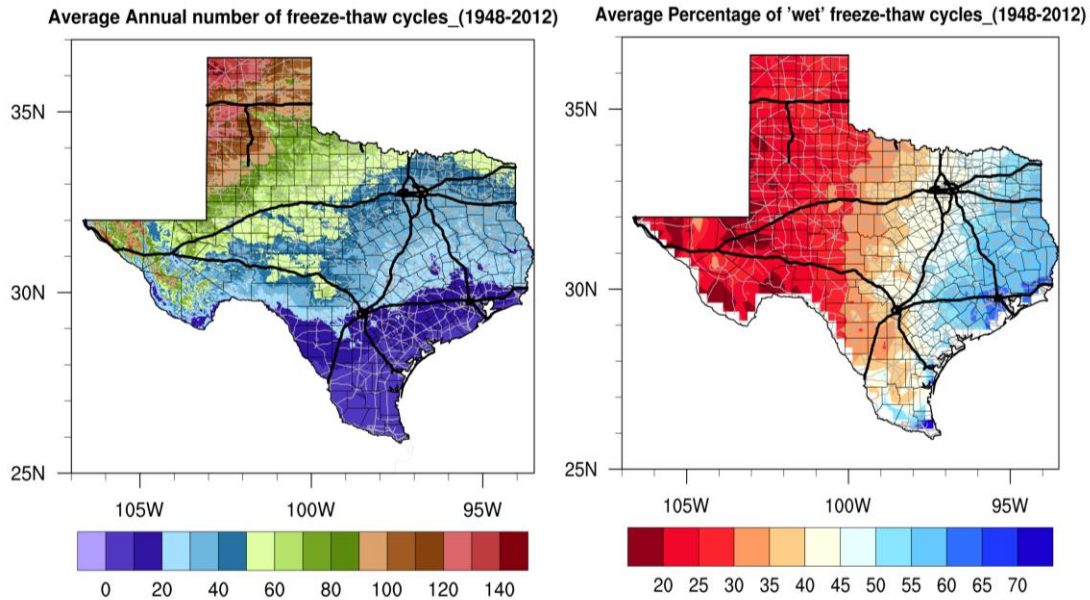


Figure 11: Left panel: Average annual number of freeze thaw cycles in Texas, based on data from 1948-2012 taken from the Topographic Weather dataset (Oyler et al. 2012). Counties, highways and interstates are overlaid (think black, grey, and thick black lines respectively). FTC frequency ranges are discussed in the text, but freeze-thaw days are rare in south Texas, elevated over the Texas hill country (40-60 per year), and reach a maximum over the western Texas panhandle (120-140 per year). **Right panel:** The percentage of freeze-thaw cycles that occurred within 3-days of precipitation >0.01 inch. Eastern Texas east of I-35 has the highest percentage with 50-65%, decreasing north and west to a minimum in the Chihuahuan desert (20-25%) and southern high plains (25-30%).

Climate change is expected to lead to a universal reduction in FTCs across Texas (Figs. 13 and 14) particularly for the late 21st century with a high emissions scenario (Fig 14). The areas historically experiencing the greater number of FTCs do so in the future but with much reduced frequency. Areas such as Amarillo decrease from more than 120 FTCs to 80-100 FTCs per year by mid-century, and 50-60 FTCs per year late century with high emissions (a 50-60% decrease). Dallas Fort Worth, with historically 40-50 FTC days per year, decreases to 20-30 by mid-century, and less than 20 days with high emissions, which would equate it's future toward present day FTC frequencies of southern Texas.

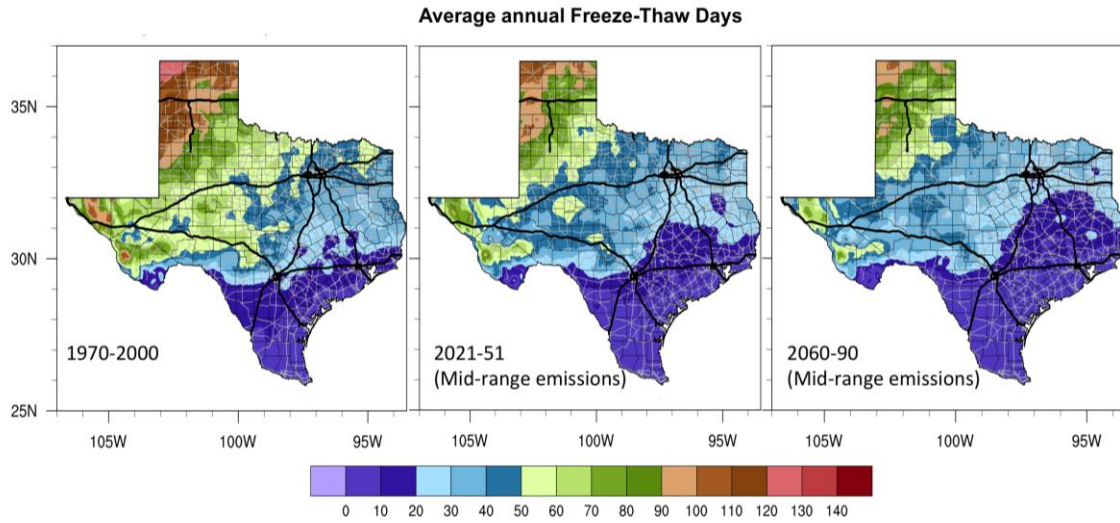


Figure 12: Multi-model average climate projections of annual average number of freeze thaw cycles for Texas using mid-range emissions scenarios (RCP4.5/B1), based on 21 models. **Left panel:** 1970-2000, **Center panel:** 2021-51, **Right panel:** 2060-90. Description of results provided in the main text.

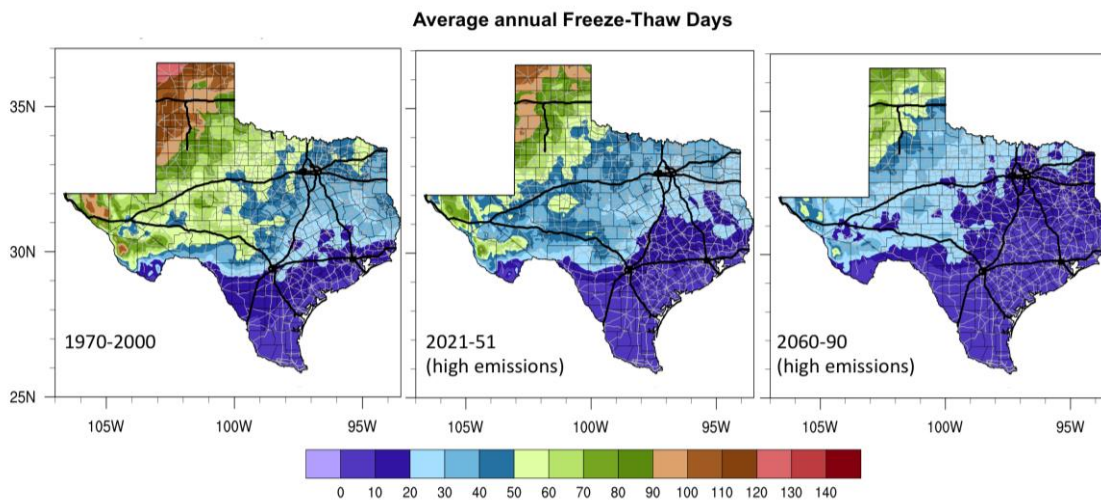


Figure 13: As Fig. 12, but for multi-model average climate projections of annual average number of freeze thaw cycles for Texas using high emissions scenarios (RCP8.5/A1Fi), based on 19 models.

(c) New Mexico

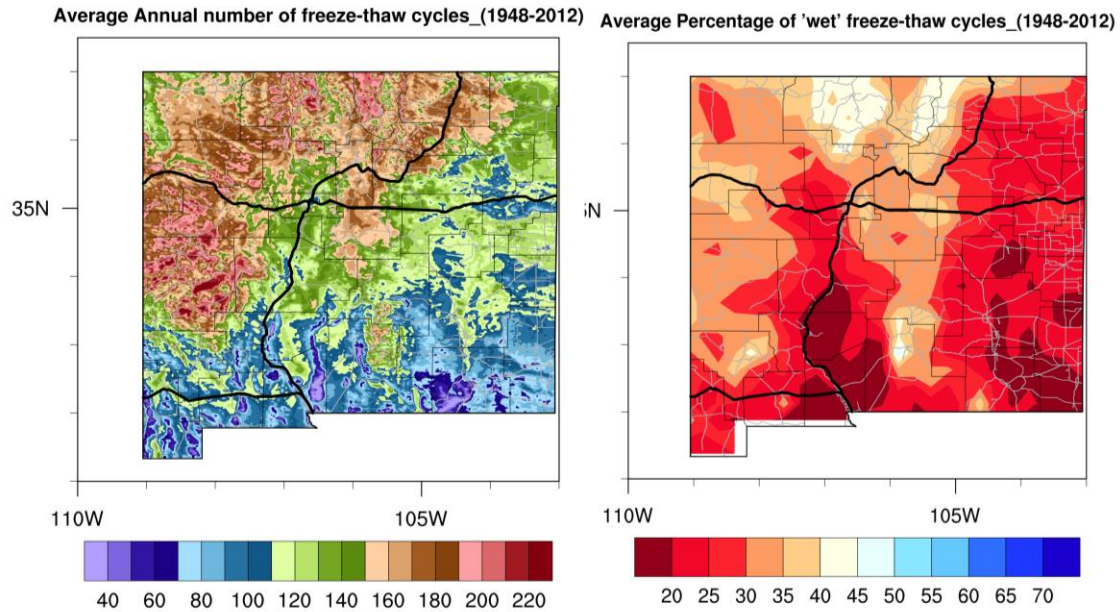


Figure 14: Left panel: Average annual number of freeze thaw cycles in New Mexico, based on data from 1948-2012 taken from the Topographic Weather dataset (Oyler et al. 2012). Counties, highways and interstates are overlaid (think black, grey, and thick black lines respectively). FTC frequency is strongly dependent on altitude, with over 180-200 or more days per year in the mountains and high plains of northern and western New Mexico. The Tularosa valley and other low-lying regions of southern NM have the least number of FTCs annually (<50). **Right panel:** The percentage of freeze-thaw cycles that occurred within 3-days of precipitation >0.01 inch. The northern Sangre De Cristo Mountains have the highest frequency of proximal precipitation (some of which may be snowfall) at 45-50%, while the valleys and Chihuahuan desert have the lowest (20-25%).

In the SPTC domain, New Mexico has the most frequent and intense FTCs (Fig. 14). The elevated terrain of the northern and western state promotes frequent freezing and thawing throughout the autumn and spring months, in addition to most days through the peak of winter experiencing an FTC. Daytime mean temperatures are in excess of 50°F, while night temperatures can be below 15°F, particularly along and west of I-25 in the northern half of the state (not shown). Snowfall and snowmelt contribute to wetter FTCs in the mountains, while the valleys and plateaus of the southeastern and south central portions of the state are predominantly dry. Albuquerque experiences lower FTC than the surrounding area, with 100-120 per year. Taos experiences closer to 200 FTCs per year, and Raton 160-180 FTCs per year. Las Cruces, in contrast, averages 80-100 days. Figures 15 and 16 show the projected future FTC days for the state. Note that these values are more smoothed compared with the historical data, which is of higher spatial

resolution. The nearer term reductions in FTC are predominantly in the southern and southeastern portions of the state, and in the lower-altitude regions. Albuquerque decreases to 80-100 FTC days per year, Taos remains closer to 200 days per year, Raton 140-160, and Las Cruces stays near 80-100 days per year. By late century, and with high emissions, Albuquerque annual mean FTC days are closer to 60-70, Taos 160-180, Raton 100-120, and Las Cruces 40-60.

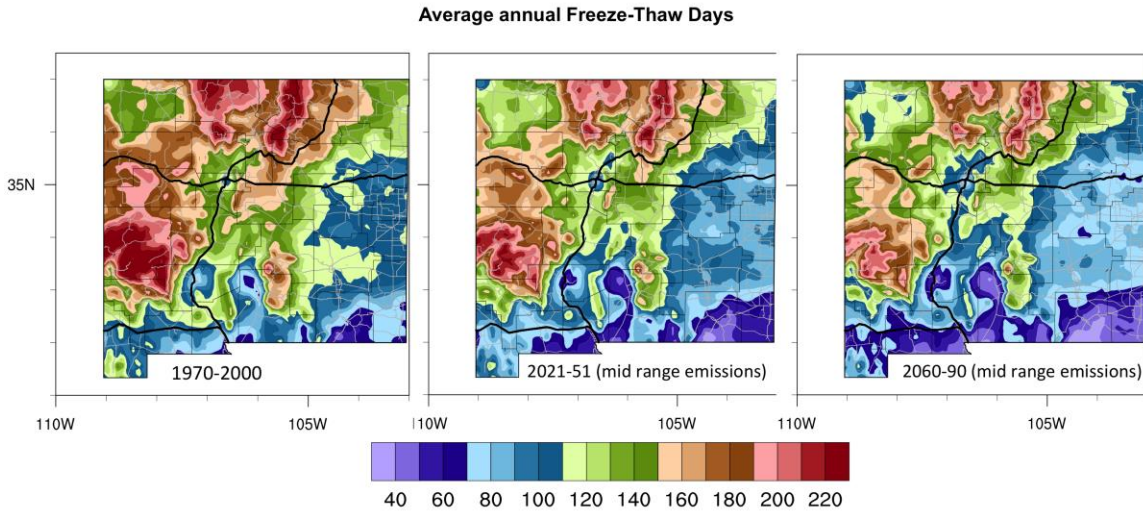


Figure 15: Multi-model average climate projections of annual average number of freeze thaw cycles for New Mexico using mid-range emissions scenarios (RCP4.5/B1), based on 21 models. **Left panel:** 1970-2000, **Center panel:** 2021-51, **Right panel:** 2060-90. Description of results provided in the main text. Note the different color bar magnitudes for this state (which range from 40-220 FTCs).

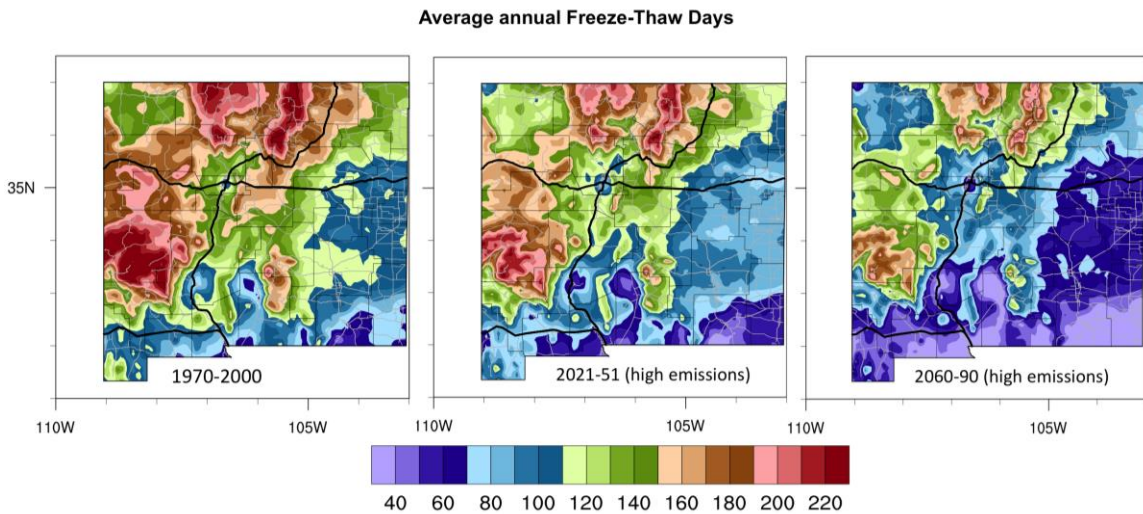


Figure 16: As Fig. 15, but for multi-model average climate projections of annual average number of freeze thaw cycles for New Mexico using high emissions scenarios (RCP8.5/A1Fi), based on 19 models.

(d) Arkansas

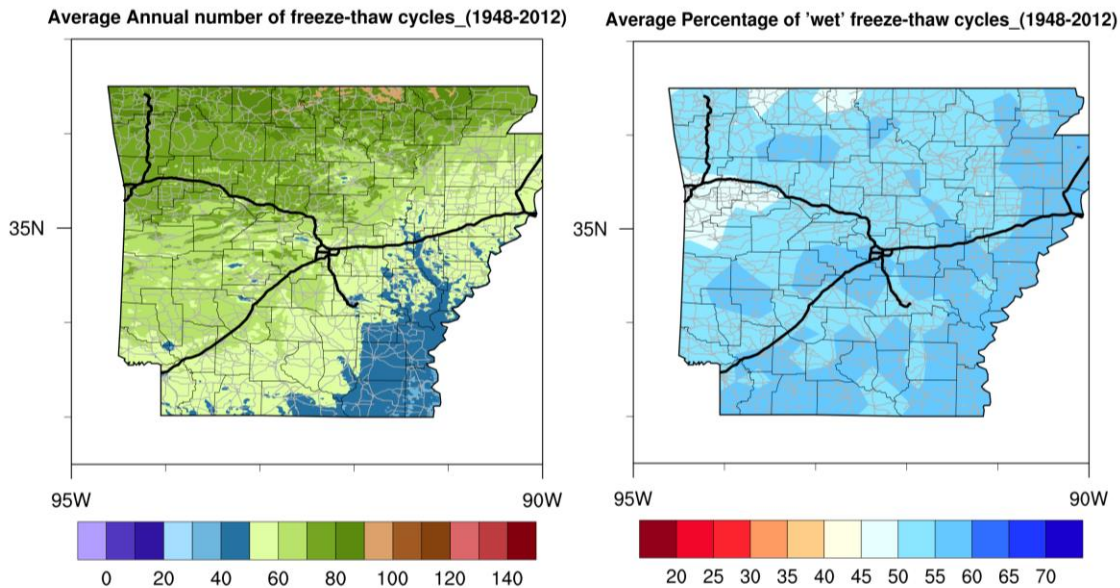


Figure 17: Left panel: Average annual number of freeze thaw cycles in Arkansas, based on data from 1948-2012 taken from the Topographic Weather dataset (Oyler et al. 2012). Counties, highways and interstates are overlaid (think black, grey, and thick black lines respectively). FTC frequency is greatest over far northern Arkansas, and along the Ozark and Ouachita ranges (70-90 per year), and decreases southeast toward the Mississippi (40-60 per year). **Right panel:** The percentage of freeze-thaw cycles that occurred within 3-days of precipitation >0.01 inch. Arkansas has relatively abundant precipitation year-round, and 50-55% (North) to 60% (south) of FTC days are proximal to precipitation.

Arkansas has a north-south and east-west gradient in freeze-thaw activity (Fig. 17). In the higher western terrain, including the Ozark and Ouachita mountains, the number of FTCs is higher, particularly along the ridgelines. The lowest number of FTCs is along the Mississippi river, particularly in the southeastern portions of the state. Arkansas is a state with a humid subtropical climate in the summer, and the winter and spring months generally receive the most precipitation. Precipitation occurs within 3 days of a FTC event in at least 50% of cases in the north, and up to 60% in the east and south. The presence of more moisture may exacerbate FTC issues in some cases. Locations such as Fayetteville average 80-90 FTCs per year, Little Rock 50-60 FTCs per year, and Memphis 40-50 FTCs per year.

Future projections in freeze-thaw cycles for Arkansas are show in Figures 18 and 19. The spatial depiction of FTCs is different in the climate models, and the historical observations from which they are based, compared with the higher-resolution historical dataset (Fig. 17). Fayetteville suggests 60-80, Little Rock 30-40, and Memphis 30-40

FTC days per year by mid-century. Later in the century, and with high emissions, the frequency declines further over the state, and FTCs become relatively rare over the southern Mississippi valley. Fayetteville decreases to 40-50, Little Rock 20-30 and Memphis 20-30 FTC days per year.

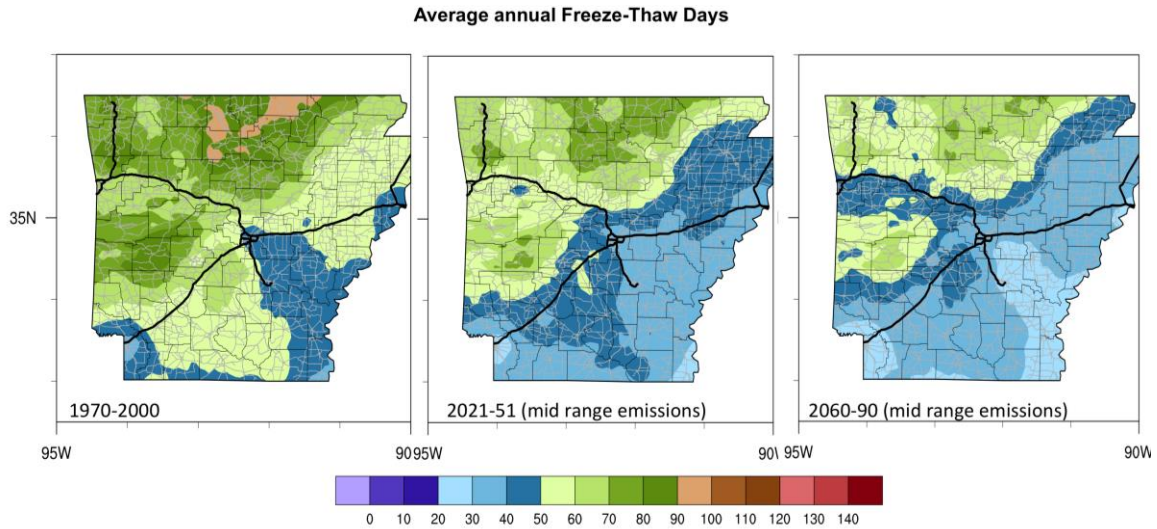


Figure 18: Multi-model average climate projections of annual average number of freeze thaw cycles for Arkansas using mid-range emissions scenarios (RCP4.5/B1), based on 21 models. **Left panel:** 1970-2000, **Center panel:** 2021-51, **Right panel:** 2060-90. Description of results provided in the main text.

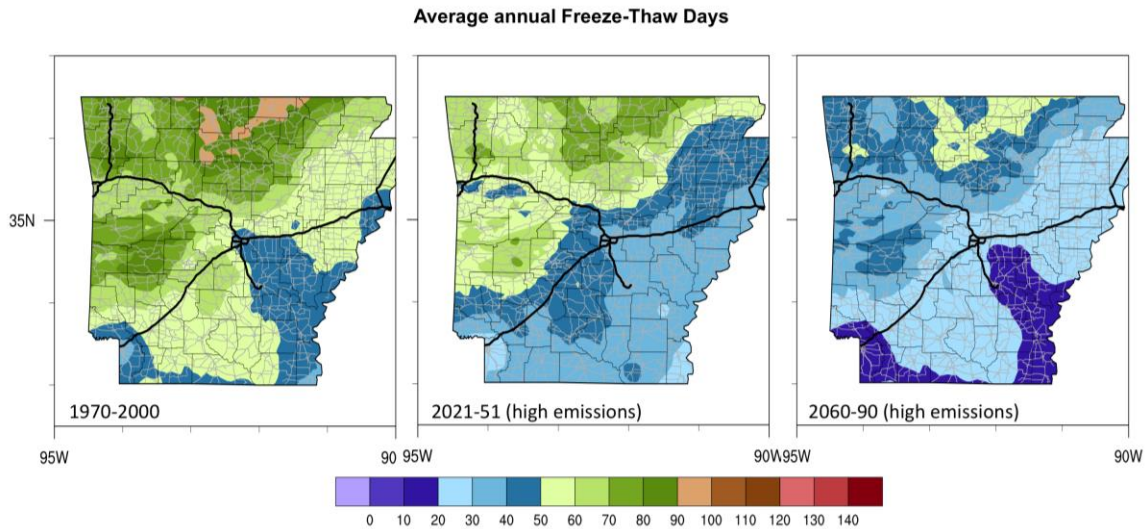


Figure 19: As Fig. 18, but for multi-model average climate projections of annual average number of freeze thaw cycles for Arkansas using high emissions scenarios (RCP8.5/A1Fi), based on 19 models.

(e) Louisiana

Louisiana, being close to the Gulf of Mexico, and a largely sub-tropical state, generally experiences few freeze-thaw cycles, with the exception of the northernmost part of the state, as shown in Figure 20. Areas south of I-40 experience fewer than 10 FTC days per year, while Shreveport has 40-50 FTC days per year. Louisiana also has relatively abundant winter rainfall (over 15 inches on average). At least 55-60% of FTCs have a proximal precipitation event, increasing to near 70 closer to the Gulf coastline.

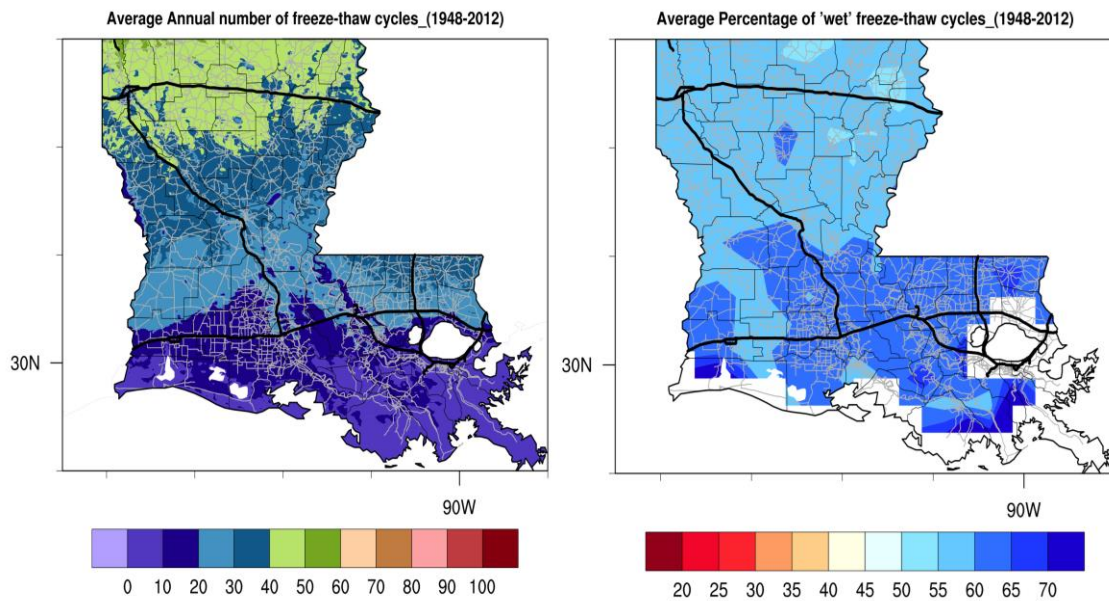


Figure 20: Left panel: Average annual number of freeze thaw cycles in Louisiana, based on data from 1948-2012 taken from the Topographic Weather dataset (Oyler et al. 2012). Counties, highways and interstates are overlaid (think black, grey, and thick black lines respectively). FTC frequency is greatest over far northern Louisiana (40-50 days), and decreases to the south. South of I-10 freeze-thaw days are rare (0-10 per year). **Right panel:** The percentage of freeze-thaw cycles that occurred within 3-days of precipitation >0.01 inch. Louisiana has relatively abundant precipitation year-round, and 55 (north)-70 (south)% of FTC days are proximal to precipitation.

The graphical projections of Louisiana FTCs are not presented here, since freeze-thaw activity is generally less of a concern in this state. However, based on our analysis, the reduction of FTC days is of similar proportions as that evidenced in the other states, with typically a 20-40% reduction by mid-century, and 50-70% reduction by late century (assuming high emissions). South of I-10, the degree of change is lower since FTCs are

already rare; however, nights below freezing may virtually disappear by the late 21st Century.

3.2 COLD TEMPERATURES: SPATIAL PROJECTIONS FOR THE SOUTH-CENTRAL U.S.

Cold temperature impacts on transportation are largely a result of their relationship to other conditions, such as the frequency of freeze-thaw cycles, or winter precipitation (ice and snow). Nonetheless, extreme and unusual cold can weaken rail lines (Rossetti 2007), may result in delays to aviation due to deicing, and can place high demands on gas pipeline operations. Cold weather preceded by rainfall, or during freezing rain can promote the formation of black ice, particularly on bridges.

Here we present results of a cold climate classification methodology, defined and described earlier in this document (Section 2.4). Projections in the cold climate class are shown for the entire SPTC region. Observations are also plotted so that the reader can refer to this for historical context. The cold climate classification attempts to class a location based on the frequency and intensity of its winter cold temperatures. Thus, a region ranked more highly would note a location where very cold temperatures are more common.

Figure 21 presents the cold climate classes of the SPTC domain, based on Livneh and Maurer observations, and the multi-model mean of all climate models, for the period 1970-2000. The observations show a climatology that reflects the latitudinal and topographical dependence of cold temperatures. Colder winter conditions are common to the north and west of the region, particularly over New Mexico, the Texas Panhandle, and northwestern Oklahoma. Further south and east, the potential for frequent extreme cold is reduced, with freezing conditions becoming very infrequent toward the Gulf Coast, and throughout the southern third of Texas. The climate model mean is slightly warmer than the observations suggest, especially over eastern and southern Texas. This may suggest that some models are not correctly representing the frequency of cold conditions in these southern regions, which are generally contributed by cold air outbreaks (e.g., Grotjahn et al. 2016). This may indicate that these models could underestimate cold air outbreaks in the future, but further work would be necessary to establish this conclusively.

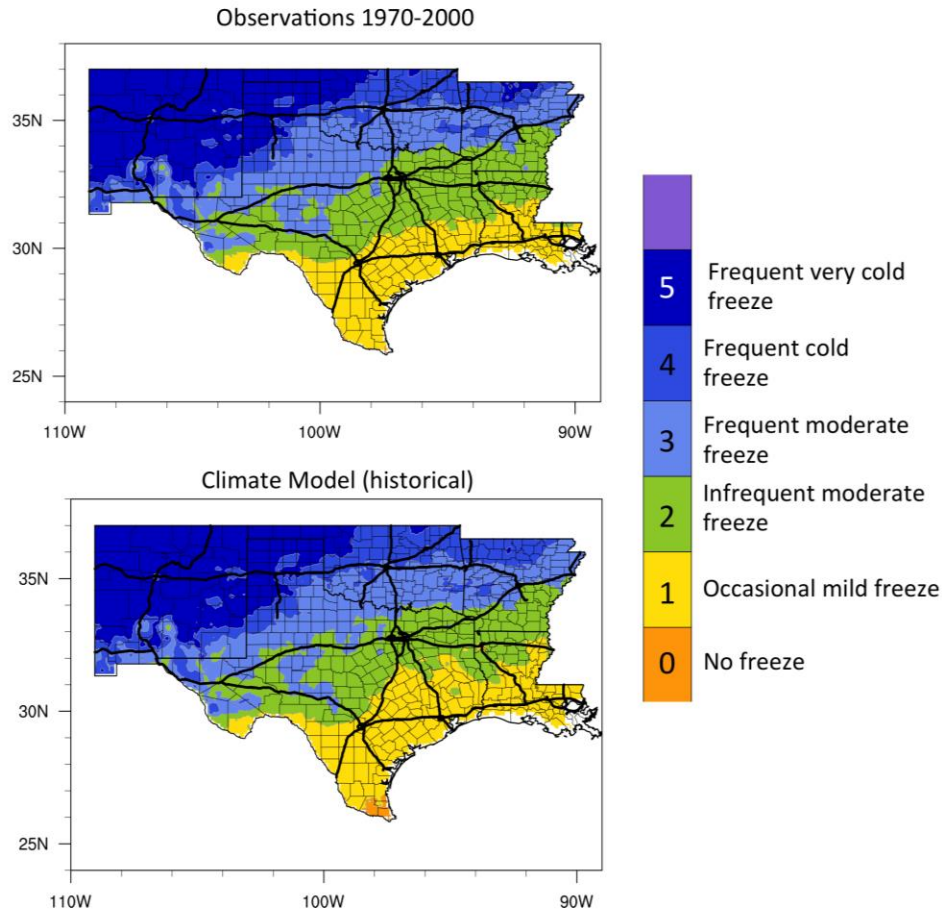


Figure 21: Cold climate class across the SPTC DOT region 6, expressed as the average for the period 1970-2000, calculated based on the frequency and magnitude of cold calculated from 4 temperature-related variables using applicable thresholds, described in section 2.4(iii), and Table 4. **Top panel:** The average of Livneh and Maurer observations (Maurer regridded to Livneh grid prior to calculation), **Bottom panel:** Climate model average, based on 21 models.

Figure 22 displays the cold climate class for the mid-century projections based on moderate and high emissions scenarios. In some locations, the cold climate class does not change (e.g., around Oklahoma City, Dallas Fort Worth, and much of northern and western New Mexico). However, in most areas, there is a reduction in extent of the coldest class, and an increase in the range of the warmer classes. The differences between mid and high emissions are negligible over this period, extending from 2021-51. Northern and central Oklahoma take on a cold climate more representative of the historical climate of central southern Oklahoma, and Dallas becomes similar to present day Waco.

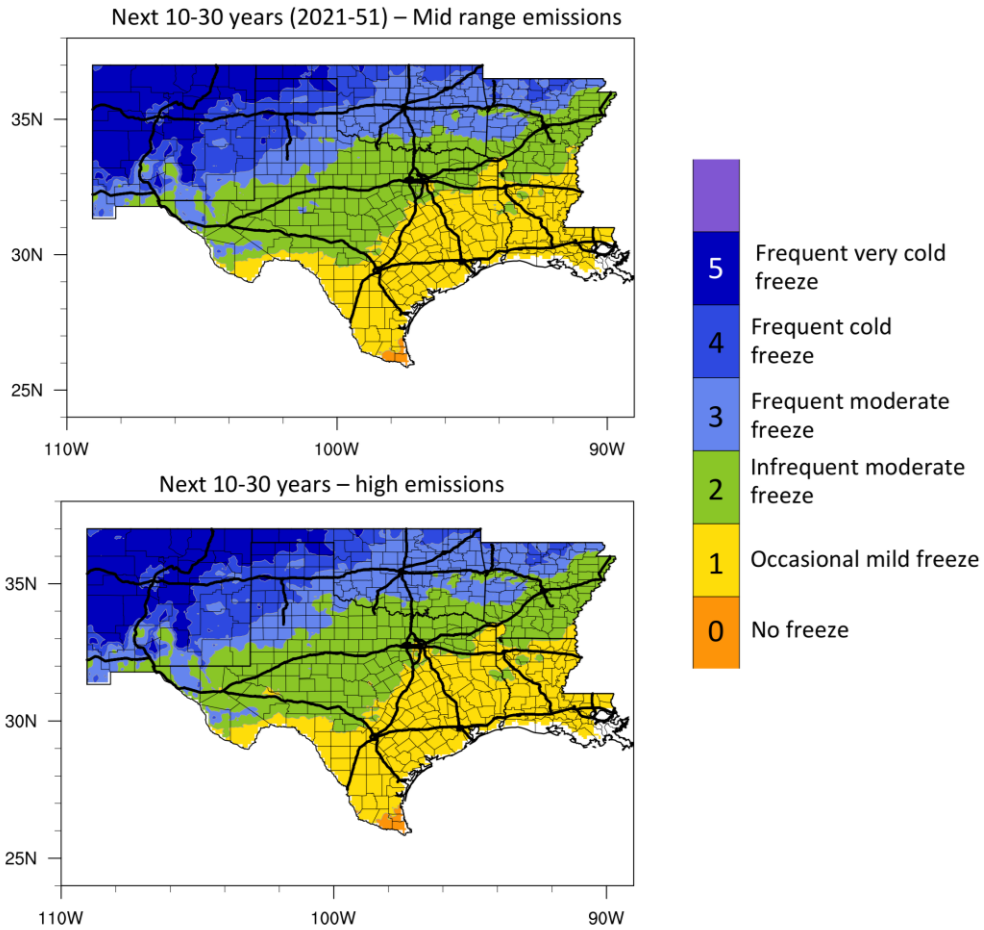


Figure 22: Cold climate class across the SPTC DOT region 6, expressed as the average for the period 2021-51. **Top panel:** mid-range emissions scenarios (RCP4.5/B1), 21 models. **Bottom panel:** high emissions scenarios (RCP8.5/A1Fi), 19 models.

Figure 23 displays the cold climate class for the late-century projections based on moderate and high emissions scenarios. There is a notable difference in the reduction of cold conditions, with the moderate emissions showing a slight further decline in cold weather relative to mid-century, but with the higher emissions leading to more substantial warming of the region, in all but the highest altitudes of New Mexico where the climate class does not change. Central Oklahoma now has winter cold temperature more akin to present day Dallas/Fort Worth, while Dallas/Fort Worth is more similar to present day San Antonio. Areas along the Gulf Coast may no longer experience any freezing temperatures, which while a benefit to transportation infrastructure, could have substantial implications for the regional ecosystem (e.g., inland extension of mangrove

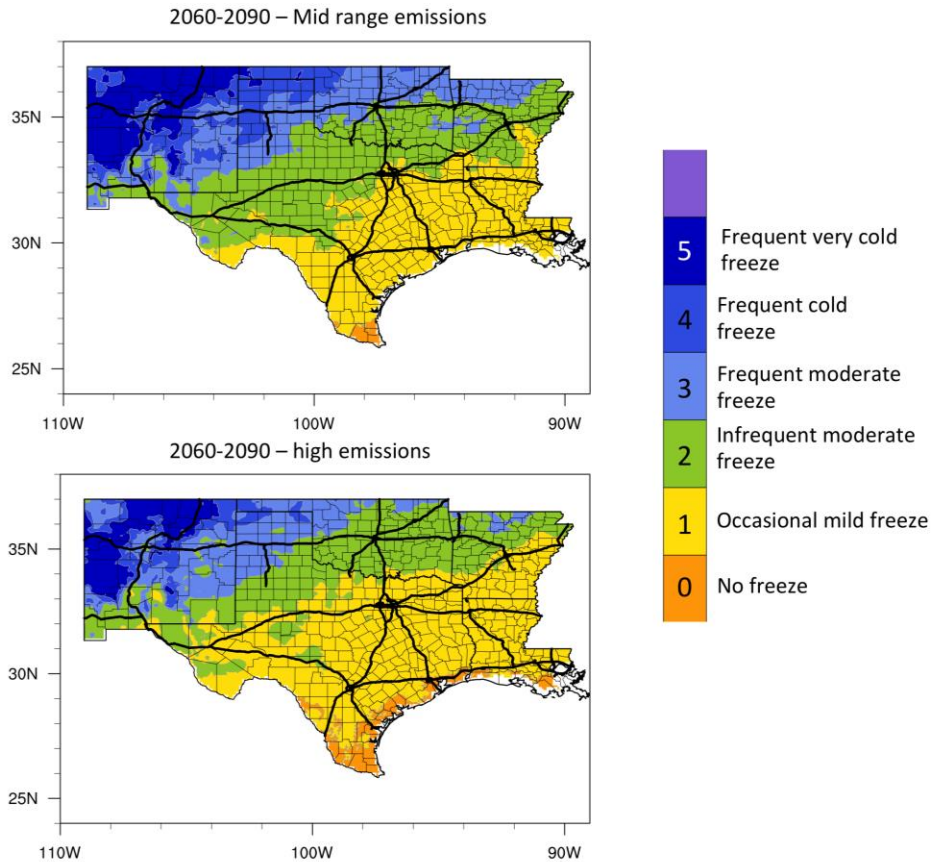


Figure 23: Cold climate class across the SPTC DOT region 6, expressed as the average for the period 2060-90. **Top panel:** mid-range emissions scenarios (RCP4.5/B1), 21 models. **Bottom panel:** high emissions scenarios (RCP8.5/A1Fi), 19 models

habitat). Portions of southwest Texas show the greatest change in class, with portions of the Chihuahuan Desert transforming from frequent cold freeze to rare mild freeze by late 21st Century.

While not shown, spatial trends for the warmest and coldest of the climate models used in the ensemble were evaluated. These would represent the upper and lower bounds to the climate classes shown. By late century, the coolest model (GFDL-ESM2G), showed a moderation of extreme cold over the entire region, but no change in class for locations such as Oklahoma City and Dallas/Fort Worth. The warmest model (HadCM3) suggested that rare mild freeze conditions could extend throughout the eastern half of the region as far north as the Kansas border, while the no-freeze zone occupied most of south Texas.

3.3 WINTER WEATHER (SNOW AND ICE)

Ice and snow storms have particularly salient impacts on the transportation sector due to their effects on traffic safety, movement, and maintenance. Precipitation, including ice and snow, has the greatest impacts to the road sector of any weather type (OFCM, 2002). Road accidents and delays tend to increase substantially during winter weather, even if volumes also decrease (e.g., Strong et al. 2010). Notably, Black and Mote (2015) recently identified substantial underreporting of the dangers of winter weather to transportation. When indirect crashes were also attributed to conditions, winter precipitation was a factor in nearly 28,000 aviation and vehicular accidents, contributing to over 32,000 fatalities between 1975 and 2011, with most of these being on the roadway. In the SPTC domain, Black and Mote showed lower mortality clustered in the Gulf Coast states, including southern Texas and Louisiana, where winter weather is already highly infrequent. Higher mortality was measured in far western Oklahoma, west Texas, and portions of northern and western New Mexico. In addition to its safety implications, melt water from snow and ice seeping into tracks or into the subsurface can exacerbate pavement and bridge damage through repeated freezing and thawing.

A key component of this project was to create a reliable, long-term, spatial historical dataset of freezing precipitation that can be used for multiple applications related to assessing transportation hazards. Our dataset was rigorously evaluated against existing observations, and found to represent the regional climatology and trends of freezing precipitation (freezing rain and sleet). It also was able to capture the spatial location and approximate duration of high-impact ice storms (see Section 2.5, and Mullens and McPherson 2017). It is therefore a tool that transportation researchers and planners may wish to consider when conducting risk assessments, or surveying past crash statistics or vulnerabilities related to winter weather. Examples of model-derived versus observed climatologies for three stations are shown in Figure 24. Examples of the spatial climatology extracted from the dataset are shown in Figure 25. Additionally, Figure 26 shows a spatial map of accumulated freezing precipitation versus the locations of 1-in-50-year ice storm events, the latter obtained from a [GIS database developed by the Army Core of Engineers](#). While accumulated liquid-water versus ice-storm accretion are not directly comparable metrics, the density of storm events versus higher

accumulations in similar locations implies some degree of spatial precision in our dataset.

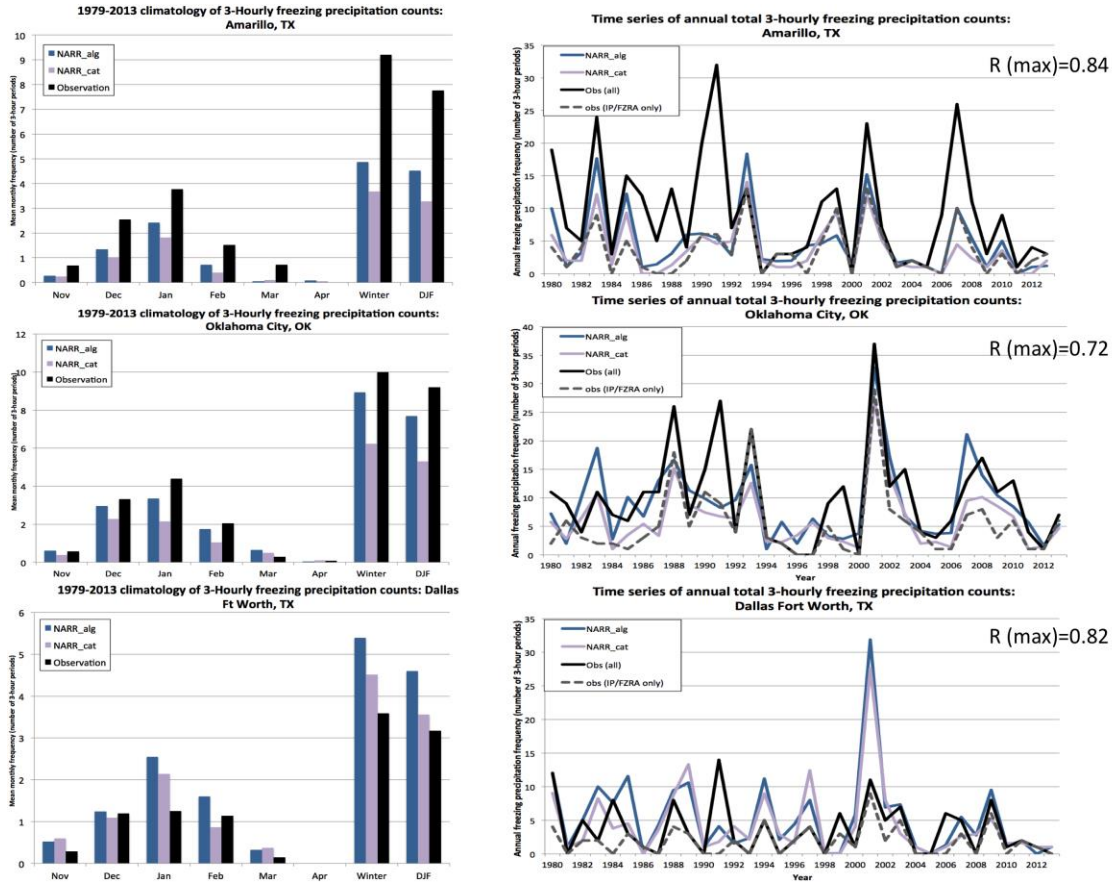


Figure 24: Left panels: Seasonal climatology of freezing precipitation (freezing rain FZRA, freezing drizzle FZDR, and sleet IP) frequency, expressed as the average number of 3-hour periods with ice (1979-2013). ‘NR-Alg’ is the algorithm mean results, based on application of three precipitation type algorithms to the NARR data (see section 2, ‘year 1 activities’), while ‘NR_Cat’ is the NARR native estimates of ice. Observations are from National Weather service observing station sites (‘ASOS’) at Amarillo (top), Oklahoma City (center) and Dallas Fort Worth (bottom). **Right panels:** Time series of winter (November-April) total ice frequency (also 3-hourly). Shown are both NARR-derived products, observations of all freezing precipitation types, and observations excluding freezing drizzle. It is evident from the Amarillo data that magnitudes of the reanalysis-derived ice frequencies are closer to estimates excluding freezing drizzle, as drizzle is not well resolved by the reanalysis. The maximum linear correlations between observations and reanalysis-derived data are shown, indicating high correlations in excess of 0.7 in all three locations.

The climatology of ice and snow in the region shows a very different spatial pattern for ice (freezing precipitation), versus snowfall. The former (Fig. 25a,b) increases north and east, which is consistent with other studies that have sought to develop spatial

climatologies from station observations. The number of hours shown are known to be overestimated in the southern third of the domain, particularly north-central Texas through central Arkansas (e.g., Fig. 24 Dallas Fort Worth). Snowfall (Fig. 25d) shows a latitudinal (south to north) increase in snow frequency, and high frequencies of snowfall over the Rocky Mountains (over 100 3-hour periods). Comparing the frequency of ice to snow via simple ratio (Fig. 25c) reveals an increase in the proportion of winter events in the form of ice to the south, peaking in east central Texas and northern Louisiana. Conversely, farther north and west, more winter precipitation is in the form of snow, with the 1-1 line along the I-44 corridor in Oklahoma, east into northern Arkansas. Freezing precipitation is rare west of the New Mexico border.

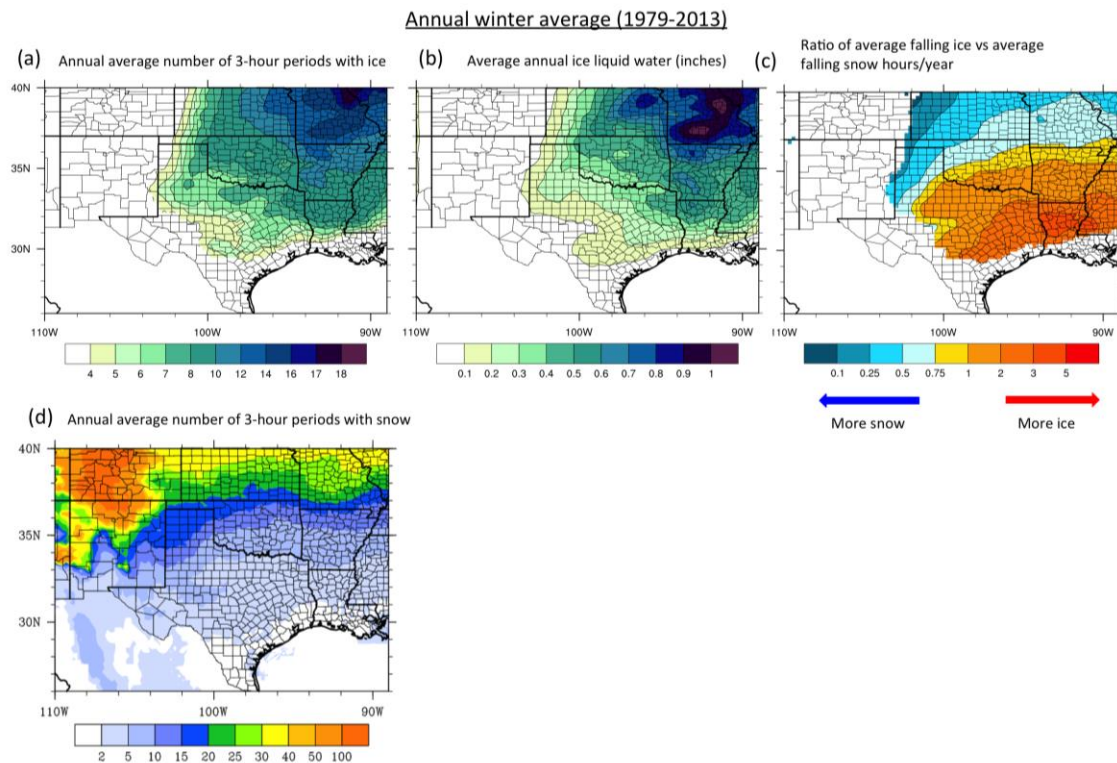


Figure 25: General ice and snow climatological information, derived from a product developed by Co-PI Mullens and PI McPherson, available from 1979-2014 (2015 and 16 data coming soon). **Panel a** depicts the average annual number of 3-hour periods with freezing precipitation, revealing a northeastward increase in frequency through the region. Values over the far southeast domain, including Northern Texas, Louisiana, and south central Arkansas are known to be overestimated compared with observations, and regions to the northwest do not account for freezing drizzle. **Panel b** shows the average annual freezing precipitation accumulation in the form of liquid water equivalent (inches), also showing a northeastward increase. **Panel c** shows the climatological ratio of freezing precipitation to snowfall, with values greater (less) than one implying more (less) freezing precipitation compared with snow. **Panel d** shows the annual average frequency of snowfall (also 3-hourly), which shows a maximum over the southern Rocky Mountains, and a latitudinal dependence over the region.

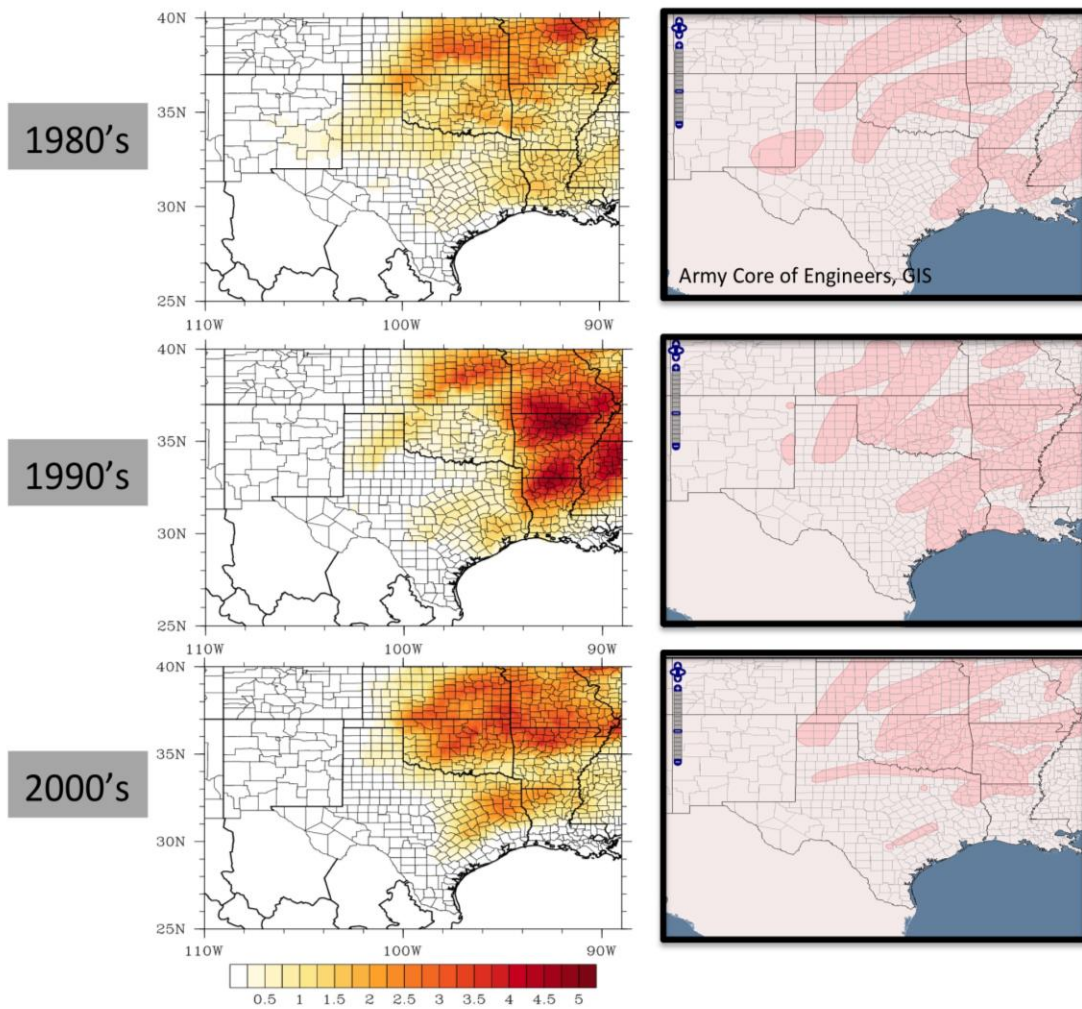


Figure 26: Distributions of multi-algorithm mean freezing precipitation LWE for three decadal periods (inches, left) and locations of 1 in 50 year ice/damaging ice (right) obtained from the Army Core on Engineers [online GIS database](#). While not strictly comparable (more work is needed), qualitatively the regions of high ice liquid water often correspond with areas impacted by multiple events in the historical storm event database.

To evaluate future projections in winter precipitation, we use a simple proxy for winter weather, since the statistically downscaled data did not permit derivation of precipitation type. This proxy was described in Section 2.4. Here, the spatial trends are estimated over each climate division as the percentage difference in mean number of winter precipitation days relative to the historical period (1970-2000). We also derived a measure of winter weather ‘intensity’, as the total annual ice accumulation divided by the number of ice days, and averaged over the reference period. Because intensity tended

to vary somewhat sporadically across climate division, a statewide trend was extracted. Figures 27 and 28 show the results for the mid- and high-emissions scenarios, respectively.

Across all of the climate divisions evaluated (southernmost CDs excluded due to low winter precipitation frequency), there was a projected decline in winter precipitation frequency between 15 and 50% by mid-century, depending on location. The smallest change was projected for southwest Texas, and the greatest change in Arkansas and western New Mexico. Projections for large population centers such as Oklahoma City and Tulsa are a 30-35% decrease in frequency, while Little Rock shows a 41-42% decline, and Albuquerque a 33-35% decline. The intensity change by mid-century appears to vary more substantially with the emissions scenario, and shows a small to moderate increase in average intensity for the whole domain with high emissions (Fig. 28), and little change to slight decrease in intensity for mid-range emissions (Fig. 27). The precise reasons for this disparity have not been investigated, and changes in precipitation intensity are unlikely to be statistically significant, based on large inter-model spread. However, since global emissions are currently tracking more closely with the high emissions pathway, this result may present a near-term shift toward less frequent events exhibiting intensities at least similar to those experienced in the recent past. The late century change is strongly dictated by the magnitude of global warming, and so high emissions implies a greater decrease in winter precipitation frequency, typically ranging from 68-85%, and once again being largest over portions of Arkansas, Louisiana, and western New Mexico. Oklahoma City and Tulsa now show decreases of 72-75%, Little Rock 80%, and Albuquerque 74% (Fig. 28). A mid-range late century change estimated lesser reductions of 30-62% (Fig. 27). Conversely to the mid-century result, late century high emissions reduced winter precipitation intensities over Texas and Louisiana, and show only a small change for Oklahoma and Arkansas. Lower emissions show similar patterns, but with smaller values, generally inferring weak changes in these areas. New Mexico showed a more discernable positive change in intensity, particularly for a mid-range emissions pathway. This is largely concentrated in the mountainous northern and western climate divisions (not shown), implying that snow events in northern New Mexico will decline substantially in frequency, but could potentially contribute similar or slightly greater amounts of precipitation equivalent in a smaller space of time.

Mid-range Emissions

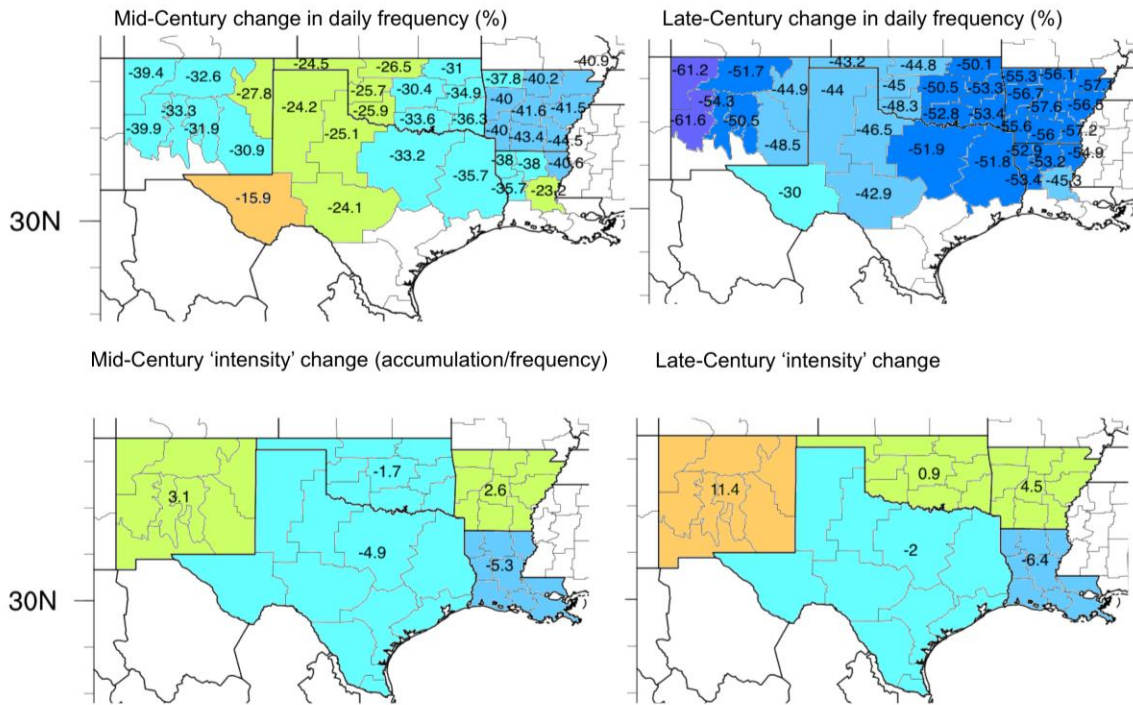


Figure 27: Mid-range emissions climate projections in winter precipitation (ice/snow) daily frequency, expressed as a multi-model mean percentage change from the historical (1970-2000) average, and aggregated over climate divisions. **Top left panel:** difference in winter precipitation frequency for the mid-century, **Top right panel:** difference in winter precipitation frequency for the late-century. The bottom two panels show the average winter precipitation intensity change for the same periods, and expressed as a state average. Values within 5% of the historical period suggest very little change. Generally, the percentage changes in frequency for mid-century are between 15 and 45%, lowest in SW Texas, followed by the southern High Plains. Decreases over New Mexico, Oklahoma, and north Texas are between 30-40%, while Arkansas is generally 40-45%. A similar pattern is projected for late century, but with reductions between 30 and 60% (the greatest reductions are over northern New Mexico). Intensity changes are within plus or minus 5% (give or take 1%) during the two periods for all states except for New Mexico, which shows an 11% positive intensity change during the late 21st Century.

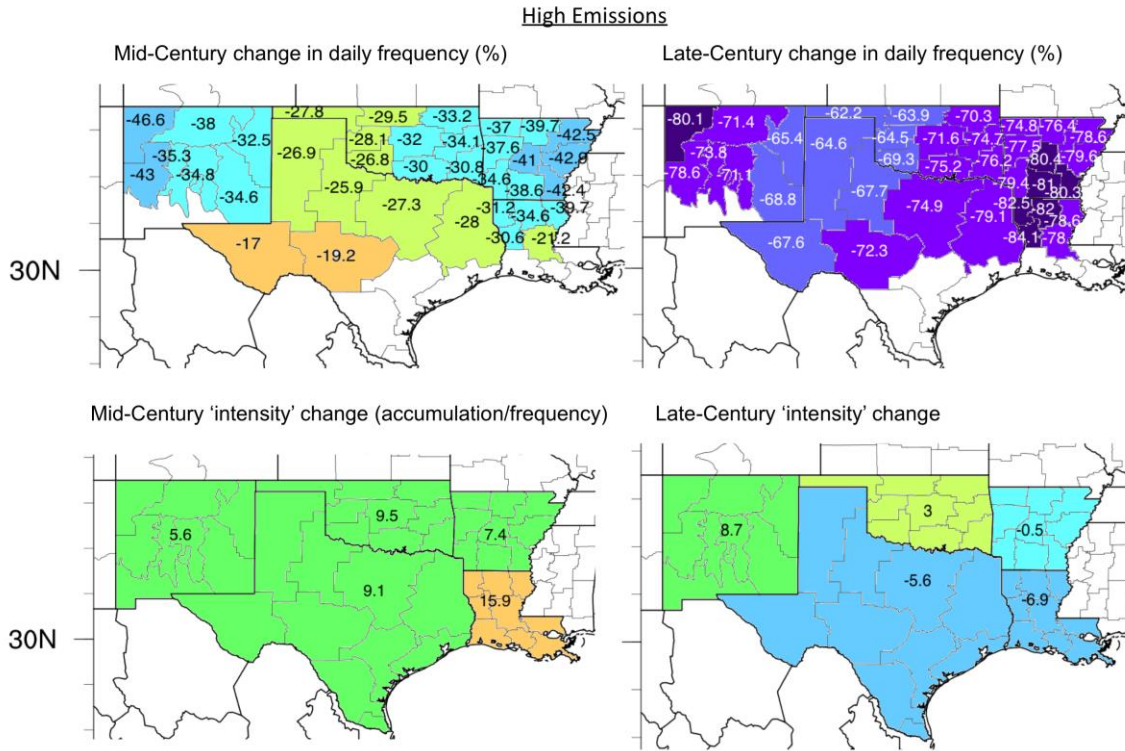


Figure 28: As Fig. 27, but for high emissions. There are some sub-regional differences compared to the mid-range, mid-century projection, however for the region as a whole, the range of the decreases are similar (15-45%), with highest decreases over Arkansas, and far western New Mexico. The spatial pattern of the decreases is similar later in the century, but the magnitude of the decrease is larger, typically 60-70% (southern High Plains), 70-80% (eastern Oklahoma into Arkansas, and North Texas), and 80-80% (southern Arkansas, northern Louisiana, and far western New Mexico). The mid-century change in intensity is an increase across all states, greater than 5% for all states, but within 10% for all except Louisiana (15.9%). The late century change is within plus to minus 7%, and is generally slightly negative with the exception of New Mexico (+8.7%).

3.4 CASE STUDY: WINTER CONDITIONS IN CENTRAL OKLAHOMA

Historically, Oklahoma City experiences an average of 65-70 freeze thaw cycles annually, oscillating between 55 and 90 for any given year during the past 65 years of record, shown in Figure 29. Enhanced freeze thaw cycles make up approximately 18% (close to 1 in 5) of FTCs, oscillating in a given year between 4 and 25 days. Probability distributions of T_{\max} and T_{\min} during FTC (Fig. 29, top), reveal typically T_{\max} in excess of 40°F , and often above 50°F . Minimum temperatures range from just below freezing, and very rarely below 0°F . Infrastructure present in the region for at least the past 50 years is estimated to have experienced nearly 3500 FTCs, and close to 700 EFTCs. Since 1948, the average annual number of FTCs and EFTCs has gradually declined, with some recovery after the year 2000. A linear trend reveals a decrease of approximately 1 FTC per decade.

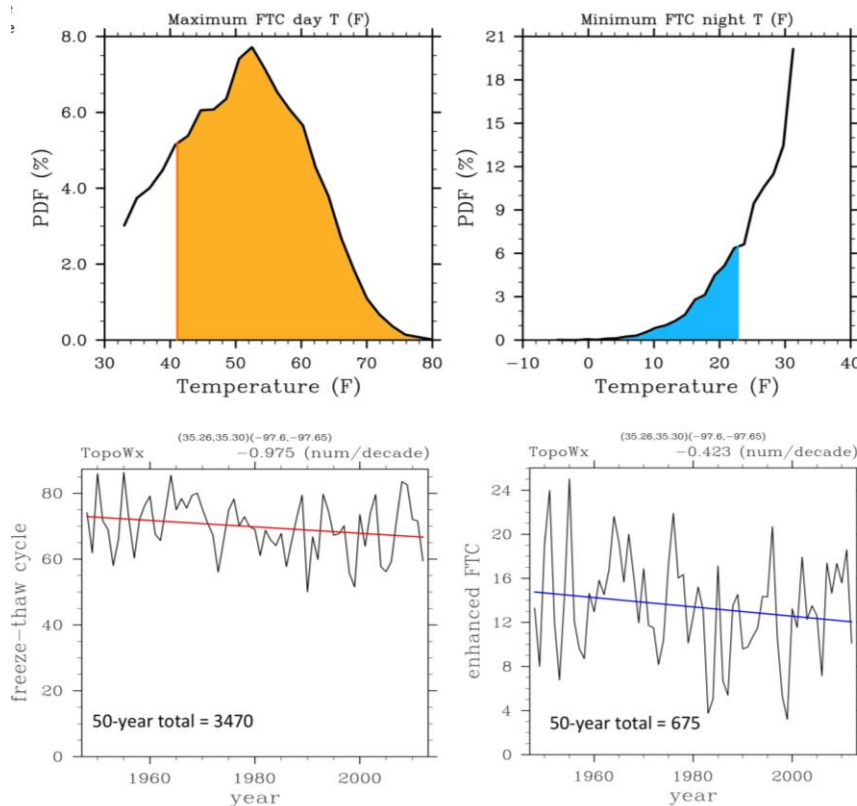


Figure 29: Freeze-thaw statistics for Oklahoma City, based on 1948-2012 data (Topographic Weather, Oyler et al. 2012). A small grid was defined that encompassed the City, and the 1-km data was averaged over this grid. **Top:** probability distributions of T_{\max} (left) and T_{\min} (right) during FTC, with values at or greater than the criteria for EFTC shaded. **Bottom:** Time series of FTC activity from 1948-2012, FTC (left), and EFTC (right), including an estimated linear trend. A description of this information is provided in the text.

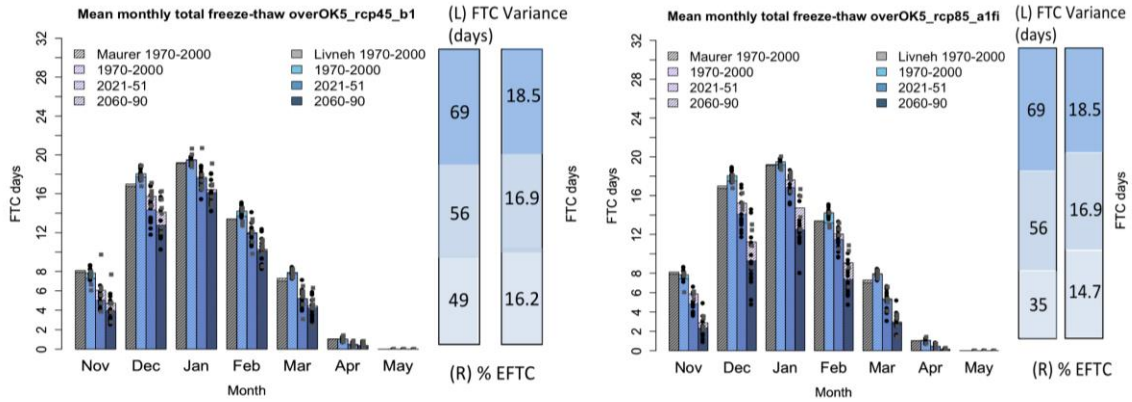


Figure 30: Future projections of monthly freeze-thaw activity. **Left panel:** Mid-range emissions showing the observations (Maurer and Livneh); the model historical average (MACA and ARRM are displayed separately and overlaid, as MACA=solid, and ARRM=stippled bars); the model mid-century; and the model late-century for months November through April. Individual model projections are shown by the black square markers (MACA), and grey square markers (ARRM). The vertical bars on the right hand side of the figure show the change in freeze-thaw cycle variance on the left, and proportion of freeze-thaw cycles that meet the ‘enhanced’ criteria (right). **Right panel:** As left panel, but for high emissions. The trends depicted in this figure are discussed in the text.

The future of freeze-thaw cycles in central Oklahoma is expected to be a continued average decline throughout the 21st century (but with year-to-year variability), with the precise magnitude being largely a function of whether or not the trend in greenhouse gas emission growth is abated. Figure 30 shows a bar plot of projected monthly freeze thaw days for the one historical and two future reference periods, also displaying the observed FTC counts. Oklahoma City is likely to experience an average reduction of FTCs of at least 20% by mid-century, and 50% by late century with high emissions, and 20% by mid century, and 30% by late-century with moderate emissions. There is variation amongst the models used for the projection, with some models showing little to no change in FTCs through peak winter, however more than ¾ of models do show a reduction in all seasons, and the vast majority of models show the most pronounced FTC decreases during early and late winter (e.g., November, December, March, April). The variance of FTC days decreases, as does the number of EFTCs, which declines from an average of 1 in 5 to 1 in 7 FTC days with the highest emissions pathway. Mean T_{max} and T_{min} during FTC show little change, however the lowest T_{min} values are a few degrees warmer in the future projections (not shown).

Oklahoma City temperature variations during peak winter were assessed by projections of average maximum and minimum temperature for each year. Figure 31 shows results for the mid and high emissions scenarios (top and bottom, respectively), and overlays the historically observed values extending back to 1960. The spread of all model results encases the observed range, so the models are adequately depicting the potential range of values through this period. Both the mean of the warmest and coldest temperatures in a given year show an increase of up to 10°F between the historical period and the year 2100. The near-term (< 10 years) projections for cold temperatures suggest that some models continue to support the possibility of extreme cold (less than -10°F), and potentially a larger range of annual winter temperature variation. In fact, most models project an increase in the seasonal temperature range, particularly for spring and fall, where the temperature range increases by 2-3°F on average (not shown). This projection is true of both emissions scenarios, but particularly for the higher emissions. After 2050, the high-emissions pathway of increasing temperature trends accelerate, and days below 0°F become rare compared to the historical period, while very warm winter days (>80°F) increase in frequency.

Winter precipitation in central Oklahoma consists of freezing rain, sleet, and snowfall. Ice and snow days are roughly equal in the long-term average, with a mean of 4 (4.5) days per year for ice (snow), with the precipitation types often occurring within the same storm system(s). Figure 32 shows recent trends and statistics for Oklahoma County compiled from our dataset. There is generally high year-to-year variation in ice and snow. Since 1980 (and before 2014), ice events peaked during the winter 2000-01 in terms of frequency, and both 2000-01 and 2007-08 in magnitude. Both ice and snow showed a slight decline in frequency; however, snowfall days appeared to be decreasing faster than freezing precipitation days. Magnitudes showed an increase in variability and intensity since the year 2000, contributing to a slightly increasing trend. The peak month for freezing precipitation was January, followed by December and February. Significant ice events occurred once every 7 years on average, with moderate icing once every 2-3 years.

Future projections in winter precipitation days for central Oklahoma, shown in Fig. 33, confirm the aforementioned decline in mean frequency, with a mid-century decrease of approximately 1 day per year, and an end of century decrease of up to 3 days per year. Most of the decline in winter precipitation frequency occurs after the year 2020.

The model range suggests the potential for seasons with higher snow/ice frequency equivalent to the historical period through mid-century, but with a more marked reduction for all models late in the 21st century. The near-term (5-25 year) future therefore suggests a general decline of ~10-20% (0.4-1 day), but with the continued potential for high impact ice and snow storms.

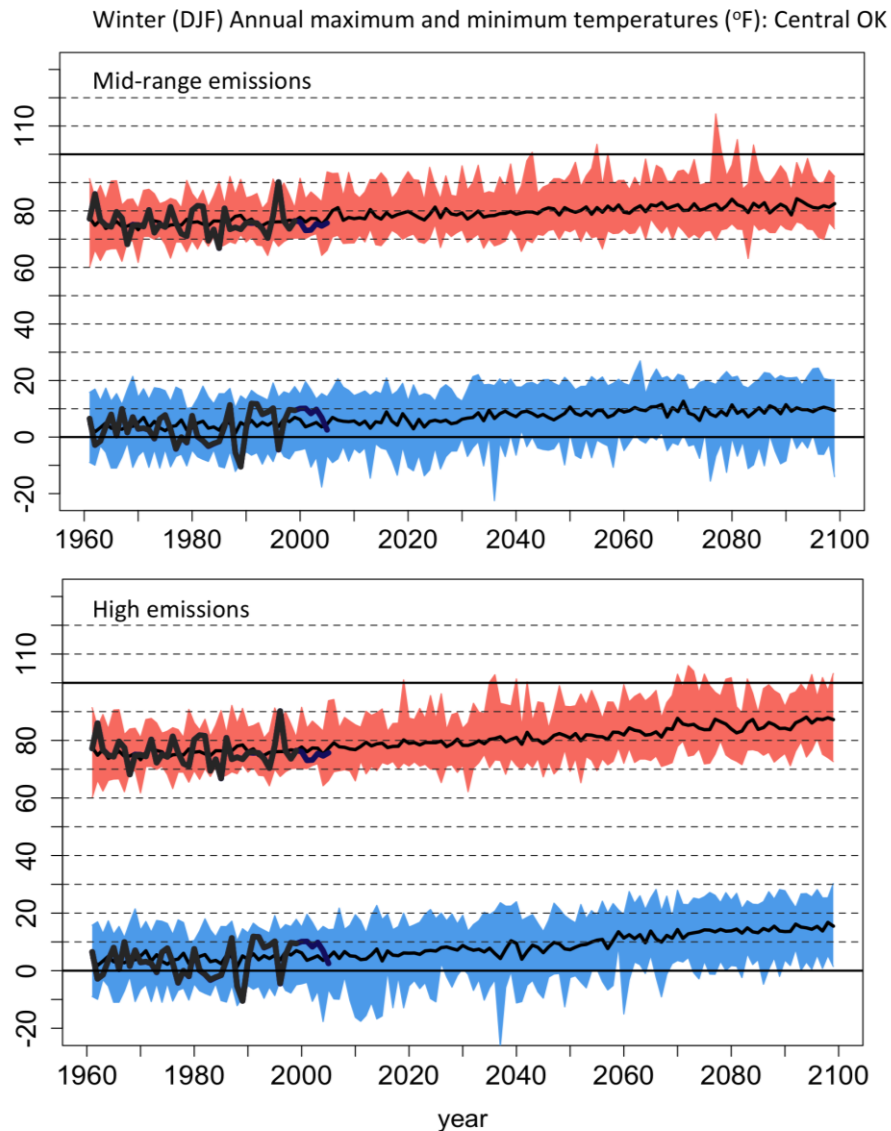


Figure 31: Annual highest and lowest temperatures in the OKC area during the peak winter season (December-January-February) as simulated by climate models. The multi-model mean is depicted by the thin black line, and the model spread the shaded polygon. The thick dark grey and blue lines show the Maurer and Livneh observed temperatures respectively. **Top panel:** mid-range emissions, **Bottom panel:** high emissions. The model spread encapsulates the range of the historical observed conditions, indicating that the past variability is relatively well constrained. The trends depicted are discussed in the text.

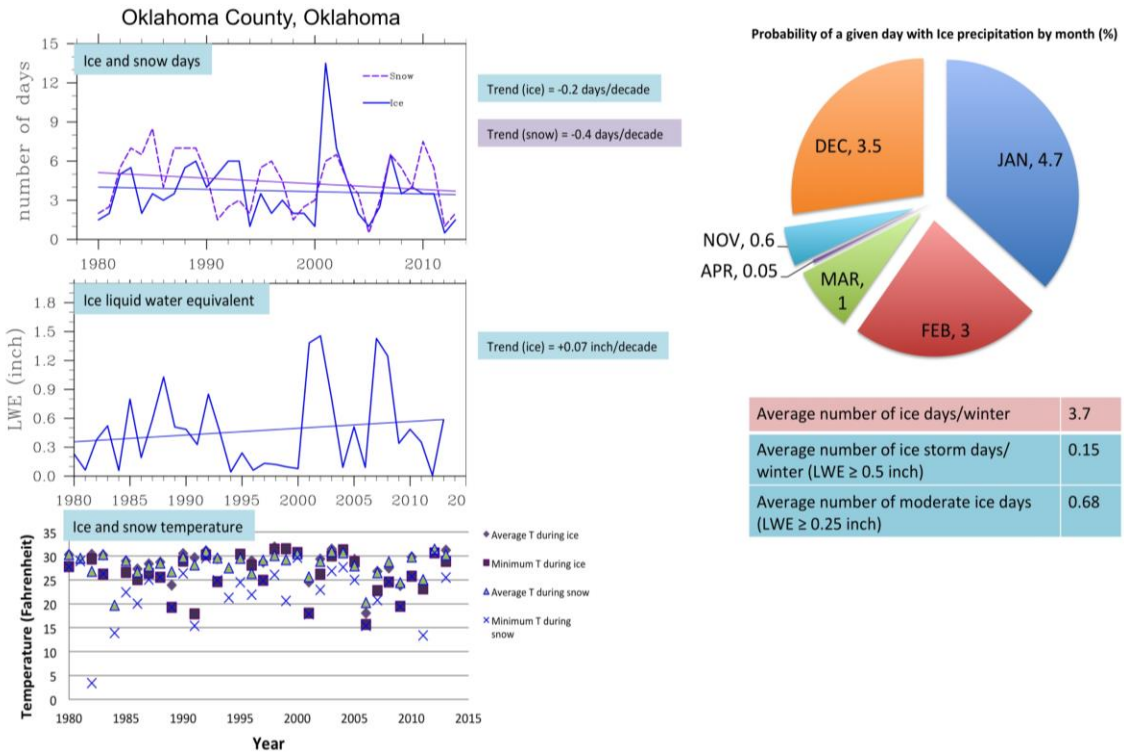


Figure 32: Output from the freezing precipitation dataset developed by Mullens and McPherson (2017), with statistics and time series shown here for Oklahoma County, OK. **Top left panel:** Time series of freezing precipitation (blue) and snowfall (purple) days 1979/80-2013/14, with a linear trend line. There is year-to-year variability in the counts, with a mean of approximately 4.5 days (snow), and 3.7 days (ice) and a general slight decreasing trend (not significant). **Center left:** Time series of freezing precipitation liquid water equivalent in inches, with a linear trend line. Prior to the year 2000 the peak LWE was lower and less variable than after 2000. **Bottom left:** Time series scatter plot of temperatures (daily average and daily minimum) during snow and freezing precipitation. In most cases temperatures range between 25 and 32°F with no apparent trend since 1979/80. **Right hand side:** Pie chart depicting the percentage probability that any given day in a given month experiences freezing precipitation. The peak month is January, followed by December, February, then March. Below this are some statistics regarding the frequency of moderate ice days and ice storm days in any given year (estimated).

In summary: For Oklahoma City, cold-season hazards, such as winter weather, cold temperatures, and freeze-thaw cycles, are projected to decline over the 21st Century. For a planning horizon of 5-10 years, there is likely to be little change from recent historical conditions and extremes, however by 20-50 years from present, transportation infrastructure is likely to benefit from reduced winter degradation, and reduced necessity for winter maintenance. Winter-related safety hazards will also decline in frequency; however, people may become less used to navigating hazardous winter conditions as

they become less common, potentially leading to exacerbated disruption when these events do occur.

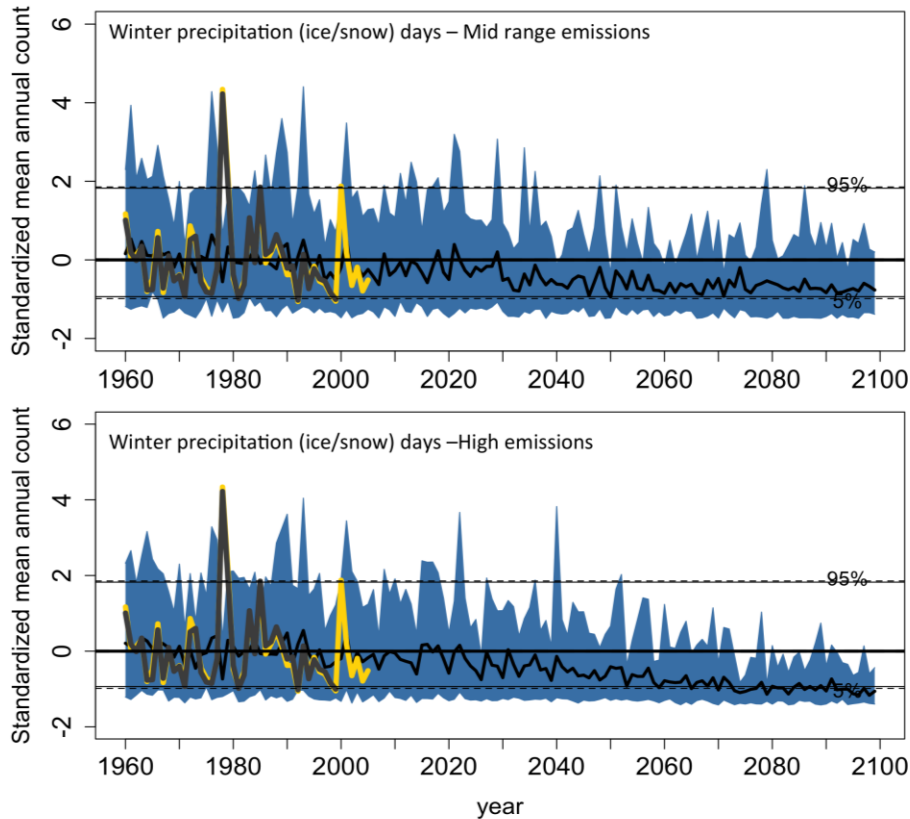


Figure 33: Time series of the standardized winter precipitation (ice/snow) frequency (days) for Oklahoma climate division 5, encompassing Central Oklahoma. Standardized units are based on the departure of values from the standard deviation of the data, so a unit of 1 for example would indicate data is roughly 1 standard deviation above the mean (the mean used was the historical period). The black line is the multi-model mean, and the blue shading the mode 5th-95th percentile range. Observed data is the grey (Maurer) and yellow (Livneh) lines, and the 5th and 95th percentiles of the observed data are shown by the horizontal dashed black lines. The model suite captures the range of historical variability, and it can be seen that with both mid and high emissions, that winter precipitation in the form of ice and snow declines over the 21st Century, particularly after mid-century with high emissions.

3.5 EXTREME HEAT: PAST AND FUTURE

Extreme heat, like extreme cold and freeze-thaw, can lead to wear and premature failure of pavement. Asphalt can soften resulting in rutting, or can crack in very dry conditions, while concrete can heave at joints. Thermal expansion of roads and bridge joints is exacerbated with unusual or persistent heat. Railroads are sensitive to heat, and

the risk of buckling of rail lines increases when temperatures exceed 110°F (OFCM, 2002). In some cases, hot days require speed restrictions due to the potential for damage on the track, e.g., Amtrak reduces speed when the track temperature is over a certain threshold (Amtrak, 2015). Road and rail maintenance activities can be more challenging during extreme heat, particularly to the health of workers. Restrictions on activities during the hottest part of the day can begin when temperatures exceed 85°F, and persistent or extreme heat may require crews to schedule work at night, or reduce the length of activity, which may prolong maintenance (OFCM, 2002).

During the summer of 2011, extreme and prolonged heat and drought affected Oklahoma and Texas, and road heaving and buckling was reported during this time ([News on 6](#), July 11 2011). Older and highly trafficked roads, or those with less suitable performance grade (PG) asphalt binders may be more susceptible to damage. Buckled highways represent a safety hazard for motorists, and high road-surface temperatures can be exacerbated in areas where traffic volumes are high, such as freight corridors. Other traffic-safety hazards during extreme heat include tire blowouts and engine overheating (Liu et al. 2015).

Historically, the frequency of days at or above 100°F in the SPTC domain are greatest in south Texas along I-35 between Laredo and San Antonio (30-40 days per year). Other areas include west Texas east of the Guadeloupe Mountains (20-30 days), and southwestern Oklahoma into northwestern Texas (20-30 days). Days above 100°F are comparatively rare (< 5 days per year) throughout Louisiana, Arkansas, and the northern half of New Mexico. These spatial distributions are shown in Figure 34. The multi-climate model historical mean (Fig. 34, right) reproduces the spatial pattern and frequency of 100°F days well. While not shown, days at or above 110°F show a similar spatial distribution, but reduced frequency.

Figure 35 shows the projection of 100°F days to mid and late century for the mid-range emissions pathway. Even by mid-century, there is a pronounced increase, a doubling to tripling, of the frequency of these temperatures (a similar trend is apparent for days above 110°F). The spatial distribution remains similar, and the peak regions are those mentioned. Areas close to the Mexico border show mid-century increases to 60-80 days per year. Portions of New Mexico and the Gulf Coast still show little change (largely

reflected by the topography or ocean moderation of temperature, respectively), while Arkansas and northern Louisiana increase to 10-20 days per year.

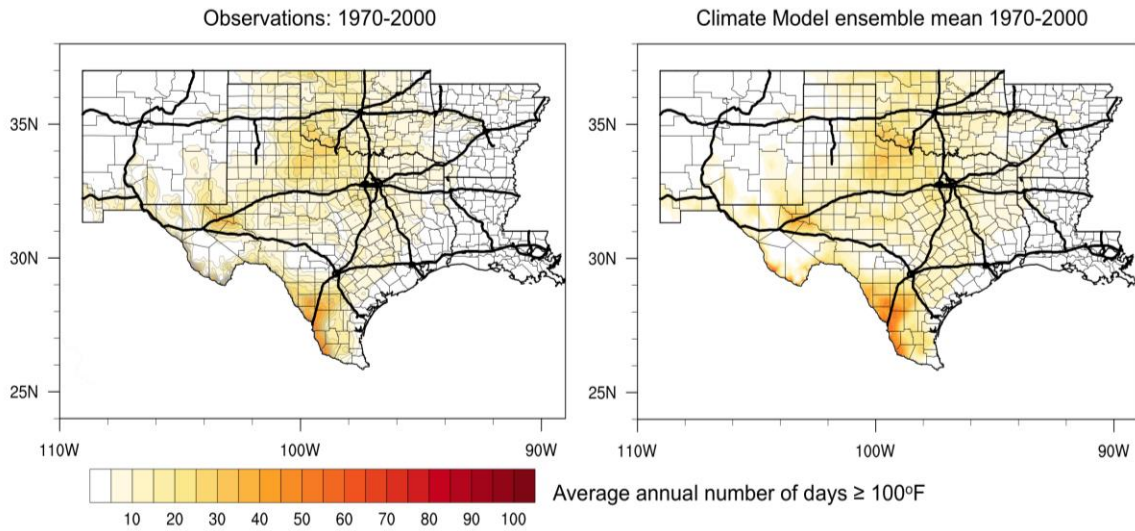


Figure 34: The average annual number of days $\geq 100^{\circ}\text{F}$ over the SPTC domain, based on historical period 1970-2000. **Left panel:** average of the two observations (Maurer and Livneh), **Right panel:** Multi-model historical mean (21 models). Interstate highways, State and county boundaries are shown. This figure is described in the main text.

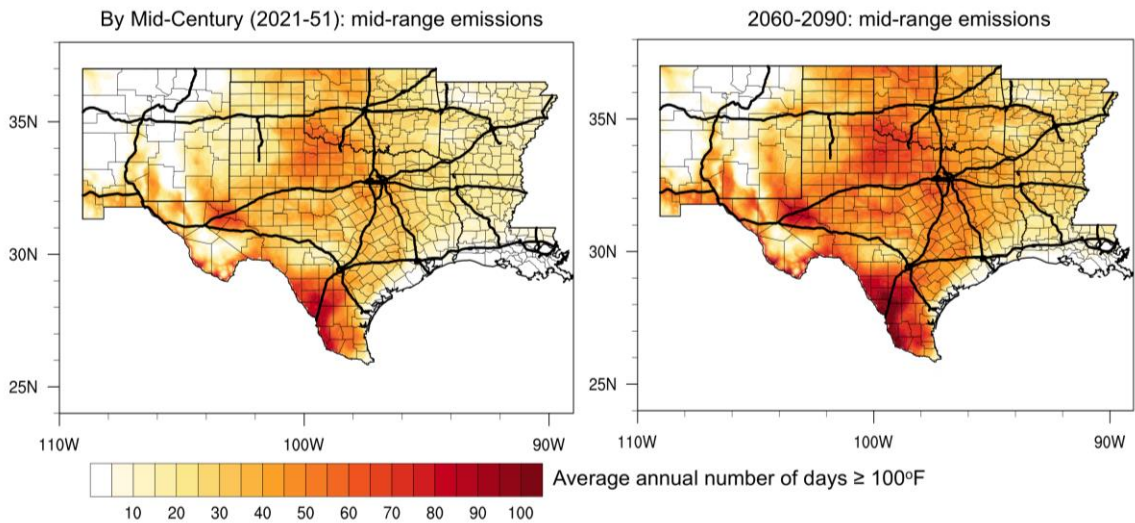


Figure 35: The average annual number of days $\geq 100^{\circ}\text{F}$ over the SPTC domain, based on future climate projections using the mid-range emissions scenarios. **Left panel:** Mid-century projections (2021-51). **Right panel:** Late century projections (2060-90). Interstate highways, State and county boundaries are shown. The results shown by this figure are described in the main text.

Figure 36 shows the projection of 100°F days to mid and late century for the high emissions pathway. While the mid-century increase is similar to the mid-range emissions scenario, the later-century change is substantial, a 600-800% increase in frequency at this, and higher, thresholds at any given location, excluding the coast and the high-elevation regions of New Mexico. By late-century, a location such as Dallas/Fort Worth could experience 70-80 100°F+ days annually, versus 10 in the historical period, and Laredo well over 100 days annually, versus 30-40 historically. Notably, this work does not include the possible impacts of and to the urban heat island. These changes have the potential to significantly stress infrastructure with a planned lifetime of 20 or more years that is being constructed today, and would be particularly important for long-duration infrastructure such as bridges and dams (with lifetimes of 50-100 years).

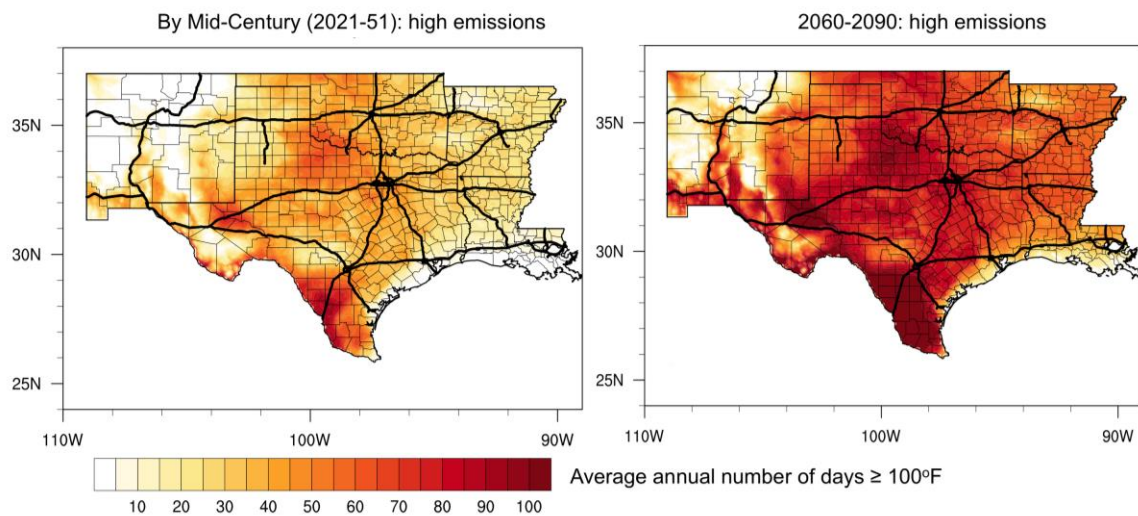


Figure 36: The average annual number of days $\geq 100^{\circ}\text{F}$ over the SPTC domain, based on future climate projections using the high emissions scenarios. **Left panel:** Mid-century projections (2021-51). **Right panel:** Late century projections (2060-90). Interstate highways, State and county boundaries are shown. The results shown by this figure are described in the main text.

3.6 CASE STUDY: EXTREME HEAT IN OKLAHOMA CITY

Central Oklahoma, including the Oklahoma City metropolitan area, experiences an average of 10 days at or above 100°F per year (temperatures exclude consideration of humidity and winds), based on a 1970-2000 average. The region also has a day over 110°F typically once every few years. The hottest air temperature recorded by in situ

observations in the city was reportedly 113°F in 1936 and 2012 ([National Weather Service](#)), and temperatures during the 1930s were historically on par with some of the recent hot extremes seen in the state (e.g., Hutchison 2008). The greatest number of 100°F days on record was 2011, with approximately 65 in central Oklahoma, and 2-5 days above 110°F.

The decadal projections of 100°F days are shown in Figure 37 for mid-range and high emissions. The historically observed values are also presented for verification of the simulated historical period. Range bars depict the 5th-95th percentile of annual counts over each decade, and bars and range bars for ARRM (stippled) are overlaid on MACA (solid). To the top of the figure, the multi-model mean number of years in each decade with at or greater than 65 100°F days is shown (top) to represent the possible future frequency of 2011-like conditions. The numbers below this are the maximum values from the multi-model ensemble, depicting the 'worst case'. The increase in 100°F days is clearly apparent from both statistically downscaled datasets, however the MACA mean (n=15) has a tendency to show a larger change than ARRM (n=4 for A1FI, n=6 for B1). Furthermore, differences between moderate and high emissions become apparent after 2040, when the latter begins to accelerate the frequency of very hot days. For the decade 2040-50, a mid-range projection suggests a 2011-like year on average every 20-years (with the warmest model every 5 years), while for the high emissions this increases to every 7 years (2 years for the warmest model). A 2011-like year is the average, occurring every other year, by later in the century for the high emissions scenarios. A similar pattern was confirmed for consecutive days above 100°F and days above 110°F.

The length of the season of very hot days also increases considerably, shown in Figure 38. The historical average onset and end dates for 100°F has been typically the second week in July through last week in August respectively. However, multi-model projections suggest a gradual lengthening of this period, to late June through the start of September by mid-century, and, with the highest emissions, late May through late September (a lengthening of approximately 10 weeks) by late 21st century. There is evidence that the change is more extensive for late spring into early summer, meaning a more rapid onset of very hot conditions in a given year. For context, the 2011-heatwave had an onset and end of 100°F days of June 25 and September 13, respectively, in Oklahoma City (National Weather Service). Cowan et al. (2016) noted that summers in

the Great Plains that follow anomalously dry springs tend to be hotter, with this heat beginning earlier in the season and lasting for longer. Their analysis examined the persistent hot summers during the 1930s. This relationship suggests that future dry summers in Oklahoma are likely to be accompanied by drought, with further implications for transportation.

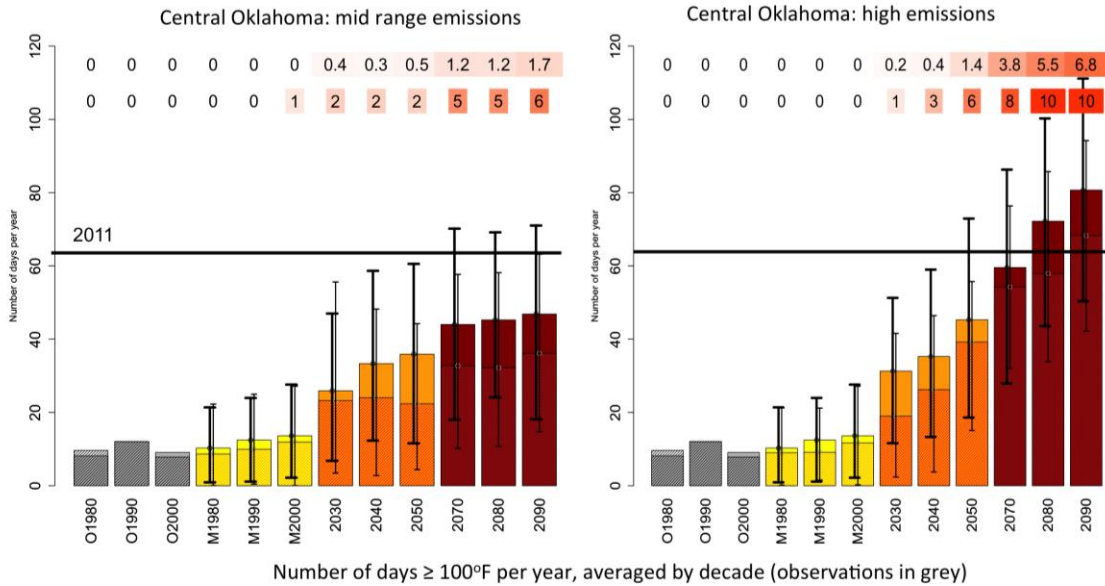


Figure 37: Decadal climate projections for average annual number of days $\geq 100^{\circ}\text{F}$, shown here for Oklahoma climate division 5, which is central Oklahoma. The decadal periods include historical, ending 1980, 1990, 2000 for observations (grey), and climate model mean (yellow), Future ending 2030, 2040, 2050 (orange), 2070, 2080, 2090 (red). The solid bars are MACA, and the stippled bars ARRM. The range bars are the 5th-95th percentile range of all annual counts of 100°F days. The horizontal line is the number of 100°F days during 2011. The values at the top of the chart show (top) the average number years with 2011-like summers in each decade, and (bottom), the maximum number of 2011-like summers in each decade. **Left panel:** mid-range emissions, **Right panel:** high emissions. The results of this graphic are described in the main text.

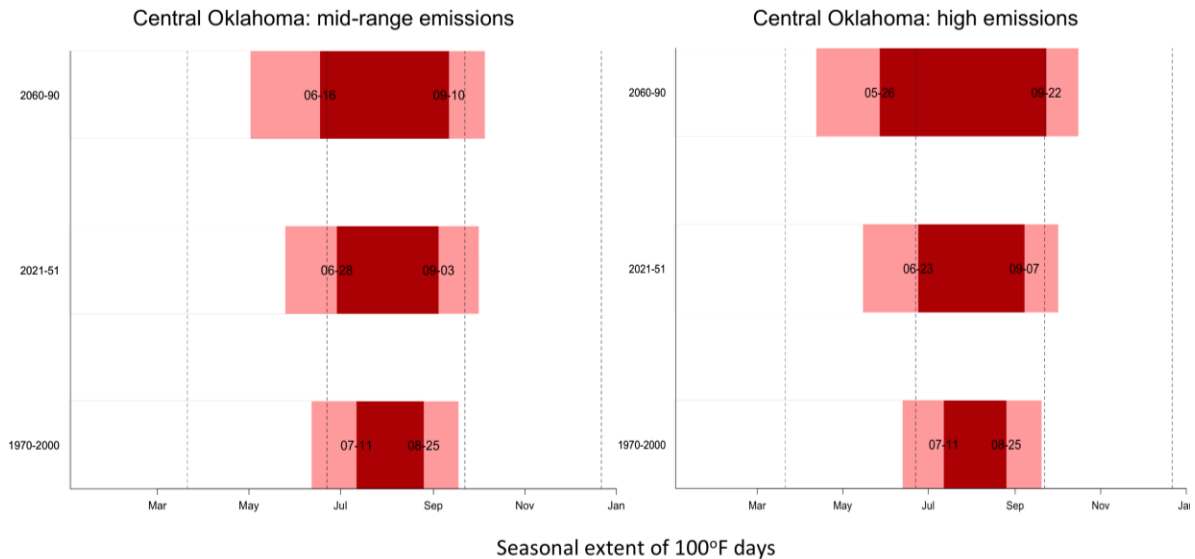


Figure 38: Historical and future projections of the average onset and termination of 100°F days for a given year, based on all MACA and ARRM models used in this work. Bottom: 1970-2000, center: 2021-51, Top: 2060-90. The red box and dates depicted are the mean values, while the lighter pink shading denotes the 5th-95th percentile earliest/latest dates. Vertical dashed lines depict the equinox dates. **Left panel:** mid-range emissions, **Right panel:** high emissions.

Peak temperatures during the hottest part of the year in Oklahoma are also projected to increase. Figure 39 shows the minimum and maximum temperatures in central Oklahoma for a given year between 1960 and 2100, with historical observations overlaid, and a model spread denoted by the shaded polygon. Presently, the maximum air temperature in any given year averages to near 105°F for the Oklahoma City area. This value shows a gradual increase, such that, by 2030, peak maximum temperatures may be a degree or so higher; but the model spread increases, suggesting increased frequency of very high temperatures (> 110°). By late century, the high emissions scenarios project a mean annual peak maximum of 115°, with some potential for temperatures over 120°F. The high emissions pathway also warms the coolest (often nighttime) temperatures during this season.

Currently, most PG-binders for asphalt in the state occupy the range 64-22, up to 76-28. These numbers refer to the highest average consecutive 7-day high and lowest average consecutive 7-day low temperature at 20mm below the pavement surface in degrees Celsius (e.g., 64°C high, to -22°C low) that the asphalt can handle. How hot the pavement temperature gets is a function of the air temperature, traffic loads (particularly for heavy freight), and potentially also the duration of hot temperatures. Clearly, the

projected temperature increases could impact the performance of certain asphalt binders, and necessitate a change in the binder used. With the temperatures of Oklahoma City potentially approaching those of Phoenix, AZ later in the century, with a high greenhouse-gas emissions pathway, it may be prudent to examine how hot climates such as southern Arizona design and maintain infrastructure to withstand heat. Modeling of pavement temperatures based on climatological data by Yavuzturk and Ksaibati (2002) calculated PG70-10 for the Phoenix area, **suggesting that, at least for high temperatures, Oklahoma City PG grades of less than 70 may not be adequate for the anticipated temperature conditions within the next 50 years.**

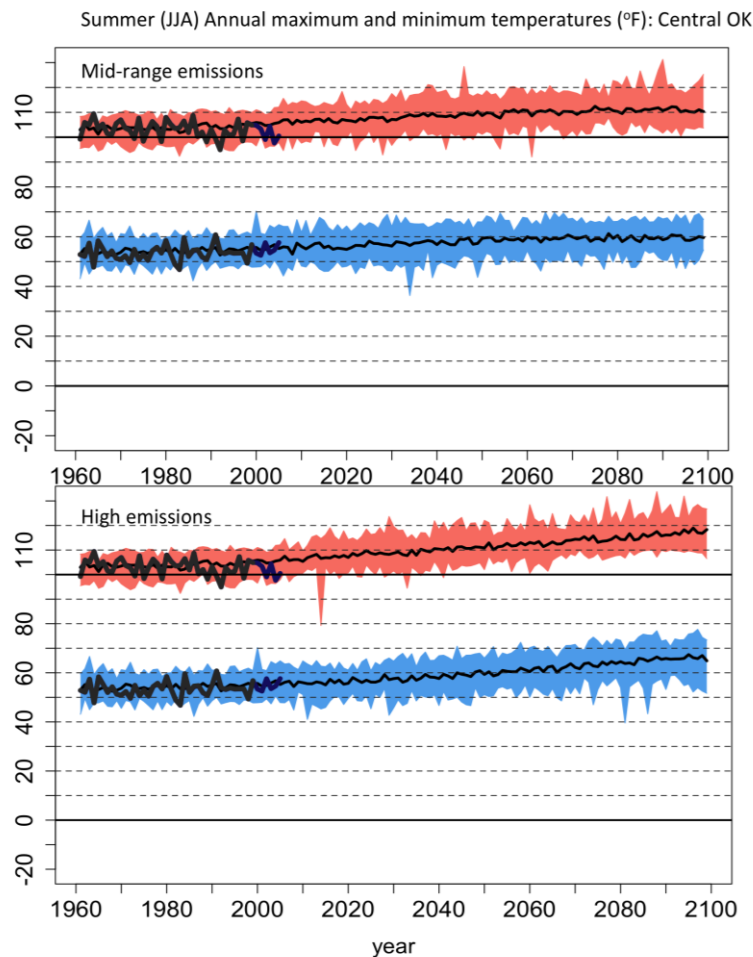


Figure 39: Annual highest and lowest temperatures in the OKC area during the peak summer season (June-July-August) as simulated by climate models. The multi-model mean is depicted by the thin black line, and the model spread the shaded polygon. The thick dark grey and dark blue lines show the Maurer and Livneh observed temperatures respectively. **Top panel:** mid-range emissions, **Bottom panel:** high emissions. The model spread encapsulates the range of the historical observed conditions, indicating that the past variability is relatively well constrained. The trends depicted are discussed in the text.

3.7 HEAVY PRECIPITATION: A CASE STUDY FOR CENTRAL OKLAHOMA

Heavy precipitation has become a particularly salient hazard for portions of the SPTC domain after recent episodes of significant flooding. According to NOAA ([NCEI, 2017](#)), since 2010, the region has experienced six billion-dollar disasters related to flooding (three in 2016 alone). These events occurred mostly in Texas, Louisiana, and Oklahoma, leading to an estimated \$22.8 billion in damages. In contrast, the prior 30-years (1980-2010) had six events amounting to \$18.4 billion (excluding tropical cyclones). Also since 2010, Oklahoma City has had three particularly noteworthy events, including 31 May 2013, when a slow moving thunderstorm produced rainfall of approximately 8 inches over 4 hours during rush hour. Nine fatalities, and widespread road and street flooding were reported. On 14 June 2010, storms produced heavy rainfall of 8-11 inches in 24 hours, setting a rainfall record for Oklahoma City's Will Rogers World Airport. The Canadian River rose 4 feet above flood stage in eastern Oklahoma City. More recently, the first-ever 'flash flood emergency' was issued from the NWS during an event that resulted in over 7 inches in 24 hours on 6 May 2015. Most of this precipitation occurred during the evening and overnight hours, and resulted once more in widespread street flooding and travel disruption.

The impacts of inland flooding on transportation systems are often most apparent in the disruption they cause to traffic movement and the risk of injuries and fatalities ("turn around don't drown"). However, heavy precipitation and road inundation may also degrade, scour, or even wash out roads (particularly if water can infiltrate the subgrade), damage bridge supports, and promote embankment slope failure.

The Federal DOT requires that road infrastructure meet certain flood-frequency standards. For Oklahoma DOT (ODOT) guidance, the flood frequency is typically based on rainfall intensity-duration-frequency (IDF) curves. The Oklahoma DOT drainage manual, [chapter 7](#) (hydrology) displays IDF curves for 8 regional zones. The data used to construct these curves was from the U.S Geological Survey, [USGS-WRI report 99-4232](#), published in 2005 (Tortorelli et al. 2005), which has been recently updated by NOAA Atlas 14 (NWS). The manual also notes the assumption that a given return-period rainfall amount would be analogous to the same return-interval flood, and it describes the limitations associated with such an assumption (e.g., location specific factors such

as soil type, antecedent moisture, hydrologic characteristics). Most freeways, principal arterial roads and high-traffic minor arterial roads at the state level (including underpasses) must be able to withstand a 1-in-50-year event; however, more local roads, and some urban roads and collectors are only required to withstand a 1-in-10-year event (ODOT Drainage Manual, Tables 7.1A, B). Some more sensitive infrastructure, such as bridges and drainage systems with no embankment overflow relief, are built to withstand a 1-in-100-year event.

In recent years, some studies have suggested that the effects of climate change are already evident in changing patterns and frequency of intense rainfall events. New York state's historical 100-year events have been estimated as a 1-in-66-year event during 1980-2010 (e.g., Eggleston et al. 2016, DeGaetano 2009). Many other regions also show a positive trend in the magnitude of precipitation associated with a given return period. This apparent non-stationarity means that return periods calculated prior to the most recent 10-20 years may already be underestimating the frequency and magnitude of extreme precipitation (e.g., Cheng and AghaKouchak, 2014).

Here, we evaluate potential changes to central Oklahoma's extreme precipitation by calculating return periods of daily accumulated rainfall from 2 to 100 years, based on annual maxima¹ in the central Oklahoma Climate Division (CD5) for the one historical and two future reference periods used throughout this study. Unfortunately, the daily data did not permit investigation of sub-daily precipitation intervals that would be used to generate IDF curves. There are some statistical approaches to disaggregating daily data; however, such an analysis was outside the scope of this work.

Our analysis is conducted for the two observational datasets (Livneh and Maurer) and for all climate models and emissions scenarios. The calculation of return-period frequency requires fitting an extreme-value distribution to the annual precipitation maxima, realizing that each distribution will tend to produce a different estimate. Some common distributions, such as Gumbel, will tend towards under-fitting peak rainfall

¹ While it is common to use block maxima, we selected the top 99.5th percentile value of annual precipitation over each CD. This was to avoid a possible effect of very small-scale (~order of a few grid points or less) precipitation maxima that could have been unrealistic when compared to its broader surrounding values. This can occasionally occur with interpolated precipitation, or result from uncertainties in the statistical downscaling process.

extremes, therefore offering a more conservative estimate, while the Generalized Extreme Value (GEV) method tends to overfit to the most extreme of the extremes (M. Richman, personal communication). Our work considered both Gumbel and GEV in a dynamic approach that evaluated each model and scenario separately, and we estimated return-period values from the best-fitting distribution — either from Gumbel, GEV, or a mixed distribution simply composed of the average between Gumbel and GEV. Importantly, the historical model and climate-model ensemble-mean values for the 24-hour return intervals considered were reasonably similar (within approximately 1-inch) to those of [NOAA-Atlas 14](#) and USGS-WRI report 99-4232. Both these data sources use a time series over different durations and different methods to estimate return intervals, compared with our work.

Figures 40-42 shows the historical and future 10-year, 50-year, and 100-year return periods calculated for daily precipitation accumulation, respectively, and for both mid-range and high emissions scenarios. Each figure panel also overlays the model spread, and it depicts individual models by markers. The multi-model mean and its value are shown by the blue bars, and the observations are denoted by a grey bar. In each case, the mean value of the future, multi-model return period increases, as does the model spread. This spread between models is most apparent toward the late 21st Century, and with higher emissions. Compared with the historical period, future daily-accumulated extreme precipitation by the mid-21st Century is 31-38% higher at the 10-year event, 53-71% higher at the 50-year event, and 66-85% higher for the 100-year event for mid-range and high emissions respectively. These values increase by 0.5-1 inch more by later in the 21st Century; however, most of the change is between the recent past, through the next 30-40 years, meaning that large increases in extreme precipitation magnitude, and possibly frequency, are anticipated in the relatively near future.

There is pronounced variations between models, more so than differences in return values due to emissions scenarios, and some climate models show the mid-21st Century to have the greatest change in return period magnitude, followed by a drop again later in the century (but still remaining higher than the historical period). This may be due to model depictions of atmospheric drivers of heavy rainfall, and drought. Nonetheless, by mid-century, the majority of models (over 75%) increase the magnitude of the return period rainfall at 50 and 100-years by at least 25%, and the proportion of models in this category increases further by late century and with higher emissions.

Figure 43 schematically represents the projected changes in terms of revised event frequencies, relative to the historical period. With mid-range emissions, and by later in the 21st Century, the 1-in-2-year to 1-in-10-year events become about twice as common, whereas the 1-in-50-year event increases by a factor of 5 (mid-range emissions) to 10 (high emissions), and the 100-year event occurs on average once every 10 years.

These types of changes, if realized, would likely have profound impacts on existing infrastructure, and could necessitate changes in how future infrastructure is designed.

Presently, designs for drainage must provide a certain level of protection against extreme rainfall, which must also be balanced by considerations such as asset criticality, traffic volume, facilities cost, budgetary constraints and political considerations. While this analysis cannot provide an estimate of design-relevant IDF parameters for climate change, we might anticipate that if daily events are substantially greater in magnitude, then IDF estimates may also increase proportionately. The level of redundancy in existing infrastructure and the impacts of floods at various scales should be assessed in order to better understand existing vulnerability and the degree to which climate change could necessitate design modifications. We have compiled return-frequency projections for each climate division in the SPTC domain, so additional heavy precipitation projections will be available.

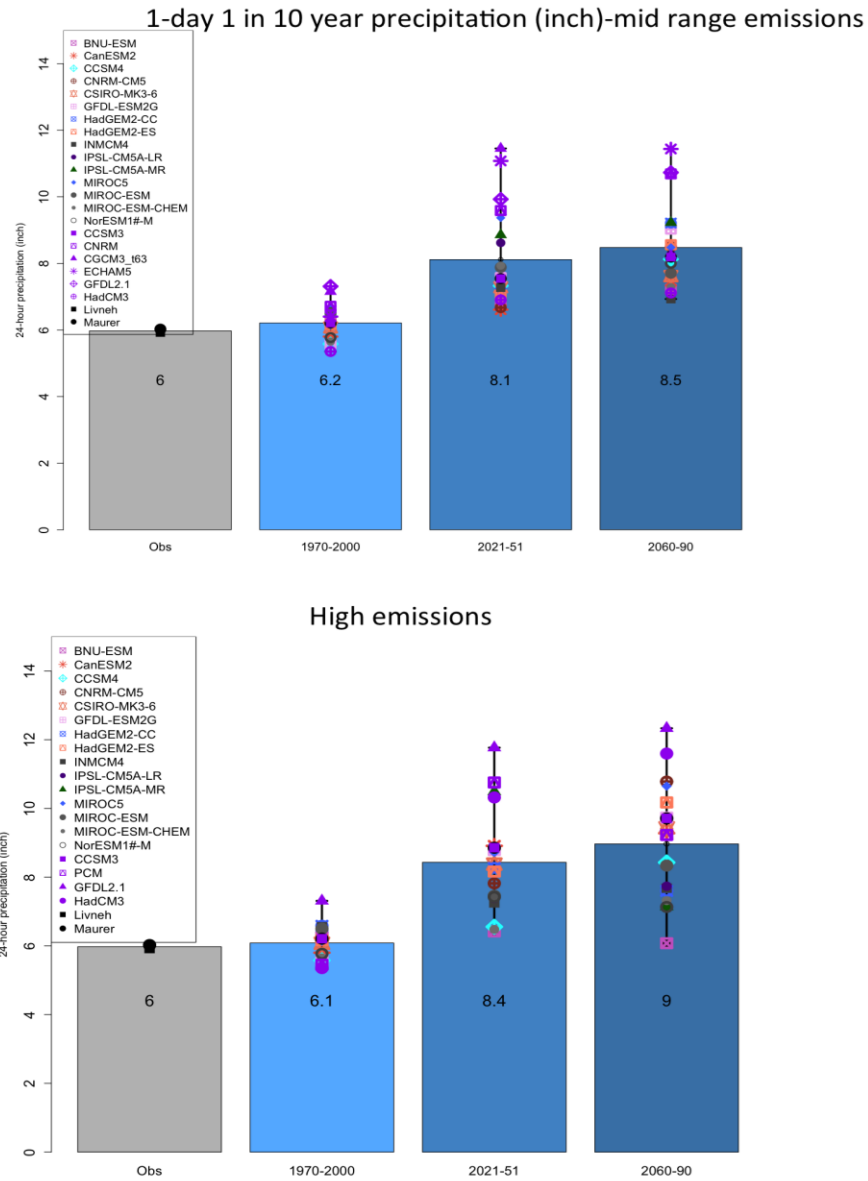


Figure 40: 1 in 10-year 1 day return period precipitation events for Oklahoma climate division 5 (central Oklahoma) for **Top:** mid range emissions, and **Bottom:** high emissions. The return value in inches is shown by and in the bars, where grey is the observations (Livneh and Maurer), light blue is the historical period, and dark blue the mid and late century periods. The model spread is depicted by the range bars, and each individual model is displayed by a marker. The results shown by this figure are described in the main text.

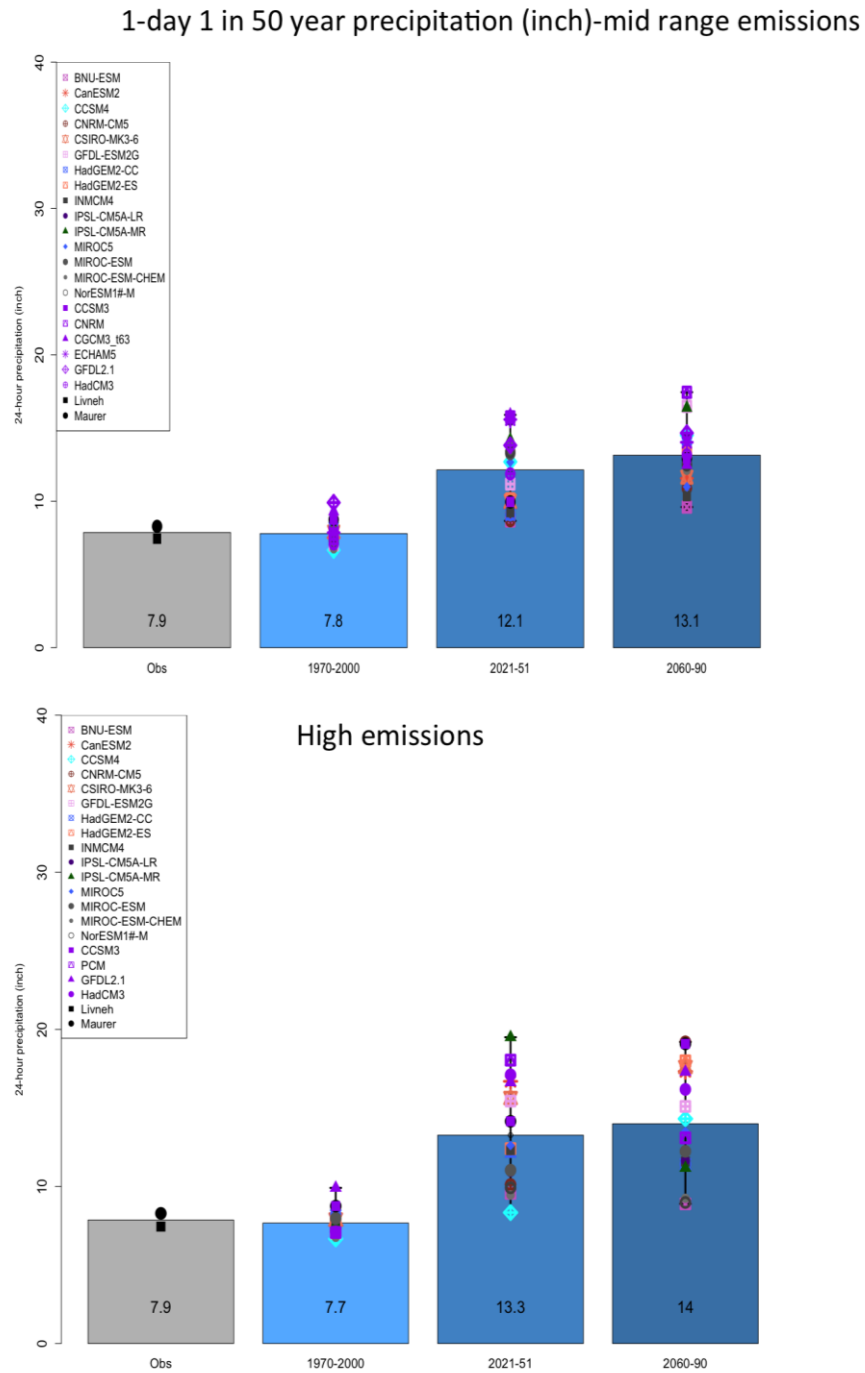


Figure 41: 1 in 50-year 1 day return period precipitation events for Oklahoma climate division 5 (central Oklahoma). The layout of the chart is the same as that of Fig. 40, however the y-axis range has been expanded to account for the higher values.

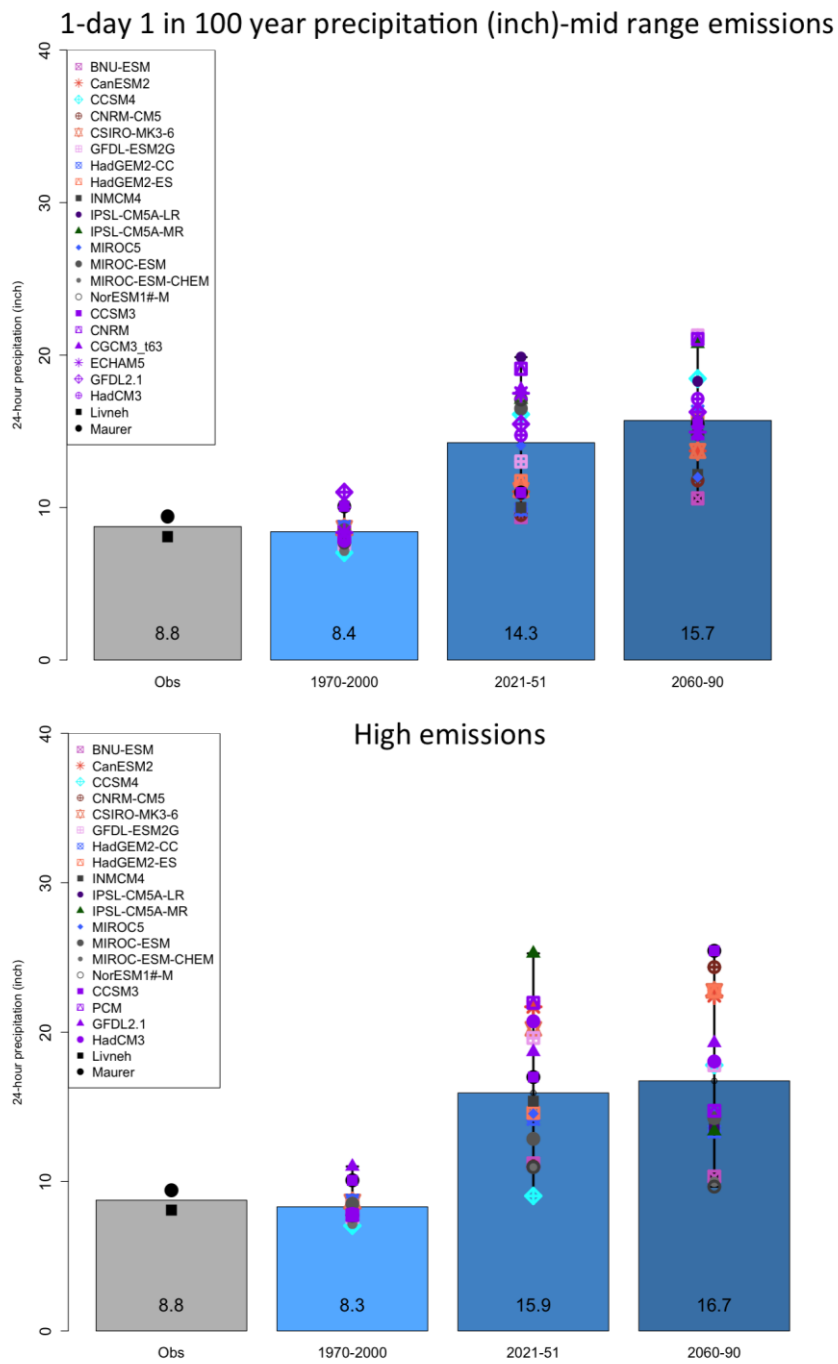


Figure 42: 1 in 100-year 1 day return period precipitation events for Oklahoma climate division 5 (central Oklahoma). The layout of the chart is the same as that of Fig. 40.

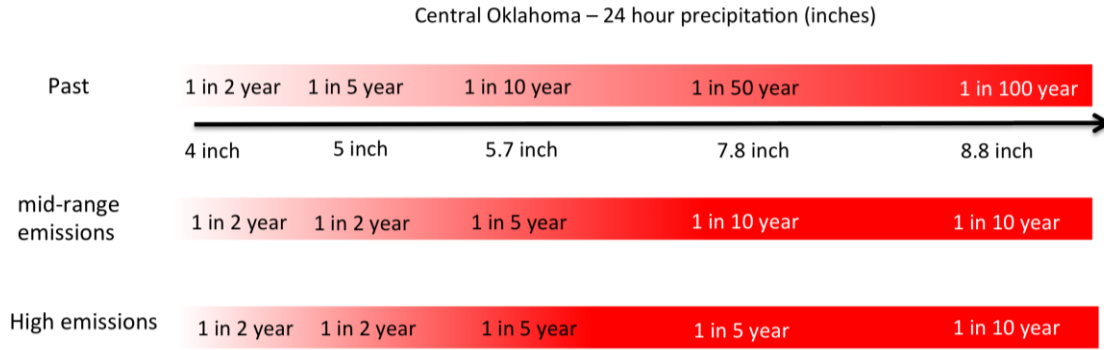


Figure 43: Schematic representation of the change in return period frequency, based on 1-day multi-model mean return periods. The top shaded bar depicts the current estimated return periods and their precipitation values for 1 in 2 years to 1 in 100-year events. The middle panel shows how the return frequency of these events changes by later in the century for mid-range emissions, and the bottom panel is the same, but for high emissions. Return periods of 10 years or less approximately double in frequency (e.g., 1 in 5 year), while 1 in 50 to 100 year return intervals increase in frequency by a factor of 5-10, according to our estimates.

4. DISCUSSION

4.1 IMPLICATIONS

This work has examined multiple sources of climate data, including historical and future, to develop regionally specific trends for the SPTC domain of responsibility. Expert input was solicited in order to better constrain the variables and metrics that reflect transportation concerns. We have provided some historical climatological context, and future trends for the region, and more specific results for central Oklahoma and the Oklahoma City Metropolitan area.

While information on hazards and possible impacts associated with these trends was provided in each subsection, here we summarize some general sensitivity to climate stressors across select transportation assets. This investigation used the ‘*Sensitivity Matrix*’ framework, developed by Rowan et al. (2012), currently available as an excel spreadsheet [from the FHWA](#). This tool provides details on each transportation asset, including some known thresholds and climatic stressors. Sensitivity of an asset is defined as the possible change in condition of that asset when exposed to the climate-related stressor. The information was developed through expert input, but does not attempt to provide detailed information on specific damage functions, since these are often not known or well-constrained for multiple inhomogeneous regions. We may therefore apply the climate change projections of our region, in this case, for central Oklahoma, to determine the possible level of climate-related threat that a given asset may be exposed to. In addition to linking the climate variable to the asset, we provide a measure of the degree of impact from the climate stressor based on the trends that we have identified. Readers should note the following assumptions:

- We assume the level of possible impact is over the full lifetime of an asset, and assume that the asset is developed/constructed under present-day conditions, and using current technology and practices, *without* building in additional redundancy that could mitigate the effects of climate change.
- For relatively short-term considerations, such as maintenance, operations, and safety, we consider a trend between the recent past, and the mid-century (2021-51).
- For longer-term hazards (> 40 years), we use the high emissions projection to inform our trend.
- The trends are based on the multi-model mean

- For assets with no known climate stressors, or unclear relationships between asset and climate are left blank.

Since there are multiple stressors that can alleviate or compound climate-related stress, such as asset age, construction quality, traffic use, among others, the climate-related impact can be difficult to quantify. In some cases, the historical degree of association and causal relationship between a given asset condition and its environmental exposure is not well known. If this is the case, the impact of future trends can be qualitatively estimated, but not quantitatively known. Nonetheless, this conceptual ‘first-order’ assessment of potential risk may be useful to transportation planners, in conjunction with other information, such as adaptive capacity (regional resilience to hazards, ability to recover and repair from extreme events etc.)

The sensitivity matrix for temperature (in tabular form, but rendered as an image in Figure 44) suggests that the majority of transportation assets may benefit from the reduction in cold-season related hazards, such as freeze-thaw cycles and cold temperatures. Freeze-thaw cycles are projected to decline in frequency by up to 20% by mid-century, and 50% (30% with a mid-range emissions pathway) by late century in central Oklahoma. For most maintenance and safety activities, which occur on a season-to-annual basis, little change is expected in the next 5-10 years, however most models thereafter project a steady decline in these hazards. Notably, some models continue to depict occasional extreme cold, with minimum temperatures below 0°F, particularly before the mid-21st Century. Despite the average warming of the Oklahoma City area, these extremes will continue to affect transportation, but in general, to a lesser extent than they would have historically. Fewer freeze-thaw cycles, and cold extremes may result in reduced degradation to paved road and bridge surfaces, and may eventually reflect in lower maintenance costs associated with potholes and other winter-related damage. Year-to-year variability in cold weather conditions will continue, and so these benefits may not be evident in all years.

In contrast to cold conditions, mean surface temperatures and hot temperatures are projected to increase. Figure 44 depicts the impacts on longer-duration infrastructure (e.g., bridges and buildings) as moderate to high, particularly for hot extremes. The duration, intensity, and frequency of very hot temperatures are expected to increase,

and years similar to the 2011 heat wave will become substantially more common by the mid-21st Century. The frequency of 100°F days, for example, increases by 200-300% by mid-Century, and close to 500% after 50 years. The anticipated impacts to infrastructure may include increased risk of railroad track buckling, pavement buckling and rutting, and insufficient asphalt binders in some locations. Buildings may require more energy usage (e.g., air conditioning). While maintenance, operations and safety are unlikely to experience conditions that differ much from present for the next 5-10 years, eventually heat-related hazards will likely contribute to adverse impacts, such as limitations to maintenance activities in summer and during the day, and increased heat-related damage control.

Temperature variation, defined here as the difference between the seasonal and/or annual highest and lowest temperatures for a given year, is not shown to change much. Both the coldest and warmest annual temperatures rise at similar rates, yielding little change, or even a very small increase in the seasonal and annual temperature range.

Our level of confidence is *high* that our climate system is trending toward increased heat extremes, and reduced cold extremes. The level of confidence in the increase in hot temperature extremes is *high*, accounting for the agreement between models, all of which show increasing trends, and the level of consensus within the climate science community. In general, our definition of 'confidence' takes into account our findings, the level of agreement between climate models, expert knowledge, and the preponderance of evidence provided by the scientific literature. The magnitude of the decrease in cold-temperature extremes is at *medium* confidence. All models analyzed here support a decreasing trend in cold weather related extremes. However, some work in the climate science community has suggested that climate models do not well account for the impact of high-latitude (e.g., Arctic) changes on mid-latitude weather, or show weak relationships (e.g., Tang et al. 2013, Cohen et al. 2012, Woollings et al. 2014). Investigations into climate change-related effects on high-latitudes have shown that in some cases there is a tendency toward cold air outbreaks in the mid-latitudes; however, the science in this area is still evolving (e.g., Yang and Christensen 2012, Screen 2014, Francis and Vavrus 2015), and the projections shown here reflect the current understanding regarding the direction of trends.

The sensitivity matrix for precipitation (Figure 45) examines changes in winter weather (ice/snow), and precipitation extremes (drought and heavy rainfall), based also on climate projections for the Oklahoma City metropolitan area. Ice and snow hazards to road surface infrastructure are largely associated with attendant issues such as freeze-thaw (particularly in the presence of melt water), cold temperatures, and the quantity and frequency of deicer use. Snow and ice days in central Oklahoma are likely to decrease by up to 25% (roughly one day per year on average) by mid-Century, and up to 3 days (75%) by late 21st Century, assuming the high emissions scenario (a mid-range scenario is closer to 60%). Shorter-term activities will therefore not experience a perceivable change within the next 5-10-years, and winter maintenance activities are likely to remain the same. Longer-term, there are expected slight to moderate benefits to the region's infrastructure, safety, and movement of transportation, including aviation.

The projections for winter weather intensity remain roughly the same as present, suggesting that events will be of similar intensity range to those experienced in the recent past, despite their lower frequency. Thus, winter weather is still expected to present adverse impacts in the future. The decrease in winter weather frequency, particularly after the mid-21st Century, is at *high* confidence, and the projected minimal change in intensity is at *medium* confidence. One caveat of the analysis when examining winter precipitation intensity is the use of liquid water equivalent. Increased liquid water does not always translate directly to high amounts of snow or ice. During freezing rain, for example, liquid water can be more abundant when temperatures are closer to freezing, which can in some cases reduce the potential for ice accretion on roadways and structures. Unfortunately, limitations with the available data preclude a more thorough investigation on the nature of winter precipitation changes (such as phase and accumulation) at this time.

Precipitation extremes, marked by very high rainfall rates, and, on the flip side, drought, are both anticipated to increase in central Oklahoma. During the summer months (June-August), mid-century precipitation declines by an average of 3-6%, with more than two-thirds of models depicting drier conditions (not shown). Later in the century, and with higher emissions, the mean decline is near 13%.

The duration of time where 100°F days can occur lengthens by 4-7 weeks, depending on the emissions pathway, and by over 10 weeks later in the 21st Century with high emissions. The plausible decrease in summer precipitation (currently the second wettest season), coupled with an increase in the duration and intensity of hot days, suggests that drought onset and/or persistence during the summer could become more common. Typically, a drought is assumed to largely result from precipitation deficit; however, Williams et al. (2015) note that the recent California drought, which was associated with precipitation deficit, was intensified primarily through anomalously warm temperatures, which more rapidly depleted soil moisture. For transportation, drought is a concern for surface infrastructure in regions where soil is prone to movement (e.g., 'shrink and swell' associated with clay soils, which are present in central Oklahoma). Drought causes soil to shrink, and can lead to pavement and foundation damage. In some areas, e.g., the Southern High Plains, and New Mexico, drought can exacerbate blowing dust, which is a transportation safety hazard (Ashley et al. 2015).

Heavy precipitation, particularly extreme rainfall, is shown by our analysis to increase in central Oklahoma, with a substantial change in return-period frequency and magnitude (particularly at the 50- and 100-year thresholds) by mid-century, *regardless of emissions pathway*. The multi-model mean estimated magnitude change by mid-century is approximately 15-20% (1 in 5 year), 24-28% (1 in 10 year), 34-41% (1 in 20 year), 50-61% (1 in 50 year), and 66-80% (1 in 100 year). The model spread for each of these return-period intervals is much broader, particularly at the longest return periods (e.g., 1 in 100 year), indicating that there is a notable range of uncertainty that could be difficult to incorporate into current design paradigms. However, the majority of models do show an increase in the return-period magnitude (Fig. 39-41), particularly between the historical and mid-century periods. Analysis of changes in the frequency of fixed threshold precipitation events (e.g., 1-6 inches per day) show relatively little change at the lower thresholds, such as 1-3 inches per day, but more substantial increases at the higher thresholds (4-6 inches per day, not shown). The implication is that days with extremely heavy precipitation will undergo a pronounced increase, but moderately heavy precipitation or very wet years do not show much of a trend, meaning that the contribution of intense precipitation days to annual precipitation could potentially increase.

The impacts of extreme precipitation (flood and drought) were readily apparent from events in the Oklahoma City area over the past 6 years, and lead to damage and disruption on multiple types of transportation assets. The sensitivity matrix depicts the potential for moderate increase in the frequency of adverse impacts within the next 5-30 years, and high potential for adverse impacts after this time, based on the degree of change shown by the models. Nonetheless, given the large range of uncertainty, we caution the use of the numbers shown as being a precise 'forecast' for the future. While we anticipate with *medium-high* confidence an increase in the frequency of drought and extreme precipitation, the precise magnitude of the changes are considered as *low-medium* confidence. In addition to model uncertainty, the values provided by the return-period calculation are heavily dependent on the methods selected to estimate the extreme value distribution (e.g., Hayhoe et al. 2015). For example, a 1-in-100 year event in central Oklahoma by mid-century showed a multi-model mean magnitude increase of 30-40% (approximately half the degree of change estimated by the combined GEV/Gumbel method) using only the Gumbel extreme value distribution.

Asset Type Description and typical field lifetime (if known)	Climate Stressor					
	Freeze-Thaw Cycles	Freeze-Thaw Intensity	Extreme and/or frequent cold	Mean summer temperature	Extreme heat duration and/or intensity	Temperature variation
Roads						
Paved (surface and subsurface), asphalt (10-20 years)	Light Blue	Light Blue	Light Blue	Light Red	Light Red	Grey
Paved – concrete (30-40 years)	Light Blue	Light Blue	Light Blue	Light Red	Light Red	Grey
Unpaved roads	White	White	White	White	White	White
Storm water and drainage (varies, for Culverts 50-100 years)	White	White	White	White	White	White
Maintenance	Light Blue	Light Blue	White	Light Red	Light Red	White
Traffic safety/flow/volume	White	White	Light Blue	Light Red	Light Red	White
Bridges						
Superstructure (girders, deck, railings, etc.) (50-75 years)	Light Blue	Light Blue	Light Blue	Light Red	Light Red	Grey
Substructure (abutment etc.) (50-75 years)	Light Blue	Light Blue	Light Blue	Light Red	Light Red	Grey
Maintenance and safety	Light Blue	Light Blue	Light Blue	Light Red	Light Red	White
Rail						
Transit support infrastructure (bridges, tunnels, stations) (50+ years)	White	White	White	White	White	White
Tracks, ties, ballast, embankments (varies, typically multi-year)	White	White	Light Blue	Light Red	Light Red	White
Electrical equipment	White	White	White	Light Red	Light Red	White
Operations, maintenance and safety	White	White	White	Light Red	Light Red	White
Airports						
Surface infrastructure (runway and taxiway) (50 years)	Light Blue	Light Blue	Light Blue	Light Red	Light Red	White
Aircraft (in and out of flight) (25 years)	White	White	Light Blue	Light Red	Light Red	White
Buildings (50-years)	White	White	White	Light Red	Light Red	White
Operations and maintenance	Light Blue	Light Blue	Light Blue	Light Red	Light Red	White

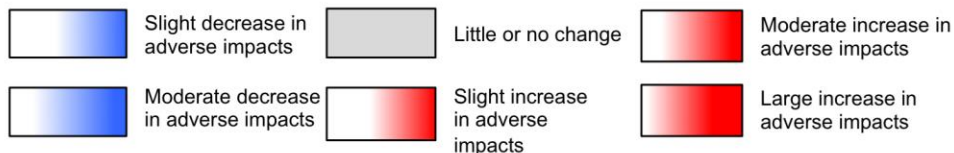


Figure 44: A ‘sensitivity matrix’ for central Oklahoma, including the Oklahoma City Metropolitan area, specifically examining temperature-related climate stressors and their potential impact on various transportation assets, including roads (paved, unpaved, asphalt and concrete), bridges (superstructure and substructure), rail (tracks, transit support infrastructure, power systems), and aviation (airports, runways, aircraft). The climate stressors examined include freeze thaw cycles, freeze thaw intensity (based on the temperature range of a cycle), extreme cold, extreme heat, mean summer temperatures, and temperature variation. The table (which is rendered as a figure here) identifies sensitive assets or activities, and approximates the degree of positive or negative impact based on the climate projections over the lifetime of the asset. The method used to construct this table, and its results are described in the main text.

Asset Type	Climate Stressor				
	Winter weather (ice/snow) frequency	Winter weather Intensity	Drought	Heavy and/or persistent rainfall and flooding	
Roads					
Paved (surface and subsurface), asphalt (10-20 years)	Blue	Grey	Red	Red	
Paved – concrete (30-40 years)	Blue	Grey	Red	Red	
Unpaved					
Storm water and drainage (varies, for Culverts 50-100 years)			Red	Red	
Maintenance	Blue	Grey	Red	Red	
Traffic safety/flow/volume	Blue	Grey	Red	Red	
Bridges					
Superstructure (girders, deck, railings...) (50-75 years)	Blue	Grey		Red	
Substructure (abutment etc.) (50-75 years)				Red	
Maintenance and safety	Blue	Grey		Red	
Rail					
Transit support infrastructure (bridges, tunnels, stations) (50+ years)				Red	
Tracks, ties, ballast, embankments (varies, typically multi-year)	Blue	Grey		Red	
Electrical equipment				Red	
Operations, maintenance and safety	Blue	Grey		Red	
Airports					
Surface infrastructure (runway and taxiway) (50 years)	Blue	Grey		Red	
Aircraft (in and out of flight) (25 years)	Blue	Grey		Red	
Buildings (50-years)					
Operations and maintenance	Blue	Grey		Red	







 Slight decrease in adverse impacts	 Little or no change	 Moderate increase in adverse impacts
 Moderate decrease in adverse impacts	 Slight increase in adverse impacts	 Large increase in adverse impacts

Figure 45: As Fig. 44, but for precipitation-related climate stressors and their potential impact on various transportation assets. The climate stressors examined include winter weather frequency, winter weather intensity (the amount of winter precipitation associated with a given event), drought, and heavy precipitation. The table (which is rendered as a figure here) identifies sensitive assets or activities, and approximates the degree of positive or negative impact based on the climate projections over the lifetime of the asset. The method used to construct this table, and its results are described in the main text.

4.2 CAVEATS AND LIMITATIONS

This study is intended to provide a comprehensive assessment of trends in transportation-relevant climate conditions using a suite of state-of-the-art climate observational and numerically modeled products that have been carefully analyzed and evaluated against historical conditions. The majority of data utilized was based on global climate models — sophisticated computer models that simulate various components of the earth system — and their response to natural and anthropogenic radiative forcing. The results provide transportation planners and other decision-makers with a general guide regarding future climate states and the potential implications of climate change on transportation. Nonetheless, the precise values for any given variable (e.g., temperature, precipitation) are uncertain, particularly for extreme precipitation where model-to-model variability is high. For example, during our investigation, we identified some extremely large future daily precipitation amounts that appeared non-physical (not shown). After communication with the original data developers (MACA, Abagatzou), we identified possible uncertainties with the downscaling technique linked to certain heavy precipitation events, particularly near the Gulf of Mexico coast. The other statistical downscaling method, ARRM, tended to overestimate historical return-period precipitation related to higher annual maxima in certain GCMs. Historical products, such as the freezing precipitation dataset developed in year 1, also have some limitations in data availability and representativeness, which users should bear in mind (see Mullens and McPherson, 2017).

Climate science is a dynamic science, and the data products used for this work are generally updated, improved, or eventually retired as new products become available and new model simulations are obtained. For example, the next CMIP project is currently underway (i.e., CMIP6), with expected release of data during 2019-2020. Users of our data products and the information contained in this report should recognize that other datasets may diverge in estimates of precise values, and in some cases (largely for precipitation), trends. Therefore the exact values shown should not be considered as the ‘final word’ on the magnitudes of future changes. Nonetheless, the general trends depicted have been supported across numerous studies, and various iterations of models, suggesting that in general, there is sufficient confidence to anticipate general temperature and precipitation hazards, irrespective of precise quantitative information. Decisions that involve risk should be prepared to incorporate uncertainty by considering

a range of climate scenarios and/or historical observations (where possible) and associated magnitudes of change. Any questions regarding the use of our data and information can be directed to Co-PI Mullens.

4.3 FUTURE EFFORTS

In addition to the data generated by this project, we are in the early stages of developing summary products, in the form of accessible summary reports, highlighting key climate projections for each state in the SPTC domain. These reports, which are expected to be made available on the South Central Climate Science Center website, will visualize trends in all the variables considered in this final report, present some general information on potential impacts, and identify resources that transportation professionals may wish to consider if they plan to use this information in their planning. The anticipated release of these documents will be late summer 2017. Interested parties can contact Co-PI Mullens for further information.

5. RECOMMENDATIONS

This work has provided the climate science background for understanding the hazards presented by climate change on the transportation sector, with more specific information provided for the Oklahoma City/central Oklahoma area. Given that this research has largely focused on weather and climate contributions to risk, we do not have the expertise necessary to provide specific prescriptive recommendations to transportation decision-makers on their use of this information. Nonetheless, in recent years, the sector has benefitted from considerable efforts to expand the consideration of weather and climate extremes in infrastructure planning, safety, asset management, and resiliency building. This section will therefore provide some examples of these activities and some recommendations that have been identified by the transportation community. With respect to the use of the data and images described in this report (and detailed further in the appendix), information regarding data limitations and caveats will be made available in the same location as the raw data or images. Users should peruse this information in order to be aware of ways in which the data can be most effectively used or interpreted.

In 2014, the Federal Department of Transportation released an [adaptation plan](#) that noted the detrimental effect that climate change is likely to have on the fundamental mission of the agency to promote safety, state of good repair, and environmental sustainability. The plan identified three key strategic adaptation goals: (1) *planning that includes climate change information*, (2) *including climate change impact data in asset management*, and (3) *providing tools, case studies, outreach activities, and best practices* that help transportation agencies develop their resources, and foster the kind of flexible approaches to planning that are necessary to incorporate information on evolving hazards. Key strategies included incorporating climate change into planning for new infrastructure, hardening existing infrastructure, and building additional redundancy into key assets, while developing provisions for rapid recovery.

Parsons Brinkerhoff has also been active in building resiliency to climate hazards, and led the development of the National Cooperative Highway Research Program (NCHRP) [report 750](#) (Vol 2). This report recommends steps that transportation agencies could take to prepare for extreme weather, manage their operations during extreme

weather, and conduct post-recovery operations. They also consider the effect that climate change may have on certain transportation-relevant extremes. An article published in the magazine [Network](#) (September 2015) provides some guidance on developing vulnerability assessments that specifically examine climate stressors on transportation. Our work is essentially the first stage of this process, and further steps toward a detailed assessment will require capitalizing on regional expertise in transportation design and operational performance characteristics of various assets. The article also notes the importance of considering costs associated with a given strategy, which is especially relevant in a climate of budget constraints and resource limitations, and identifying the effectiveness of a given strategy to meet goals such as safety and good repair, if it is implemented.

The FHWA has supported a series of pilot and case studies that establish frameworks, guidance and tools for transportation professionals to assess the role of climate variability and change in infrastructure planning. The '[Gulf Coast Study](#)' was a comprehensive analysis of vulnerability along sections of the Texas, Louisiana, and Alabama coastline. The project resulted in the development of vulnerability assessment and sensitivity matrix tools that are now publically available. [New York State \(2011\)](#) examined climate change projections for their area, and identified some recommendations for transportation planners, including incorporating climate change adaptation into designs for new and rehabilitated infrastructure, which was seen to be most cost-effective. They also suggested that programs and projects that require infrastructure design should be building in flexible methods and approaches that can better incorporate information that is consistently evolving.

Inland within the SPTC domain, the North Central Texas Council of Governments (NCTCOG, 2015), in collaboration with the Texas State Climatologist, examined the potential [impacts of climate change in the Dallas Fort Worth metropolitan area](#). Stakeholders in the region found that the size and complexity of the transportation network and infrastructure in this city alone require prioritizing data collection to gather only the most essential information. They also identified the need to improve weather-related monitoring of the transportation system, in order to connect adverse conditions to specific impacts on the system. In New Mexico, a multi-agency project (2015) entitled '[Integrating Climate Change in Transportation and Land-use Scenario Planning](#)'

specifically examines climate-related challenges in the Albuquerque region, testing different climate and land-use change scenarios and their impacts. Participating stakeholders were able to examine each scenario and identify a preferred option that best promotes resiliency and sustainability. Climate information was used here to put forward some general plausible ‘scenarios’ of future climates (e.g., warm/wet, warm/dry, hot/dry, hot/wet), rather than identifying specific projections as our work has done. The work also included projections of population, growth, and land-use changes. A key recommendation included the need to plan beyond traditional planning horizons, for example, a state’s 10-year strategic plan should not discount climate information because the impacts are felt most after this time. In addition to the studies discussed, climate information assessments related to transportation have been conducted in Arizona, California, Austin TX, Connecticut, Iowa, Maine, Maryland, Massachusetts, Michigan, Minnesota, Oregon, Tennessee, and Washington.

For the SPTC domain, and specifically for states, regions, or municipalities that have currently not considered climate futures in their planning process, some recommendations suggested by the broader transportation sector include:

- Use available resources, such as those provided here, to assess the potential effects of climate change in a given region or for a given asset.
- Keep abreast of information and resources provided by state agencies and federal entities related to climate change and transportation.
- Pursue collaborations between weather/climate experts and those in transportation design, safety, engineering, hydrology, etc. to address the complex challenges of climate change (e.g., Meyer 2013). The SPTC’s strategic goals of climate resilient transportation have created a forum for these types of collaborations; however, relationships take time to develop and mature, so efforts should be made by transportation researchers, DOTs, and climate scientists to communicate with one another over matters of mutual concern on a regular schedule.
- Incorporate climate information into assessments of vulnerability, using strategies put forward by the FHWA, AASHTO, and other governmental and non-governmental transportation organizations.
- Identify cost-effective ways to increase weather and climate monitoring of key assets and compile historical records of structural information on assets,

including any maintenance reports that have cited weather-related impacts to specific damage or degradation, accidents, or fatalities.

- Within the context of current constraints, identify cost-effective ways to evaluate and implement additional redundancy into new infrastructure or when rehabilitating existing infrastructure. Reassess design paradigms to evaluate how future climate extremes, and non-stationary trends in temperature and precipitation could modify existing guidance. Cultivate a 'long-term' perspective on asset management that transcends traditional planning horizons.

6. REFERENCES

- Abatzoglou J.T. and A. Brown, 2012: A comparison of statistical downscaling methods suited for wildfire applications. *International Journal of Climatology*, doi: [10.1002/joc.2312](https://doi.org/10.1002/joc.2312).
- Amtrak, 2015: What are heat restrictions? June 2015. <http://blog.amtrak.com/2015/06/heat-restrictions/>. Accessed 02/24/17.
- Ashley, W., S. Strader, D. Dziubla, and A. Haberlie, 2015: Driving Blind: Weather-Related Vision Hazards and Fatal Motor Vehicle Crashes. *Bull. Amer. Meteor. Soc.*, **96**, 755–778, doi: [10.1175/BAMS-D-14-00026.1](https://doi.org/10.1175/BAMS-D-14-00026.1)
- ATSM C666/C666M-15. *Standard Test method for resistance of concrete to rapid freezing and thawing*. ASTM International, West Conshohocken, PA, 2015, https://doi.org/10.1520/C0666_C0666M-15
- Black, A. W., and T.L. Mote, 2015: Characteristics of winter-precipitation-related transportation fatalities in the United States. *Weather, climate, and society*, **7**, 133-145, doi: [10.1175/WCAS-D-14-00011.1](https://doi.org/10.1175/WCAS-D-14-00011.1).
- Cheng, L., and A. AghaKouchak, 2014: Nonstationary Precipitation Intensity-Duration-Frequency Curves for Infrastructure Design in a Changing Climate. *Science Reports*, **4**, 7093, doi: 10.1038/srep07093
- Chin S., O. Franzese, D. L. Greene, H. L. Hwang, and R. L. Gibson, 2002: Temporary losses of highway capacity and impacts on performance. Oak Ridge National Lab, ORNL/TM-2002/3. <http://csmb.ornl.gov/~webworks/cppr/y2001/rpt/112739.pdf>. Accessed 03/22/14.
- Cohen, J., J.C. Furtado, M.A. Barlow, V.A. Alexeev, and J.E Cherry, 2012: Arctic warming, increasing snow cover and widespread boreal winter cooling. *Environmental Res. Letters*, **7**, doi: <https://doi.org/10.1088/1748-9326/7/1/014007>
- Cowan, T., G. Hegerl, I. Colfescu, M. Bollasina, A. Purich, and G. Boschat, 2016: Factors contributing to record-breaking heat waves over the Great Plains during the 1930s Dust Bowl. *J. Climate*, **0**, doi: [10.1175/JCLI-D-16-0436.1](https://doi.org/10.1175/JCLI-D-16-0436.1).
- DeGaetano, A., 2009: Time-Dependent Changes in Extreme-Precipitation Return-Period Amounts in the Continental United States. *J. Appl. Meteor. Climatol.*, **48**, 2086–2099, doi: [10.1175/2009JAMC2179.1](https://doi.org/10.1175/2009JAMC2179.1).
- Eggleston, K., A. DeGaetano, and C. Castellano, 2016: Duration Frequency (IDF) curves for NY. Presentation, 14th annual Climate Prediction Applications Science Workshop (CPASW), Burlington VT. <https://www.uvm.edu/~cpasw/presentations/wed/Session2/6DeGaetanoEgglestonWedSession2CPASW16.pdf>. Accessed 02/01/2017.

- FEMA, 2015: Disaster declarations for 2015. <https://www.fema.gov/disasters/grid/year/2015>. Accessed 01/30/2017.
- Francis, J.A., and S.J. Vavrus, 2015: Evidence for a wavier jet stream in response to rapid Arctic warming. *Environmental Res. Letters*, **10**, doi: <https://doi.org/10.1088/1748-9326/10/1/014005>
- Grotjahn, R., and 12 Co-authors, 2016: North American extreme temperature events and related large scale meteorological patterns: a review of statistical methods, dynamics, modeling, and trends. *Climate Dynamics*, **46**, 1151-1184, doi: 10.1007/s00382-015-2638-6
- Guttman, N. B., and R.G. Quayle, 1995: A historical perspective of U.S Climate Divisions. *Bulletin of the American Meteorological Soc.*, **77**, 293-303, doi: [http://dx.doi.org/10.1175/1520-0477\(1996\)077<0293:AHPOUC>2.0.CO;2](http://dx.doi.org/10.1175/1520-0477(1996)077<0293:AHPOUC>2.0.CO;2)
- Haley, J.S., 2011: *Climatology of freeze-thaw days in the conterminous United States: 1982-2009*, Thesis, Kent State University Dept. Geography, Retrieved from <https://etd.ohiolink.edu/>
- Hayhoe, H., A. Stoner, S. Abeyundara, J.S Daniel, J.M. Jacobs, P. Kirshen, and R. Benestad, 2015: Climate Projections for Transportation Infrastructure Planning, Operations and Maintenance, and Design. *TRB: Journal of the Transportation Research Board*, **2510**, 90-97, doi: <http://dx.doi.org/10.3141/2510-11>
- Hershfield, D., 1974: The Frequency of Freeze-Thaw Cycles. *J. Appl. Meteor.*, **13**, 348–354, doi: [10.1175/1520-0450\(1974\)013<0348:TFOFTC>2.0.CO;2](https://doi.org/10.1175/1520-0450(1974)013<0348:TFOFTC>2.0.CO;2).
- Hutchison, P. J., 2008: Journalism and the perfect heat wave: Assessing the reportage of America's worst heatwave, July-August 1936. *American Journalism*, **25**, Iss 1, 2008, doi: <http://dx.doi.org/10.1080/08821127.2008.10678091>
- IPCC: Stocker, T.F., D. Qin, G.-K. Plattner, M. Tignor, S.K. Allen, J. Boschung, A. Nauels, Y. Xia, V. Bex, and P.M. Midgley. (eds), 2013: Climate Change 2013: The Physical Science Basis. [Contribution of Working Group I to the Fifth Assessment Report of the Intergovernmental Panel on Climate Change](#), 1535 pp, Cambridge Univ. Press, Cambridge, U. K. and New York.
- Jackson, N., and J. Puccinelli, 2006: *Long-Term Pavement Performance (LTPP) Data Analysis Support: National Pooled Fund study TPF-5(013) - Effects of Multiple Freeze Cycles and Deep Frost Penetration on Pavement Performance and Cost*. Report FHWA-HRT-06-121, 123210-8, 262pp. <https://www.fhwa.dot.gov/publications/research/infrastructure/pavements/ltp/06121/>
- Knutti, R., R. Furrer, C. Tebaldi, J. Cermak, and G. Meehl, 2010: Challenges in Combining Projections from Multiple Climate Models. *J. Climate*, **23**, 2739–2758, doi: [10.1175/2009JCLI3361.1](https://doi.org/10.1175/2009JCLI3361.1).

- Liu, G., L. Zhang, B. He, X. Jin, Q. Zhang, B. Razafindrabe, and H. You, 2015: Temporal changes in extreme high temperature, heat waves, and relevant disasters in Nanjing metropolitan region, China. *Natural Hazards*, **76**: 1415. doi:[10.1007/s11069-014-1556-y](https://doi.org/10.1007/s11069-014-1556-y)
- Livneh B, E.A. Rosenberg, C. Lin, V. Mishra, K. Andreadis, E.P. Maurer, and D.P. Lettenmaier, 2013: A Long-Term Hydrologically Based Dataset of Land Surface Fluxes and States for the Conterminous United States: Update and Extensions. *Journal of Climate*, **26**, 9384–9392. doi: <http://dx.doi.org/10.1175/JCLI-D-12-00508.1>
- Maurer, E. P., A. W. Wood, J. C. Adam, D. P. Lettenmaier, and B. Nijssen, 2002: A long-term hydrologically-based data set of land surface fluxes and states for the conterminous United States, *Journal of Climate*, **15**, 3237–3251, doi: [http://dx.doi.org/10.1175/1520-0442\(2002\)015<3237:ALTHBD>2.0.CO;2](http://dx.doi.org/10.1175/1520-0442(2002)015<3237:ALTHBD>2.0.CO;2)
- Melillo, J. M., T. C Richmond, and G. W Yohe. (eds), 2014: Climate Change Impacts in the United States: The Third National Climate Assessment (US Global Change Research Program), <http://nca2014.globalchange.gov/download> Accessed 02/01/2017.
- Mesinger, F., and coauthors, 2006: North American Regional Reanalysis. *Bulletin of the American Meteorological Soc.*, **87**, 343–360, doi: <http://dx.doi.org/10.1175/BAMS-87-3-343>
- Meyer, M. D., P. Brinckerhoff, E. Rowan, C. Snow, and A. Choate (ICF International, AASHTO), 2013: Impacts of extreme weather on transportation: national symposium summary, June 28 2013. http://environment.transportation.org/pdf/2013_symposium/AASHTO_EWESymposium_2013.pdf. Accessed 03/01/2014
- Mills, B., and J. Andrey, 2002: Climate change and transportation: potential interactions and impacts, in The potential impacts of climate change on transportation, Federal Research Partnership Workshop, October 1-2 2002. <http://2climate.dot.gov/documents/workshop1002/workshop.pdf#page84>. Accessed 02/28/2014.
- Mullens, E.D., and R.A McPherson, 2017: A Multi-Algorithm Reanalysis-based Freezing Precipitation Dataset for Climate Studies in the South-Central US. *J. Applied Meteorology and Climatology*, **56**, doi: 10.1175/JAMC-D-16-0180.1
- Nakicenovic, Nebojsa, and Robert Swart, 2000: [*Special report on emissions scenarios*](#). Special Report on Emissions Scenarios, Edited by Nebojsa Nakicenovic and Robert Swart, pp. 612. ISBN 0521804930. Cambridge, UK: Cambridge University Press, July 2000.
- NCEI, 2017: Billion Dollar Weather and Climate disasters: Table of events. <https://www.ncdc.noaa.gov/billions/events>. Accessed 01/21/2017.

- NCHRP, 2013: *Strategic Issues facing transportation, Volume 2: Climate change, extreme weather events, and the highway system. Practitioner's guide and research report*. TRB National Cooperative Highway Research Program Report 750. Project Number 20-83(05). DOI: [10.17226/22473](https://doi.org/10.17226/22473)
- OFCM, 2002: Weather Information for Surface Transportation, National needs Assessment report. Office of the Federal Coordinator for Meteorological Services and Supporting Research. http://ofcm.gov/wist_report/pdf/entire_wist.pdf. Accessed 03/22/2014.
- Oklahoma Climatological Survey, 2015: Monthly summaries. <http://climate.ok.gov/index.php/climate/summary>. Accessed 01/30/2017.
- Oklahoma Dept. Transportation (ODOT), 2017: *8-year construction work plan*. https://www.ok.gov/odot/Programs_and_Projects/8_Year_Construction_Work_Plan/. Accessed 02/03/2017.
- Oklahoma Dept. Transportation (ODOT), 2014: *Roadway drainage design manual*. https://www.ok.gov/odot/Doing_Business/Pre-Construction_Design/Roadway_Design/Support_Units/Oklahoma_Roadway_Drainage_Manual.html. Accessed 01/20/2017.
- Ongel, A., and J. Harvey, 2004: *Analysis of 30 years of pavement temperatures using the Enhanced Integrated Climate Model (EICM)*. Report Developed for the California Dept. Transportation. http://www.ucprc.ucdavis.edu/PDF/Climate_30_Years.pdf. Accessed 02/01/2017.
- Oyler, J.W., A. Ballantyne, K. Jencso, M. Sweet, and S.W Running, 2014: Creating a topoclimatic daily air temperature dataset for the conterminous United States using homogenized station data and remotely sensed land skin temperature. *International. J. Climatology*, **35**, 2258-2279, doi:[10.1002/joc.4127](https://doi.org/10.1002/joc.4127)
- Pierce, D., D. Cayan, and B. Thrasher, 2014: Statistical Downscaling Using Localized Constructed Analogs (LOCA). *J. Hydrometeorology*, **15**, 2558–2585, doi: [10.1175/JHM-D-14-0082.1](https://doi.org/10.1175/JHM-D-14-0082.1).
- Rosenberg, E.A., P.W. Keys, D.B. Booth, D. Hartley, J. Burkley, A.C. Steinemann, D.P. Lettenmaier, 2010: Precipitation extremes and the impacts of climate change on stormwater infrastructure in Washington State. *Climatic Change*, **102**: 319. doi:[10.1007/s10584-010-9847-0](https://doi.org/10.1007/s10584-010-9847-0)
- Rossetti, M.A., 2007: Analysis of Weather Events on U.S. Railroads. Available at <http://ntl.bts.gov/lib/47000/47000/47093/118791.pdf>. Accessed 02/27/2017.
- Rowan, E, C. Evans, M. Riley-Gilbert, R. Hyman, R. Kafalenos, B. Beucler, B. Rodehorst, A. Choate, and P. Schultz, 2012: Assessing the sensitivity of transportation assets to extreme weather events and climate change. *Transportation Research Board (TRB): Journal of the TRB*, **2326**, 16-23.
- Rupp, D. E., J. T. Abatzoglou, K. C. Hegewisch, and P. W. Mote, 2013: Evaluation of

- CMIP5 20th century climate simulations for the Pacific Northwest USA, *J. Geophys. Res. Atmos.*, **118**, 10,884–10,906, doi: [10.1002/jgrd.50843](https://doi.org/10.1002/jgrd.50843)
- Screen, J.A., 2014: Arctic amplification decreases temperature variance in northern mid- to high-latitudes. *Nature Climate Change*, **4**, 577-582. doi:[10.1038/nclimate2268](https://doi.org/10.1038/nclimate2268)
- Stoner, A. M. K., Hayhoe, K., Yang, X. and D.J. Wuebbles, 2013: An asynchronous regional regression model for statistical downscaling of daily climate variables. *International. J. Climatology*, **33**, 2473–2494. doi:[10.1002/joc.3603](https://doi.org/10.1002/joc.3603)
- Strong, C. A., Z. Ye, and X. Shi, 2010: Safety effects of winter weather: the state of Knowledge and remaining challenges. *Transport Reviews: A Transnational Transdisciplinary Journal*, **30**, 677-699, <http://dx.doi.org/10.1080/01441640903414470>
- Sunyer, M.A., H. Madsen, and P.H. Ang, 2012: A comparison of different regional climate models and statistical downscaling methods for extreme rainfall estimation under climate change. *Atmospheric Research*, **103**, 119-128, doi: <http://dx.doi.org/10.1016/j.atmosres.2011.06.011>
- Tang, Q., X. Zhang, X. Yang, and J. A. Francis, 2013: Cold winter extremes in northern continents linked to Arctic sea ice loss. *Environmental Res. Letters*, **8**, doi: <https://doi.org/10.1088/1748-9326/8/1/014036>
- Tebaldi, C., and R. Knutti, 2007: The use of the multi-model ensemble in probabilistic climate projections. *Philosophical Transactions of the Royal Society A.*, **365**, 2053-2075, doi: [10.1098/rsta.2007.2076](https://doi.org/10.1098/rsta.2007.2076).
- Tortorelli, R.L., A. Rea, and W.H. Asquith, 2005: *Depth Duration Frequency of precipitation from Oklahoma*. U.S. Geological Survey Water-Resources Investigations Report 99–4232. <https://pubs.usgs.gov/wri/wri994232/>. Accessed 02/01/2017.
- UNFCCC (United Nations Framework Convention on Climate Change), Conference of Parties 21, 2015: Paris Climate Change Conference. Available at http://unfccc.int/meetings/paris_nov_2015/meeting/8926.php. Accessed 02/27/2017.
- Van Vuuren., and 14 Co-authors, 2011: The representative concentration pathways: an overview. *Climatic Change*, **109**, doi: [10.1007/s10584-011-0148-z](https://doi.org/10.1007/s10584-011-0148-z)
- Weigel, A., R. Knutti, M. Liniger, and C. Appenzeller, 2010: Risks of Model Weighting in Multimodel Climate Projections. *Journal of Climate*, **23**, 4175–4191, doi: [10.1175/2010JCLI3594.1](https://doi.org/10.1175/2010JCLI3594.1).
- Williams, A. P., R. Seager, J. T. Abatzoglou, B. I. Cook, J. E. Smerdon, and E. R. Cook 2015: Contribution of anthropogenic warming to California drought during 2012–2014. *Geophysical Research Letters*, **42**, 6819–6828, doi:[10.1002/2015GL064924](https://doi.org/10.1002/2015GL064924).

- Woollings, T., B. Harvey, and G. Masato, 2014: Arctic warming, atmospheric blocking, and cold European winters in CMIP5 models. *Environmental Res. Letters*, **9**, doi: <https://doi.org/10.1088/1748-9326/9/1/014002>
- Yang, S., and J.H. Christensen, 2012: Arctic sea ice reduction and European cold winters in CMIP5 climate change experiments. *Geophys. Res. Lett.*, **39**, L20707, doi:[10.1029/2012GL053338](https://doi.org/10.1029/2012GL053338)
- Yavuzturk C., and K. Ksaibati, 2002: Assessment of temperature fluctuations in asphalt pavements due to thermal environmental conditions using a two-dimensional, transient finite difference approach. <https://ntl.bts.gov/lib/13000/13100/13135/MPC02-136.htm>. Accessed 02/01/2017.
- Ye, Z., D. Veneziano, and X. Shi, 2013: Estimating statewide benefits of winter maintenance operations. *TRB: Journal of the Transportation Research Board*, **2329**, 17-23, DOI: [10.3141/2329-03](https://doi.org/10.3141/2329-03)

APPENDIX

A.1 RESOURCES ON PUBLICALLY AVAILABLE STATISTICALLY DOWNSCALED DATASETS

All of the data products that are specifically listed below have a minimum temporal resolution of 1-day, and have both historical and future climate projections. Web links are provided where possible. *Before using the data in any capacity, peruse (if available) data FAQs, descriptions, and guidance for use.* Be aware that different downscaling techniques have some influence on the magnitudes of any variable output from the dataset. Detailed assessments for error and uncertainty due to these methods have not yet been examined in many cases. Statistical downscaling has a few key assumptions:

- Many downscaling methods were developed for a specific application or region, and have been scaled up to cover larger portions of the U.S. Their specific method may therefore perform best in the region it was originally designed for.
- The methods require gridded observations, and so it is assumed that those observations are reliable.
- The methods are trained and built by establishing relationships in the historical period, and it is assumed that these relationships are also true in the future (so called 'stationarity assumption'). There is ongoing work at the [Geophysical Fluid Dynamics Lab](#) to establish the degree to which this assumption is valid.

A1.1 Delta Method

The most basic form of this method examines model projected temperature and precipitation by calculating changes in model projections relative to each model's average climatology over a given time period, usually a historical period where high-resolution surface observations are also available. Subsequently, the changes are downscaled to a high-resolution grid by adding them to the high-resolution observation for temperature (or multiplying in the case of precipitation). This method is simple to implement, but also makes very limiting assumptions regarding the physical behavior of the climate. It is generally not recommended for applications that consider extreme events. The delta method has been applied for specific regional projects.

A1.2 Bias correction and Quantile Mapping

Bias correction is applied in all downscaling methods, and can take a number of forms. Its aim is to remove biases that are present in the GCM (e.g., when temperature or precipitation climatology for a given region departs significantly from observations). One technique generates cumulative distribution functions for a given variable and time period for historical and future GCM, and observations. High-resolution data is coarsened to the same grid as the GCM. The GCM data is then 'quantile mapped' on to the observations. Additional steps can include generating and applying factor fields (differences or ratios between an observed and GCM variable), followed by interpolation to the high-resolution observation grid.

BCSD – [Bias Corrected Spatial Disaggregation](#) (data typically only available monthly)

EDQM – Equidistant quantile mapping applied in the Red River projection (see below).

A1.3 Regression techniques

A downscaling technique that relates coarse-resolution GCM variables to a high-resolution counterpart variable using regression equations. These can take multiple forms, ranging from linear and univariate relationships to non-linear multivariate forms.

ARRM – [Asynchronous regional regression model](#)

A1.4 Multivariate techniques

A multivariate method involves a statistical analysis that incorporates more than one variable. For statistical downscaling, this can mean that instead of downscaling variables independently, they can be downscaled jointly. This can be important for variables with strong dependencies, e.g., temperature, humidity, and precipitation.

MACA – [Multivariate adaptive constructed analogues](#)

A1.5 Weather analogue techniques

Constructed analogues (CA) examine synoptic (large-scale atmospheric) patterns (typically daily) from a GCM dataset, and determine patterns that are similar to those derived from observations. This method therefore incorporates a higher degree of physical meteorology into its process, and can better represent processes in complex terrain (such as mountains). The CA approach does not bias correct on its own, so downscaling methods must bias correct data before and/or after applying the analogues. Various different techniques can be applied within this general framework, such that the three datasets referenced below differ in their methods, and output data characteristics.

MACA – [Multivariate adaptive constructed analogues](#)

LOCA – [Localized constructed analogues](#)

BCCA – [Bias corrected constructed analogues](#)

A1.6 Other

[The Red River Project](#)

This project statistically downscaled three CMIP5 GCMs, using three different statistical downscaling techniques, two of which were based on bias correction and quantile mapping techniques, and one a cumulative distribution transform method. The downscaling was for the Red River basin, stretching from the Texas Oklahoma border, through southern Oklahoma into Arkansas and Louisiana. In addition to downscaled temperature and precipitation, climate projections for streamflow were conducted using the Variable Infiltration Capacity (VIC) model. This data is publically available.

The 3rd project (not currently available)

This project, in collaboration with GFDL, uses three GCMs, three downscaling methods, and three different observations to examine historical and future climate in the South Central U.S. The project will generate multiple data products for temperature and precipitation over the next couple of years that have been rigorously evaluated and quality controlled. Contact PI McPherson for more information.

A.2 LIST OF DATA PRODUCTS GENERATED BY THIS PROJECT

Visual Graphics

The graphics described below will be available online in static .pdf format. Each of the 5 States in the SPTC domain will be available separately, unless otherwise mentioned.

Datasets

Quantitative output will be in spreadsheet-readable form (‘.txt’, ‘.csv’), for select regional subsets. In most cases, this will be climate divisions and/or county averages. The raw data will remain in scientific ‘NetCDF’ format. A description of this file format is provided in section 7.3

Dataset location

The data and images described below will be available approximately Fall 2017, via the South Central Climate Science Center basic data portal. For further information on locating the portal, and timeline for data, contact Co-PI Mullens (esther.white@ou.edu)

User access/agreement

All datasets and graphics are freely available for non-commercial use. Users of any graphical data should acknowledge Esther Mullens (Postdoctoral Associate, South Central Climate Science Center) as the author of these images. For data files, users should cite this final report, and the original developers of the data (e.g., MACA, ARRM). If any of these data products have a digital object identifier (DOI) citation, these should also be referenced. If users are unsure of how to cite this work, please contact PI McPherson or Co-PI Mullens.

A.2.1 Freeze Thaw Cycles

Visual Graphics

- Climatologies of historical FTC and EFTC from 1950-79 and 1980-2009 from all four observation datasets.
- Future decadal and 30-year climatologies from 2010 to 2099 from each climate model, and the multi-model mean, based on the climate scenarios (mid-range, and high emissions) used in this work.

- Time series of observed FTC and EFTC by climate division for TopoWx (1948-2012), Daymet (1980-2015), Livneh (1950-2005), and Maurer (1950-1999).

Datasets

Quantitative data will be available for the variables and metrics listed in Table 7.

- NetCDF file format datasets for historical and future projections, and observations
- Climate division (CD) spreadsheet-readable data files (these are typically expressed as a spatial average over the CD).

A.2.2 Cold temperatures

Visual Graphics

- Cold climate class, by state and for the whole domain, based on the three defined climate reference periods, and all applicable emissions scenarios. Graphics for each model, observation (Maurer and Livneh only), and multi-model mean.
- 0.1th percentile of T_{\min} for each decade 1950-2100, using historical observations, and all models and emissions scenarios.
- Climate division-based multi-model mean seasonal range of days with $T_{\min} < 32^{\circ}\text{F}$, past and future, with a range encompassing model spread.

Datasets

Quantitative data will be available for the variables and metrics listed in Table 8 as gridded NetCDF for the whole domain, and as tabulated climate division averages in textfile format.

A.2.3 Winter Precipitation

Visual Graphics

- *For the historical freezing precipitation dataset:* Spatial climatologies of freezing precipitation for decadal periods between 1980 and 2010, and for the whole duration of record. Frequencies of higher-impact events by magnitude.

- *For the analysis of statistically downscaled climate data:* Climate division-based time series of observations and model projected changes in winter weather frequency, liquid water equivalent, and intensity, 1950-2100. Model range included as a spread around a multi-model mean.

Datasets

- *For the historical freezing precipitation dataset:* Gridded spatial NetCDF files of 3-hourly, daily, monthly, and annual freezing precipitation frequency, liquid water equivalent, and other meteorologically relevant variables from 1979-2016. County average spreadsheet readable files of freezing precipitation frequency and liquid water equivalent, storm-mean surface temperatures, and wind speeds.
- *For the analysis of statistically downscaled climate data:* Climate division average historical and future time series of daily winter precipitation frequency and liquid water equivalent in textfile format. Original gridded dataset in NetCDF format. Data range from 1950-2100.

A.2.4 Hot Temperatures and temperature range

Visual Graphics

- Decadal averages of number of days above 95°F, 100°F and 110°F from historical observations and all models (individually, and as a multi-model mean), 1950-2100.
- 99.9th percentile value of T_{\max} (°F) for each decade 1950-2100, using historical observations (Livneh and Maurer), and all models and emissions scenarios.
- Climate division-average decadal time series in the multi-model mean (and spread) projections for numbers of days above 95, 100, 110°F.
- Climate division-based changes in seasonality of the 100°F season (using the three climate reference periods from the text).
- Climate division-based multi-model mean seasonal minimum and maximum temperatures from 1950-2100, expressed a time series with a range encompassing model spread. Observations are overlaid.

Datasets

Quantitative data will be available for the variables and metrics listed in Table 9. As with the other variables, data will be available as gridded spatial NetCDF files, and climate division averages in textfiles.

A.2.5 Precipitation, including average and extremes

Visual Graphics

- Climate division-based bar plots showing historical and projected magnitudes of 1 in 10, 1 in 50, and 1 in 100-year daily precipitation amounts, with individual models and the multi-model mean displayed.
- Climate division-based frequency intensity curves of historical and projected extreme precipitation, with model range also displayed.
- *For both of the above, separate plots showing block maxima extreme values estimated using Gumbel distribution, and the mixed Gumbel GEV method employed in this research.*

Datasets

- Quantitative data will be available for the variables and metrics listed in Table 11 in gridded NetCDF and textfile CD averages (return period calculations for climate divisions only).

A.3 INTERPRETING DATA FORMATS

A.3.1 Spreadsheet Readable formats

Files with a .txt ('text') or .csv ('comma separated') are common file formats used for numerical tables. They can be imported into Microsoft Excel from file->open. These files contain headers to define each column variable.

A.3.2 NetCDF

NetCDF is short for 'Network Common Data Form.' It is a file format commonly used for storing large array data. An array is data with a n -dimensional structure (where $n=1,2,3...$ and so on). For climate data, gridded datasets often possess arrays on the form (time, latitude, longitude). In other words, every data point for a variable (e.g.,

temperature) has a time coordinate, a latitude coordinate, and a longitude coordinate. The file structure includes 'metadata', which describes the information that is included within the file, such as variable names and array sizes/dimensions. An example of metadata for a freeze-thaw dataset derived from this study is shown below.

```
netcdf FTC_TopoWx_Livneh_res_1967 {
dimensions:
    months = 12
    lat = 238
    lon = 337
variables:
    int months(months)
    double lat(lat)
        lat:max = 39.96875
        lat:min = 25.15625
        lat:units = "degrees_north"
        lat:long_name = "latitude"
    double lon(lon)
        lon:max = -89.03125
        lon:min = -110.03125
        lon:units = "degrees_east"
        lon:long_name = "longitude"
    float total_ftc(lat, lon)
        total_ftc:min = 0.f
        total_ftc:max = 258.2498f
        total_ftc:long_name = "freeze thaw cycles - annual total"
        total_ftc:units = "days in year"
        total_ftc:_FillValue = -2.147484e+09f
    float total_enhanced_ftc(lat, lon)
        total_enhanced_ftc:units = "days in year"
        total_enhanced_ftc:long_name = "enhanced freeze thaw cycles - annual
total"
        total_enhanced_ftc:max = 155.7499f
        total_enhanced_ftc:min = 0.f
        total_enhanced_ftc:_FillValue = -2.147484e+09f
    float total_ftc_monthly(months, lat, lon)
        total_ftc_monthly:min = 0.f
        total_ftc_monthly:max = 31.f
        total_ftc_monthly:long_name = "monthly FTC"
        total_ftc_monthly:units = "cycles per month"
        total_ftc_monthly:_FillValue = 9.96921e+36f

// global attributes:
    :Conventions = "None"
    :source = "TopoWx 2014 version, see Oyler et al. (2014) and
http://www.ntsg.umd.edu/project/TopoWx"
    :title = "TopoWx derived diurnal freeze thaw cycles for the south
central states - annual and monthly totals only. Year=1967"
}
```

The metadata shows the list of variables in the file *FTC_TopoWx_Livneh_res_1967.nc* (*lat*, *lon*, *months*, *total_ftc*, *total_enhanced_ftc*, *total_ftc_monthly*). It shows the number of latitude and longitude points, the value(s) given to missing data, and describes attributes of each variable, and where the original data was sourced. The file name in

this case refers to TopoWx 1 km data that has been regridded to the resolution of the Livneh data (6.6km).

Reading and writing NetCDF files requires a specific set of libraries. Software that is able to read, display and even convert NetCDF data to other formats is available:

Geographic Information Systems (GIS): GIS has the ability to use and analyze NetCDF files and its data. It is supported in ArcGIS9.2 and higher. Web-resources for NetCDF and GIS can be found on the [National Center for Atmospheric Research website](#) and through [ArcGIS/ESRI](#).

R statistical software: R packages ncd, ncd4, raster, and RNetCDF provide support for reading and writing NetCDF, though users should check their version of R and the very latest guidance, as packages can be retired or changed with time. Documentation on these packages and examples of reading, writing and examining NetCDF in R can be found on the [R website](#).

Many other types of software are available, [listed by UCAR](#). In addition, for visualizing and sub setting, NASA has provided a free tool called '[panoply](#)' which can be run on a Windows platform.

A.4 LEVELS OF CONFIDENCE IN CLIMATE PROJECTIONS

The confidence levels discussed in section 4 adheres to the general principles of confidence as defined by the 3rd National Climate Assessment.

High confidence refers to moderate-strong evidence in the direction of change, the magnitude of change, and a confirmed scientific consensus. Multiple studies should support the result, despite using diverse methods and tools. Methods used to establish the result should be scientifically sound and robust.

Medium confidence refers to suggested evidence, some consensus regarding the direction and magnitude of trends. Studies may show differences in results, uncertainties in trends, and/or more limited documentation of approaches.

Low confidence suggests that evidence is inconclusive. Trends may be highly uncertain and vary between different studies leading to a lack of consensus. Documentation on methods and/or reliability of methods may be limited, absence of research may also constitute limited or uncertain evidence.

An additional element of confidence in this work considers the agreement between models on the direction and magnitude of change, and known model/method uncertainties contributed by physical processes or architectural/methodological uncertainty.